



Design and Performance Analysis of Energy Harvesting Communications Systems

Arooj Mubashara Siddiqui

A thesis submitted in partial fulfillment for the degree of
Doctor of Philosophy

in the

Faculty of Science and Technology
School of Computing and Communications, InfoLab 21
Lancaster University
September 2017

Declaration

I, Arooj Mubashara Siddiqui, declare that this thesis titled, "**Design and Performance Analysis of Energy Harvesting Communications Systems**" and the work presented in it are my own. I confirm that:

- Where I have consulted the published work of others, this is always clearly attributed.
- Where I have quoted from the work of others, the source is always given. With the exception of such quotations, this thesis is entirely my own work.
- I have acknowledged all main sources of help.
- Where the thesis is based on work done by myself jointly with others, I have made clear exactly what was done by others and what I have contributed myself.
- Detailed breakdown of the publications is presented in the first chapter of this thesis.

Signed: _____

Arooj Mubashara Siddiqui

Date: September 2017

Dedication

To my most beloved parents.....

Nisar Ahmed Siddiqui and Fareeda Naheed Afzal

Without them none of my success is possible.

Acknowledgement

In the name of ALLAH, The beneficent, The merciful

I would like to thank Almighty ALLAH for his countless blessings bestowed upon me during my PhD journey. I would express my gratitude to my supervisors Dr. Leila Musavian and Prof. Qiang Ni for their endless efforts, support, guidance and encouragement towards my doctoral studies. I would especially acknowledge Dr. Leila for her sincere and rent-less efforts towards completion of my PhD studies. She has been a source of inspiration and motivation for me to carry forward this research with her continuous devotion and supervision.

I would further thank my beloved parents, my sisters Aysha, Amna, Fateeha, my nephews Ibraheem, Ismaeel, Ishaaq, Sulaiman, Musa and brother-in-laws Ali, Intiaz, Zuhaib for their endless love, warmth and prayers.

Also, I am thankful to COMSATS Institute of Information and Technology, Pakistan, my parent university for providing me an opportunity to pursue my goals.

I would further thank brilliant teachers including Zhiguo Ding, my internal Ioannis Chatzigeorgiou, external Toktam mahmoodi, chair Keivan Navaie and university staff including Vicky, Debbie and Gillian.

I would especially acknowledge and thank my collaborator Sonia Aissa for giving me a chance to be part of her research team.

I would also like to thank all my friends, Beenish, Zohra, Nargis, Haris, Wenjuan, Amjad, Ethem, Mahmood, Gaurav and people whom i met during this course of

PhD and who have somehow inspired me during my doctoral studies. To all of them, I dedicate this thesis.

Abstract

The continuous growth of high data rates with huge increase in the number of mobile devices and communication infrastructure have led to greenhouse gas emission, higher pollution and higher energy costs. After the deployment of 4G and immense data rate and QoS requirements for 5G, there is an urgent need to design future wireless systems that aim to improve energy efficiency (EE) and spectral efficiency (SE). One of the possible solutions is to use energy harvesting (EH), which promises to reduce energy consumption issues in information and communication technology sector. In order to tackle these challenges, this thesis is focused on the design and performance analysis of EH systems. EH has emerged as a potential candidate for green wireless communication which not only provides solution to the energy limitation problem but also prolongs the lifetime of batteries.

First, the performance evaluation of an EH-equipped dual-hop relaying system is proposed to improve the system throughput and the end-to-end signal-to-noise ratio (SNR). We derive novel closed-form expressions for cumulative distribution function of individual link's SNR and of the end-to-end SNR. In addition, the proposed model analyses the ergodic capacity which is an important performance metric for delay-sensitive services. Further, these closed-form expressions reduce the computational complexity of the receiver architecture for practical systems. An insight through system parameters provide significant improvement in end-to-end SNR especially when both transmitter and relay nodes are equipped with harvesting

sources.

Second, performance analysis and optimal transmission power allocation techniques for EH-equipped system are studied. Our proposed model investigates and provides the conditions under which the harvesting can improve the system performance. In this work, novel closed-form expressions are calculated for the maximum achievable EE, SE and EH beneficialness condition. We studied two cases such as power is adapted to variations in the channel and when transmit power is fixed. We proved that EE-optimum input power decreases with EH power level. Also, system parameters demonstrate the conditions under which EH improves overall system performance.

Finally, a multi-objective optimization problem is formulated that jointly maximizes EE and SE for point-to-point EH-equipped system. We introduce new importance weight which set the priority levels of EE versus SE of the system. The formulated problem is solved by using convex optimization method to achieve optimal solution. The proposed system model provides freedom to choose any value for importance weight to satisfy quality of service (QoS) requirements and the flexibility of balancing between EE and SE performance metrics.

Table of Contents

Declaration	i
Dedication	ii
Acknowledgement	iii
Abstract	v
Table of Contents	vii
List of Abbreviations	xiv
List of Symbols	xvi
1 Introduction	1
1.1 Thesis Context and Motivation	1
1.2 Objective and Scope	6
1.3 Thesis Contributions and Novelties	8
1.3.1 Performance evaluation of an EH-equipped dual-hop relaying system with fixed batteries.	9
1.3.2 Optimal transmission power allocation techniques for point-to- point systems and performance analysis of EH system using Harvest-use approach.	9
1.3.3 EE and SE trade-off as a multi-objective optimization problem for a Rayleigh fading channel with point-to-point EH networks. .	10
1.4 Thesis Outline	10
1.5 Author Publications and Achievements	11

2	Performance Analysis of Relaying Systems with Fixed and Energy Harvesting Batteries	13
2.1	Introduction	14
2.1.1	Motivation and Related Works	14
2.1.2	Contributions	17
2.2	System Model and Assumptions	19
2.3	Performance Analysis of Energy-Harvesting Relaying System	23
2.3.1	First Hop (Transmitter to Relay)	24
2.3.2	Second Hop (Relay to Sink)	25
2.4	Closed-form Derivations	26
2.4.1	CDF of the First-Hop SINR	27
2.4.2	CDF of the Second Hop SNR	29
2.4.2.1	Closed-Form Expression for J_1	31
2.4.2.2	Closed-Form Expression for J_2	32
2.4.2.3	Closed-Form Expression for J_3	33
2.4.3	CDF of the End-to-End SNR	33
2.4.3.1	Closed-Form Expression for K_3	34
2.4.4	Ergodic Capacity	36
2.5	Numerical Results and Discussion	36
2.6	Chapter Summary	44
2.7	Experts Recommendation	45
3	Performance Analysis of Energy Harvesting Systems Using Harvest-Use Approach: Energy and Spectral Efficiency	46
3.1	Introduction	47
3.1.1	Motivation and Related Works	48
3.1.2	Contributions	50
3.2	System Model	52
3.3	Optimum Power Allocation	55
3.3.1	Energy-Efficient Power allocation without Input Power Constraint	55
3.3.2	Effect of Q_r on \bar{P}_u	58
3.3.2.1	Special Case - Neglecting the Circuit Power	59
3.3.3	Optimal Power Allocation to Maximize SE	60
3.4	Performance Improvement Analysis	61
3.4.1	Adaptive Transmit Power Allocation	61
3.4.1.1	Effect of Harvesting on the System's η_{opt}	61

3.4.1.2	Effect of Harvesting on η_{opt} when $P_{\text{cr}2} = 0$	63
3.4.1.3	Effect of Harvesting on SE_{opt}	64
3.4.2	Fixed Transmit Power	65
3.4.2.1	Effect of Harvesting on the System EE	65
3.4.2.2	Effect of Harvesting on the System η_{fix} when $P_{\text{cr}2} = 0$	67
3.4.2.3	Effect of Harvesting on the System SE_{fix}	67
3.5	Numerical Results	68
3.5.1	Case I: Adaptive Power Allocation	69
3.5.2	Case II: Fixed Transmit Power	72
3.6	Chapter Summary	76
4	Weighted Trade-off between Energy Efficiency and Spectral Efficiency for Systems with Energy Harvesting Batteries	78
4.1	Introduction	79
4.1.1	Motivation and Related Work	79
4.1.2	Contributions	80
4.2	System Model	81
4.3	Optimal Power Allocation in EE-SE Tradeoff	82
4.3.1	EE-SE Trade-off as an MOP	83
4.3.2	Optimal Power Allocation with No Input Power Constraint	84
4.3.3	Special case: without Circuit Power $P_{\text{cr}2}$	87
4.4	Numerical results	89
4.4.1	Optimum Power Allocation	89
4.4.2	Optimum Power Allocation without Circuit Power $P_{\text{cr}2}$	92
4.5	Chapter Summary	95
5	Conclusion and Future work	97
5.1	Conclusion	97
5.2	Future Work	98
5.2.1	Optimal power allocation for multiple network topologies in 5G	99
5.2.2	Energy harvesting for Internet-of-things (IOT)	99
5.2.3	EH based Non-orthogonal multiple access relaying systems	100
A	Appendix of Chapter 2	101
A.1	Proof for Lemma 1	101
A.2	Calculating Generalized Incomplete Gamma Function	102

B Appendix of Chapter 3	104
B.1 Proof for Lemma 2	104
Bibliography	106

List of Figures

2.1	Relaying system with fixed and energy-harvesting batteries.	20
2.2	Time-switching protocol for harvesting energy and information processing.	20
2.3	Illustration of key parameters in time-switching protocol for harvesting energy and information processing.	22
2.4	The CDF of γ_{TR} (first hop), CDF of γ_{RS} (second hop), and the CDF of the end-to-end SNR $\gamma_{\text{end-to-end}}$ versus the power consumed from the fixed batteries P , when $\gamma = 0.2$, $\eta = 0.3$ and $Q_t = 1\text{dB}$	38
2.5	Average rates at the first and second hops ($\mathbb{E}(R_1), \mathbb{E}(R_2)$) versus P with $\eta = 0.3$	38
2.6	$F_{\gamma_{\text{TR}}}(\gamma)$ and $F_{\gamma_{\text{RS}}}(\gamma)$ versus Q_t at $\gamma = 0.2$ with $\eta = 0.3$ and $P = 1\text{dB}$	40
2.7	Average rates at the first and second hops, ($\mathbb{E}(R_1), \mathbb{E}(R_2)$), versus τ , with $\eta = 0.3$ and various values of Q_t	40
2.8	Average rates (first-hop and second-hop) versus the energy conversion coefficient η , for $P = 1\text{dB}$ and various values of Q_t	41
2.9	Average rates (first hop, second hop and end-to-end) versus Q_t at $\eta = 0.3$ with $P = 1\text{dB}$	42
2.10	Average SNR/SINR versus Q_t at $\eta = 0.3$ with $P = 1\text{dB}$	43
2.11	Average rates (first hop, second hop and end-to-end) versus average interference at the relay $\mathbb{E}(I_R)$, with $\tau = 0.4$, $Q_t = 1\text{dB}$ and varying μ	43
3.1	System model.	52
3.2	Illustration of key parameters in time switching protocol for harvesting energy and information transfer.	52
3.3	EE versus TS parameter τ , when $Q_r = 0.5\text{dB}$, $P_{\text{cr}} = 0\text{dB}$ and $P_{\text{cr}2}$ varies.	69

3.4	SE versus TS parameter τ , with $Q_r = 0.5\text{dB}$ and various values of P_{\max} .	70
3.5	EE versus τ with various values of P_{cr} and P_{cr2} .	71
3.6	EE versus τ with $P_{cr} = 1\text{dB}$ and $P_{cr2} = 0\text{dB}$ and various values of Q_r .	71
3.7	Q_r versus power consumed from fixed battery P at $\tau = 0$ with $P_{cr2} = 0\text{dB}$ and $P_{cr} = 0\text{dB}$.	72
3.8	EE versus TS parameter τ at $P_{cr2} = 0\text{dB}$ and $P_{cr} = 0\text{dB}$ with various values of harvesting power Q_r and power consumed from fixed battery P.	73
3.9	SE versus TS parameter τ at $P_{\max} = 1\text{dB}$ with various values of harvesting power Q_r .	74
3.10	EE versus power P at $\tau = 0.5$ for various values of P_{cr} and P_{cr2} .	74
3.11	EE versus TS parameter τ at P = 1dB for various values of P_{cr} and P_{cr2} .	75
3.12	EE versus power from the fixed battery P with various values of τ , P_{cr} and P_{cr2} .	76
4.1	EE versus SE for various values of circuit power P_{cr} with $\tau = 0.8$, $Q_r = 0\text{dB}$ and $P_{cr2} = 0\text{dB}$.	89
4.2	EE versus SE with $Q_r = 0\text{dB}$, $P_{cr} = 0\text{dB}$ and $P_{cr2} = 0\text{dB}$ for various values of TS parameter τ .	90
4.3	EE vs Q_r with $\tau = 0.5$ with $P_{cr} = 0\text{dB}$ and $P_{cr2} = 0\text{dB}$, for various values of Δ .	91
4.4	SE vs Q_r with $\tau = 0.5$ with $P_{cr} = 0\text{dB}$ and $P_{cr2} = 0\text{dB}$, for various values of Δ .	92
4.5	EE and SE vs importance weight Δ with $Q_r = 1\text{dB}$, $\tau = 0.5$ with $P_{cr} = 0\text{dB}$ and $P_{cr2} = 0\text{dB}$.	93
4.6	EE vs τ with $\Delta = 0.7$, $Q_r = 1\text{dB}$ for various values of P_{cr} and P_{cr2} .	93
4.7	EE vs τ for various values of Δ with $Q_r = 1\text{dB}$ and $P_{cr} = 0\text{dB}$.	94
4.8	SE vs τ for various values of Δ with $Q_r = 1\text{dB}$ and $P_{cr} = 0\text{dB}$.	94
4.9	EE vs Q_r with $\tau = 0.5$ with $P_{cr} = 0\text{dB}$ and $P_{cr2} = 0\text{dB}$, for various values of Δ .	95

List of Tables

2.1 Simulation parameters	37
-------------------------------------	----

List of Abbreviations

AF	Amplify-and-forward
BS	Base station
CSI	Channel-state-information
CDF	Cumulative distribution function
CR	Cognitive radio
DF	Decode-and-forward
EH	Energy harvesting
EARTH	Energy aware radio and network technologies
EE	Energy efficiency
EC	Effective capacity
GDP	Gross domestic product
HU	Harvest-use
HSU	Harvest-store-use
ICT	Information and communication technology
i.n.i.d	Statistically independent and not necessarily distributed
KKT	Karush-Kuhn-Tucker
MIMO	Multiple-input-multiple-output
MRC	Maximal ratio combining
MISO	Multiple-input and single-output
MOP	Multi-objective optimization problem
NOMA	Non-orthogonal multiple access
OFDMA	Orthogonal frequency division multiple access
PS	Power-splitting
PDF	Probability density function
RF	Radio frequency
SNR	Signal-to-noise ratio
SINR	Signal-to-interference-plus-noise ratio
SOP	Single-objective optimization problem

SWIPT	Simultaneous and wireless information and power transfer
SE	Spectral efficiency
TREND	Towards real energy-efficient network design
TS	Time-switching
WSN	Wireless sensor networks

List of Symbols

\mathbf{A}	Capital bold-faced letter defines a matrix
B	System bandwidth
B_1	Fixed battery at transmitter
B_2	Fixed battery at relay node
C	End-to-end ergodic capacity
d_R	Distance between the transmitter and the relay node
d_S	Distance between the relay and the sink node
$F_{\gamma_{TR}}$	CDF of the SINR at the first-hop
$F_{\gamma_{RS}}$	CDF of the SNR at the second-hop
$F_{\gamma_{\text{end-to-end}}}$	CDF of end-to-end SNR
f_γ	Probability density function (PDF) of γ
g	Complex channel fading gain for second-hop
h	Complex channel fading gain for first-hop
I_i	interference power
K	Frequency dependent constant
P_{LR}	Path-loss at the relay
P_R	Power at relay
P_{LS}	Path-loss at the sink
P_L	Path-loss
P_c	Circuit power
P_{c2}	Circuit power during harvesting time
η	Achievable energy efficiency
P_r	Signal-to-noise ratio
P_{cr}	Circuit-to-noise ratio
P_{cr2}	Circuit-to-noise ratio during harvesting
P_{\max}	Average transmission power limit
Q	Solar energy harvesting power level
Q_t	Harvested solar energy

Q_T	Harvesting battery power
Q_R	Power harvested at relay node
Q_r	Harvest-to-noise power ratio
SE	Transmission rate or Spectral efficiency
SE_{opt}	Spectral efficiency with adaptive transmit power
SE_{fix}	Spectral efficiency with fixed transmit power
T_{sym}	Symbol duration
T_b	Length of fading block
τ	Time-switching parameter
γ_{TR}	Transmitter-to-relay SINR
γ_{RS}	Relay-to-sink SNR
σ_R^2	Variance of the AWGN at relay
Ω_h	Variance of channel fading gain for first-hop
Ω_g	Variance of channel fading gain for second-hop
$\dot{\alpha}$	Environmental/terrain dependent path-loss exponent
σ_S^2	Variance of the AWGN at sink
w	Random variable (RV)
$\Pr(\cdot)$	Probability
μ_i	Mean of i.n.i.d. exponential random interferences
$v(\mathbf{A})$	Number of distinct diagonal elements of \mathbf{A}
$\tau_i(\mathbf{A})$	Multiplicity of μ_i
λ_{ij}	(i, j) th characteristic coefficient of \mathbf{A}
\bar{P}_u	Optimal power level
ε	Power amplifier efficiency
Δ	Importance weight
η_{opt}	Energy efficiency with adaptive transmit power
η_{fix}	Energy efficiency with fixed transmit power

Chapter 1

Introduction

In this chapter, section 1.1 explains the motivation for using energy harvesting in green communication system which is a promising candidate in next generation 5G communication systems. Section 1.2 provides the objective and scope for this thesis. The main contribution and novelties towards this dissertation is mentioned in section 1.3. Then, section 1.4 is outlined to give an overview and structure of thesis. Lastly, section 1.5 lists the author's conference and journal papers during her doctoral studies.

1.1 Thesis Context and Motivation

We are living in a mobile generation, where demand of data rate and mobile-connected devices have immensely increased over the last two decades [DG16]. According to CISCO Visual Networking Index (VNI) 2016 report [Ind15] mobile data is expected to increase to 49 exabyte per month by 2021 which will eventually exceed annual traffic to half a zettabyte, out of this 78% of total mobile data traffic will be video. Due to this advancement in wireless technology, it is challenging to satisfy the high demands of users throughput, carbon footprint of information and communication technologies, cost effectiveness and limited battery issues [DCA16].

In addition to the battery limitation, according to climate group SMART (2020) [Mel10], higher greenhouse gas emissions have increased the carbon footprint to 349 metric ton (Mt) and the electrical energy consumption to 1700 tera watt hour (TWh), which will affect cost and climate changes by at least losing 5% of the global gross domestic product (GDP) every year. Due to the increase in the carbon-dioxide emission, limited battery life advancements, and the operational costs, several projects started to look for solutions to reduce the high energy costs and the carbon footprint of communication networks [LKWG11], e.g., energy aware radio and network technologies (EARTH) [GBF⁺09] and towards real energy-efficient network design (TREND) [AMBC⁺12]. There is indeed a huge interest in the academics and industries to design and develop higher data rate devices while lowering the device energy consumption. As discussed in [CZXL11], and references therein, there are four key trade-offs between energy efficiency, spectrum efficiency, delay and deployment costs.

In addition to the information and communication technology (ICT) challenges, saving energy is one of the most critical challenges for wireless communication sector [FVDM⁺12]. In light of the challenges mentioned above, there is a need of shifting to new paradigm "Green communication" for next generation networks [ABC⁺14]. Green communications promise to overcome these challenges by reducing energy consumption impact to environment [YZLZ17] and providing possible solutions to the current energy limitation problems in the ICT sector [LDPR02].

The evolving next generation networks focus on energy saving and fulfilling the energy requirements [DGK⁺13]. Fifth generation (5G) networks promises to provide high data rate in the range of 1 Giga bits per second (Gb/s) with 1000 times improved throughput, end-to-end latency in the range of 1 mili second (ms) and 10 times prolonged battery life in order to improve energy efficiency [ABC⁺14]. There are different technologies addressing to the requirements of 5G systems which are

classified as [HH15] 1) Energy harvesting (EH), 2) Cloud-based radio access network (C-RAN), 3) Heterogeneous networks (HetNets), 4) Full duplex communication, 5) Massive multiple-input multiple-output (MIMO), 6) Device-to-device (D2D) and virtualisation of network resources.

Energy harvesting has the potential to prolong the lifetime and improve the performance of energy limited networks, e.g., wireless sensor networks (WSNs) [XCFD13]. This technology not only promises to resolve the limited battery issues, but also to reduce the carbon footprint of high data rate wireless devices, by reusing the energy from the surrounding environment [Var08]. Energy can be harvested from sources like solar, wind, vibrations, thermo-electric and also from radio frequency (RF) signals [YU10], [CYZ⁺11].

On large scale harvesting energy opens the possibility for obtaining green and sustainable energy from all the resources [WYJW14]. Also, energy harvesting on large scale is beneficial for the applications envisioned for IoT which includes home automation, health care, transportation, smart environments and surveillance [ENS⁺17].

Energy harvesting techniques have the potential to reduce the carbon consumption of high data rate wireless systems by reusing the energy available in the surrounding environment [CQZ14], and can also be used to increase the lifetime of battery-limited devices, e.g, sensors and actuators [LZC13].

Energy harvesting is considered as one of the promising candidates for 5G communication. However the growing demand of energy in the world has set new challenges to the new generation networks. Internet of Things (IoT), connected devices and development in the energy based wireless communication devices has motivated researchers and academics to pay more attention towards increasing the battery life of these devices [RJS⁺17].

The Internet of Things (IoT) in particular is an intelligent infrastructure where

devices communicate wirelessly with each other and provide services to people on a large scale through the Internet [KMS⁺15]. IoT has the potential to improve many aspects of users' quality of life. In an IoT structure, sensors are mainly used which have limited energy resources (e.g., a battery). Energy harvesting may provide a solution with improved power management which eliminates the need of these batteries are getting attention in recent years [TTS⁺16].

Solar energy is certainly one of the most commonly used ambient energy, since light can be directly converted into electricity that runs a wide range of indoor and portable devices [HD88]. Also, solar energy is by far the largest and most available source among the renewable energy sources. In a communication network for example, the BS transmitter can be equipped with high solar panels that provide it with constant energy supply [CSAA16]. Solar energy is indeed a practical source for getting additional energy in outdoor networks. In wireless sensor networks for instance, intelligent solar energy harvesting systems comprised of solar panels and control circuits are highly beneficial [LS15]. RF energy harvesting, on the other hand, can be used in recharging a wireless node having limited battery capacity [PSZS13].

Apart from conventional renewable sources, energy can also be harvested from ambient energy in the RF [Kri14]. In particular, interference in the RF which emanates from cellular communication networks is an ambient source of energy omnipresent in various environments such as urban areas [CLJ⁺15]. Energy harvested from RF can be used to run devices with energy constrained resources [RSV11a]. RF harvesting got popularity due to the fact that it is autonomous and does not depend on dedicated energy sources [HD88].

EH is one of the promising solutions for improving energy efficiency (EE) of the battery constrained-wireless devices since it meets the requirements of green communications [NJC⁺17] and [PS05]. EH is expected to have futuristic abundant

applications e.g., solar panels and wind turbines which are deployed to reduce energy consumption and prolong the operation time [GSMZ14]. EH is an ambient source of energy which significantly improves EE of the system by keeping the device energy consumption low [ZCR⁺17].

In this regard, green communications provide ecological friendly approach that aims at improving the EE and the spectral efficiency (SE) of the future communication systems [BCR⁺12]. EE, which is defined as the data transferred per unit energy consumed, with unit of b/J/Hz, has recently received a great deal of interest, e.g., [MHL10] and [SMN15]. Designing an energy-aware system to provide high network performance and save energy is proved to be challenging in recent literature [HMLN13] and [ZZZ14]. EE is one of the key performance metrics for next generation communication networks. According to 5GrEEen project [OCF⁺13], telecom vendors and leading academics are contributing significantly to improve EE in 5G communications while reducing the operational cost. One of the biggest challenges in designing a future generation network is to jointly optimize contradicting objectives, which include, e.g., EE and SE [SK]. Improving EE or maximizing throughput, has been investigated widely in literature, e.g., in [PD10] and [XZ14], which show that increasing EE in many cases results in decreasing rate. In this trend, recently, EH has emerged as a new technology that has potential to improve EE, while maintaining the SE [PKH13] and [ZZH12].

From a usage architectural point-of-view, there exists two main categories for harvesting energy [RSV11a]: (a) harvest-store-use (HSU), where harvested energy can be accumulated for future use, and (b) harvest-use (HU). In the latter approach [KZO13], energy cannot be stored and must be used immediately when it becomes available to the transmitter [MM10]. This is suitable for applications where nodes exchange short messages, such as in sensor monitoring networks [SP01], and for systems with limited battery storage capabilities for instance [OTY⁺11]. The

benefit of the HU technique is indeed the low cost and the reduced implementation complexity.

In addition, since the energy should be immediately utilized as soon as it becomes available, the time switching (TS) protocol that assures the source to either harvest energy or transmit information data can be implemented [GA14]. The TS is indeed necessary as the information and energy receivers operate with different power levels [Var08] in practice. Also, due to the circuit limitations in reality, it is not possible to harvest energy and transmit or receive information at the same time [CSAA16]. Therefore, practical receiver architectures use either TS or power splitting (PS) for energy harvesting [DdCA16]. Compared to the TS approach, where the receiver switches over time between harvesting energy and transmitting/receiving information, in the PS scheme a portion of the received power is used for the harvesting and the rest is consumed for information processing [NZDK15].

The above mentioned research problems motivated us to investigate different aspects of utilizing EH in order to improve system performance metrics in terms of EE and SE. The motivation of this thesis is to highlight the importance of using EH as a potential candidate for 5G communication networks. This thesis will provide in-depth analysis on design and performance evaluation of EH systems.

1.2 Objective and Scope

The main objective of the thesis is to analyse two prominent performance metrics, i.e., EE and SE with an EH-equipped battery. The focus of this thesis is to design parameters, implementation strategies and providing solutions for EH systems that will achieve quality of service (QoS) requirements for 5G networks while maintaining EE. Performance analysis of EH system with fixed as well as EH battery under different scenarios has been done and discussed. Also, trade-off between EE and

SE is addressed and explained in detailed. The main objectives of this thesis are as follows:

Chapter 2

- To develop a new system model with EH-equipped dual-hop relaying system.
- To study the impact of two different EH sources, i.e., solar and RF interference on system performance and throughput.
- To investigate and derive the estimated closed-form expressions for cumulative distribution function of each link's individual SNR and of the end-to-end SNR.
- To derive the closed-form expressions for the randomness in the interference at relay which makes the system design practical.
- To evaluate the impact of additional energy sources to improve system throughput by providing the closed-form expressions.

Chapter 3

- To evaluate the performance of solar EH at transmitter along with fixed battery for point-to-point system.
- To study the conditions under which EH can improve system performance in terms of maximizing EE or SE of a system.
- To investigate the optimum power allocation on maximum achievable EE and SE, respectively.
- To provide closed-form expressions for the maximum achievable EE, SE and EH beneficialness condition under adaptive and fixed transmit power scenarios, respectively.

- To investigate the impact of power from fixed battery, TS parameter and solar harvesting energy level on the system performance.

Chapter 4

- To investigate the trade-off between EE and SE with solar EH at transmitter in a system.
- To study the multi-objective optimization problem (MOP) which jointly optimize EE and SE in Rayleigh fading channel.
- To study the impact of importance weight, circuit powers and solar harvesting level on achievable trade-off performance.

1.3 Thesis Contributions and Novelties

The challenges regarding performance analysis of a system with fixed battery issues and optimal power allocation in EH are highlighted and discussed in order to pave ways for this particular research direction. There are three main contributions;

- Performance evaluation of an EH-equipped dual-hop relaying system with fixed batteries.
- Optimal transmission power allocation techniques for point-to-point systems and performance analysis of EH system using harvest-use approach.
- EE and SE trade-off as a multi-objective optimization problem for a Rayleigh fading channel with point-to-point EH networks.

1.3.1 Performance evaluation of an EH-equipped dual-hop relaying system with fixed batteries.

In chapter 2, the performance evaluation of EH-equipped dual-hop relaying system is considered in which transmitter and relay nodes are equipped with both fixed and EH batteries. We derive the end-to-end SNR and the SNR at each link by providing closed-form expressions. Analytical expression for ergodic capacity is also calculated. Furthermore, the closed-form expressions are validated by Monte-Carlo simulations. The effect of EH factor, power from fixed batteries and statistically independent and not necessarily distributed (i.n.i.d) exponential variables on the rate of the system and overall system performance is evaluated. Hence, the system model is evaluated for the randomness in the interference at the relay, which makes the closed-form challenging.

1.3.2 Optimal transmission power allocation techniques for point-to-point systems and performance analysis of EH system using Harvest-use approach.

In chapter 3, performance analysis and optimal transmission power allocation techniques for point-to-point system, equipped with a harvest-use battery, as well as a fixed battery is evaluated. We derive closed-form expressions for the following cases: 1) when power is adapted optimally to the variations in the channel and 2) when the transmission power is fixed. The analysis is provided for the conditions under which EH can improve system performance. Also, the novel closed-form expression is calculated for the maximum achievable EE, SE and EH beneficialness condition. The maximum achievable EE is obtained by using fractional programming to get optimal power level. And then we proved that the

optimal power level monotonically decreases with EH power level. The correctness of the closed-form expressions is validated by Monte-Carlo simulations. Moreover, the impact of EH power level, TS parameter, circuit powers and power from fixed batteries on system performance is investigated through numerical results.

1.3.3 EE and SE trade-off as a multi-objective optimization problem for a Rayleigh fading channel with point-to-point EH networks.

In chapter 4, a power allocation scheme that jointly optimize EE and SE for a point-to-point system is proposed. A multi-objective optimization problem using weighted sum which jointly optimize EE and SE is derived. We introduce importance weight which is varied to prioritize EE and SE level. Using Karush-Kuhn-Tucker (KKT) conditions, the optimum power allocation without input power constraint is calculated in terms of closed-form expressions. Again, the impact of importance weight, TS parameter, circuit powers and solar harvesting energy level on achievable trade-off performance is investigated.

1.4 Thesis Outline

The thesis is organized into 5 chapters.

- Chapter 1 starts with an introduction to the thesis and present the objectives and motivation for the proposed research.
- Chapter 2 describes the performance analysis of EH-equipped dual-hop relaying system which improves end-to-end signal-to-noise ratio and system throughput. It includes the system model design and deriving the closed-form expressions.

- Chapter 3 explains the performance analysis and optimal transmission power allocation techniques for EH-equipped system is studied. The proposed model is analysed to investigate whether EH can improve the system performance under different scenarios.
- Chapter 4 investigates the system in which EE and SE trade-off as a multi-objective optimization problem for a Rayleigh fading channel with point-to-point EH networks.
- Chapter 5 summarizes all the chapters by providing conclusion of the thesis and giving potential directions for future work.

1.5 Author Publications and Achievements

Most of the results presented in the thesis are submitted and/or accepted in various conference and journals are provided as follows:

- Arooj.M. Siddiqui, Leila Musavian, Qiang Ni, "Energy efficiency optimization with energy harvesting using harvest-use approach", In *Proc. IEEE Int. Conf. Commun. Work. (ICCW)*, pages 1982-1987, London, June, 2015.
- Arooj.M. Siddiqui, Leila Musavian, Qiang Ni, and Sonia Aissa, "Performance analysis of Relaying Systems with Fixed and Energy Harvesting Batteries", *IEEE Trans. Commun. (TCOM)*, Feb 2017 (Accepted for publication).
- Arooj.M. Siddiqui, Leila Musavian, Qiang Ni, and Sonia Aissa, "Performance Analysis of Energy Harvesting Systems Using Harvest-Use Approach: Energy and Spectral Efficiency", *IEEE Trans. Wireless Commun. (TWC)*, May 2017 (submitted).

Apart from publications, few awards and achievements which counts in credit for author during PhD includes:

- Best Poster award at Postgraduate Research Conference, Lancaster university, 25th April 2015.
- Runner up for the best "3 minute thesis presentation award" at Postgraduate Research Conference, Lancaster university, 25th April 2015.
- Lancaster Award winner.
- Lancaster Excellence award. The Excellence Award is a stand-alone award which rewards high achieving students who have invested time and energy into academic and non-academic activities during their PhD. Author was selected for Lancaster excellence out of 200 students.

The chapters are mapped to papers in such a way that each work is represented by individual chapter given in detail in thesis later. Chapter 2 relates to "Performance analysis of Relaying Systems with Fixed and Energy Harvesting Batteries". This chapter is already accepted for publication in IEEE TCOM. Chapter 3 represents "Performance Analysis of Energy Harvesting Systems Using Harvest-Use Approach: Energy and Spectral Efficiency". Also one half of chapter 4 is already published in ICC conference given with title "Energy efficiency optimization with energy harvesting using harvest-use approach".

Chapter 2

Performance Analysis of Relaying Systems with Fixed and Energy Harvesting Batteries

This chapter focuses on the performance evaluation of an energy harvesting-equipped dual-hop relaying system for which the end-to-end signal-to-noise ratio (SNR) and the overall system throughput are analyzed. The transmitter and the relay nodes are equipped with both fixed and energy harvesting batteries. The source for harvesting at the transmitter is the solar energy, and at the relay node, the interference energy in the radio frequency is the harvesting source. The harvested energy, along with the energy from the fixed battery, is used to forward the decoded signal to the destination. Time switching scheme is used at the relay to switch between harvesting energy and decoding information. Harvest-use approach is implemented, and we investigate the effects of the harvested power in enhancing the performance of the relaying system by deriving estimated closed-form expressions for the cumulative distribution function of each links individual SNR and of the end-to-end SNR. The analytical expression for the ergodic capacity is also derived.

These expressions are validated through Monte-Carlo simulations. It is also shown that with the additional energy harvesting at the transmitters (source node and relay), a significant improvement in the system throughput can be achieved when fixed batteries are running on low powers.

2.1 Introduction

The continuously growing demand for higher data rates with the huge increase in the number of mobile devices have led to a rapid growth in the data traffic and communications infrastructure. This excessive demand in communicating data requires more energy consumption, which, in turn, results in higher greenhouse gas emission, higher pollution and higher energy costs [HBB11]. In addition, while the wireless traffic is increasing rapidly, battery capacity is still limited. The battery advancement is much slower than the need for long-life batteries, which resulted in widening the gap between increasing the rate demands and the battery advancements [HBB11].

2.1.1 Motivation and Related Works

Referring to the famous Shannon capacity formula, the link capacity increases when the transmission power increases since the received SNR increases [XZ14]. The capacity can also increase when the distance between the communicating nodes decreases, which will effectively reduce the path loss [GW02]. Employing a relaying node between the transmitter and its end receiver, which reduces the distance between the communicating nodes, could improve the capacity. On the other hand, to increase the transmission power without spending more from the fixed battery of the device, one can employ an additional energy harvesting equipment, which gives the flexibility of not being constrained by the fixed power or limited battery

supplies [HZ12]. By implementing energy harvesting at the transmitter and at the relay, the transmission rate can be improved while limiting the energy consumption from the fixed batteries [SMN15].

Energy harvesting strategy for a point-to-point communication link with a conventional harvesting source was formulated and proposed to improve throughput in [GS10]. In [HZ12], a water-filling algorithm for finite battery capacity was proposed for improving the throughput of the communication links with battery limited devices. Directional water-filling algorithms to maximize throughput in energy harvesting networks was later proposed in [WAW14]. Throughput maximization under fixed battery at the transmitter is studied for point-to-point communication systems in [TY12]. For communication systems assisted by relaying, a comprehensive receiver architecture was proposed in [XT12] for the rate-energy trade-off, where energy harvesting is used at the relay node only. Commonly used relaying techniques include amplify-and-forward (AF) and decode-and-forward (DF) [NZDK15].

To increase the battery life of relays, wireless energy harvesting has proven to be beneficial [DPEP14]. Recent studies showed that the combination of relaying with energy harvesting is useful and practical in deploying WSNs in remote areas [THOK15]. These advantages are not limited to WSNs, but also to other types of networks including cognitive and multiple-input multiple-output (MIMO) networks [LMD⁺16]. Optimal scheduling and power allocation for two-hop EH system with non-EH relay for calculating short-term throughput maximization is explained in [LZL13].

The received signal at the relay node is a combination of unwanted signals (interference) and the desired information [GA15]. As opposed to conventional communication, where interference is discarded instead of re-utilizing [GA14], co-channel interference was recently identified as a source for energy harvesting [LZC13]. From literature [GA15], improving signal-to-interference-plus-noise ratio (SINR)

by decreasing the interference has always been a concern and different methods including multi-cell coordination, interference-alignment are used to maintain the balance. Although interference reduces capacity of the system but on the other hand, from energy point of view, it serves as an additional source of energy for harvesting system [GA15]. In fact, interference emerges as an additional source of energy that can help the communication process and improve the system performance [GA14, GA15, LZC13].

The performance analysis of RF energy harvesting relaying network is studied in [DdCA16], which focuses on energy constraint on the transmission power and transceiver hardware impairment for multi-relay EH, while not focusing on TS approach. Performance analysis of RF-powered wireless sensor in downlink wireless information and power transfer (SWIPT) using stochastic geometry is explained in [LFN⁺15].

Relay selection with residual impairments and multiple antennas devices is considered in [NK⁺16], wherein the best relay is chosen using the channel-state-information (CSI) at each hop and applying maximal ratio combining (MRC). The same performance analysis approach is used in [HGM16] for non-orthogonal multiple access (NOMA) under Nakagami- m fading. Also, cooperative NOMA with simultaneous wireless information and power transfer, where the users close to source act as EH relays is considered in [LDEP16]. Outage probability and throughput of an amplitude-and-forward EH relaying system using for Nakagami- m channel is presented in [Che16]. In addition to that, performance analysis of dual-hop under-water channel subject to $\kappa - \mu$ shadowed fading Channel with RF EH is considered in [IEBA16]. Despite the importance of energy constraint and its effects on the transceiver design issues in cooperative networks, most of the research work in the literature focused on harvesting sources at the transmitter and at the relay with no fixed batteries. It is inevitable that a limited fixed battery

is implemented within the communication system nodes [LMD⁺16]. Given the nature of the most types of harvesting energy sources, which is random and not necessarily available at all times, a limited fixed battery can provide extra flexibility and continuity in service. However, a thorough study on how energy harvesting can improve the performance of relaying-based communication with fixed batteries, but limited power, is yet to be done.

2.1.2 Contributions

In this chapter, we consider a dual-hop relaying system in which the transmitter and the relay are equipped with both fixed and energy-harvesting batteries. The harvesting at the transmitter relies on solar energy. At the relay node, on the other hand, the energy source is RF interference along with the fixed battery. The TS scheme is used at the relay to harvest energy and to pass information to the destination. Energy harvesting serving as an additional source of energy, and modelled as a continuous function with fixed rate, is considered in [VTY14] and a throughput maximization problem is solved in this chapter. The work here, however, considers continuous constant energy arrivals joined with a limited fixed battery, and thus, can be used as a basis for a system with random harvesting energy arrivals. For the relaying system considered here, we analyse and discuss the impact of energy harvesting on the system performance. First, closed-form expressions for the cumulative distribution function (CDF) of the end-to-end SNR, and also for each link SNR are obtained. To do so, we analyse the randomness in the transmission power due to the RF interference energy at the relay, and we evaluate the overall system performance in terms of the end-to-end SNR. Analytical expression for the ergodic capacity is also derived. Numerical results for the validation of the developed analysis are obtained using Monte-Carlo simulations.

The effect of different parameters, such as the energy harvesting power, the power levels of the fixed batteries, and the energy conservation coefficient, are discussed and analysed.

To summarize, the main contributions of this chapter are enlisted below:

- The benefits of having interference energy harvesting at the relay node and solar energy harvesting at the source node, along with limited power fixed batteries, on the performance of dual-hop relaying system, is investigated. To the best of the authors' knowledge, this work presented in this is the first to address this. Section 2.2 describes the system model and assumptions.
- Closed-form expressions for the CDF of the end-to-end SNR and the SNR at each link are derived. The closed-form expressions reduce the computational complexity, but are also challenging to derive due to the presence of randomness in the interference at the relay node. Since, the channel between the relay and the source is also random, the presence of multiplication of several random parameters in the received SNR, makes it difficult to analyze.¹ Performance analysis of the energy harvesting relaying system is discussed in Section 2.3. In Section 2.4, we derive the CDF of the first-hop signal-to-interference and noise ratio SINR, that of the second-hop SNR, and the one of the end-to-end SNR.
- Ergodic capacity, which is an important performance metric for delay-insensitive services, is analysed. The analytical expression for the ergodic capacity of the relaying system is also obtained. Section 2.4 also includes description about Ergodic capacity.

¹The closed-form expressions developed here are of great help when it comes to the system design in practice, where the impact of interference, solar energy and energy efficiency coefficient play a significant role in improving throughput.

- The impact of the additional energy sources to improve the overall system performance is evaluated by using mathematical closed-form expressions, which are validated through Monte-Carlo simulations. Differences between the numerical results corresponding to the analysis and the Monte-Carlo simulations are small, such that the closed-form expressions are good estimates of the results. The simulation results also evaluate the effect of the mean of the sum of the statistically independent and not necessarily distributed (i.n.i.d.) exponential variables on the interference level on the rate of the system.
- Finally, the impact of energy harvesting factor and power from the fixed batteries, on the system performance, is studied through numerical results. Also, the insightful results related to energy harvesting sources, i.e., RF interference and solar energy, on improving end-to-end rate, are analysed. The numerical results and discussion are given in Section 2.5, followed by the chapter summary in Section 2.6.

2.2 System Model and Assumptions

We consider a dual-hop DF relaying system, in which the transmitter T communicates with the sink S through an energy-harvesting relaying node R , as presented in Fig. 2.1. Node T is equipped with a fixed battery and a conventional solar energy harvesting battery. The relay node is also energy constrained with a fixed battery but can also harvest energy from RF signals in the form of interference².

²The system model considered has fixed as well as harvesting batteries. The system is assumed to finish fixed battery first and then use energy harvesting battery as soon as energy becomes available. Also, EH is not available all the time, therefore having fixed battery keeps the system working. In addition to that, EH with fixed battery provide support which prolong the battery life. The application of such system is more reliable when considering short-range communications such as wireless sensor networks (WSN) in remote areas [LWN⁺15]. Therefore, by providing fixed batteries the system model becomes more practical and realistic.

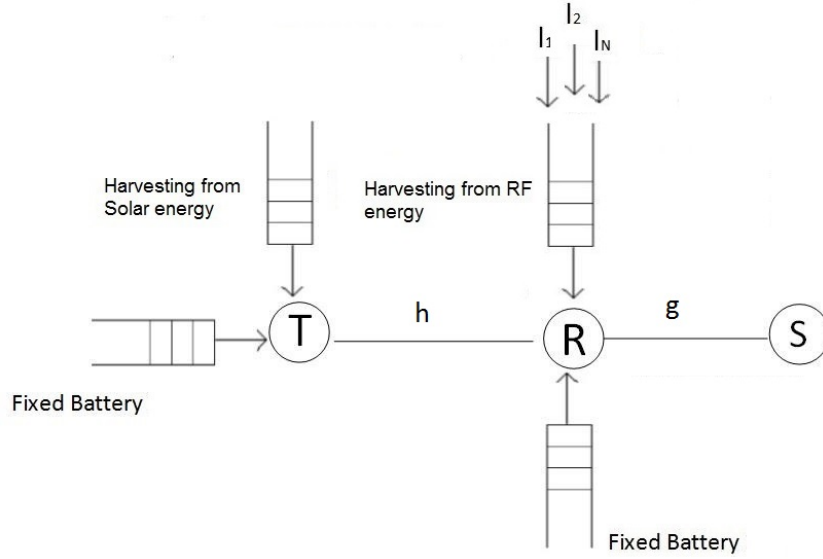


Figure 2.1: Relaying system with fixed and energy-harvesting batteries.

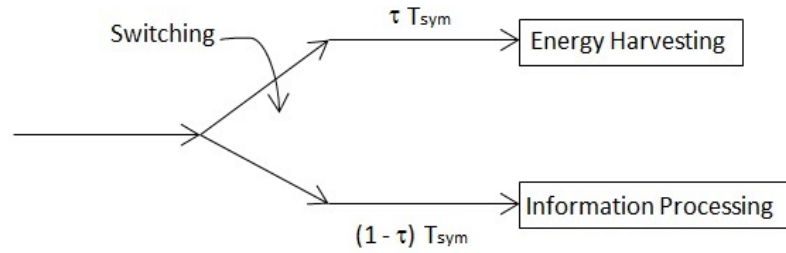


Figure 2.2: Time-switching protocol for harvesting energy and information processing.

No direct communication between transmitter T and the sink S is possible, e.g., due to shadowing.

Channels follow the block flat-fading model, i.e., each of the channel gains are invariant during each fading block, but varies independently from one block to another. The length of each fading block is denoted by T_b . The symbol duration is given by $T_{\text{sym}} = 1/B$, where B is the system bandwidth. We assume that the fading block duration is an integer multiplication of the symbol duration.³ Furthermore, the fading block duration of all channels are assumed to be same. In the considered system model, the CSI is not known to the transmitter node, as power allocation

³ If T_b is smaller than T_{sym} , then one symbol will be divided into two fading blocks and will experience different fading. Hence, the derivations of this work will not hold anymore.

is not considered. Therefore, the instantaneous knowledge of the channel is not required at the transmitter. However, the sink node knows the CSI when it is in the receiving mode [LZL13]. Additive white Gaussian noise (AWGN) is considered at the receiver and at the relay node. The first-hop and second-hop channels experience independent Rayleigh fading with complex channel fading gains given by $h \sim CN(0, \Omega_h)$ and $g \sim CN(0, \Omega_g)$, respectively. Parameter Ω_h and Ω_g denote the variance of channel fading gains h and g , respectively.

In this system model, transmitter T has a fixed battery, referred to by battery B_1 , and the relay node R also has a fixed battery, referred to by battery B_2 . These batteries operate at fixed powers, P_1 and P_2 , respectively. We also use two additional energy harvesting sources apart from the fixed batteries. At node T , harvesting is done from the solar energy, while at the relay energy from RF interference signals is used⁴. The transmitter. Here, we assume that the arrival rate of the harvested solar energy is constant, hence Q_t is a fixed value. This is a reliable assumption when we use solar energy as explained in [VTY14]. When relay is transmitting, the source node harvests energy, hence, no TS is required at the source. These harvesting batteries use harvest-use approach, in which energy cannot be stored and must be used immediately when it becomes available for signal transmission. In the harvest-use approach, energy collected through harvesting is assumed available at the end of the harvesting time [RSV11b]. As there is no buffer to store the harvested energy, the energy causality constraints are not applicable here. Rechargeable batteries, which consider energy causality constraints for energy storage through harvesting, are discussed in [RSV14].⁵ The

⁴For keeping practical circuit implementation in mind, the receiver activation threshold is not supposed to go beyond -10dBm [LWN⁺15]. Also, when RF harvested power is low, the conversion efficiency is also low [NMLC12].

⁵More information on the harvest-use approach is provided in [KHZS07]. In the present work, the EH battery level is considered fixed within a transmission cycle, while the interference from the RF source is random given the nature of ambient energy. Similar to [RSV11b] and [KHZS07], no device equipment is dedicated to store energy.

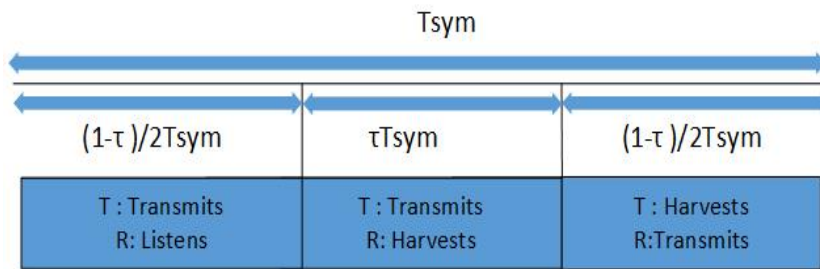


Figure 2.3: Illustration of key parameters in time-switching protocol for harvesting energy and information processing.

overall interference induced on the relay node originates from N i.n.i.d. interferers [GA14], and is represented by $\sum_{i=1}^N I_i$, where I_i denotes the interference power of the i^{th} interferer. It is assumed that the interference channels and the desired channels are independent from each other. Here, the interference imposed on the other networks from the considered relay system is not analyzed. However, the results of this chapter can pave the way for more analysis by considering both the incoming interference to the relay system, and the imposing interference from the relay system to the neighbouring networks. To do so, a further complex variable can be introduced for inter-cell interference. By that the analysis and derivations of this chapter can be further updated to be used for multi-cell applications under inter-cell interference.

We assume DF relaying is employed hence, the message received at the relay node is decoded and forwarded to the sink without any delay. Each node is assumed to have a single antenna and to work in a half duplex mode within the dual-hop communication system. The TS approach is used at the relay for harvesting energy and processing information, as described in Fig. 2.2. Let us consider τT_{sym} , for which τ varies from $0 \leq \tau \leq 1$, is the fraction of time in which the relay harvests energy from the received signals and from the external interference. $(1 - \tau)T_{\text{sym}}$ is divided in two equal parts and represents the fraction of time during which information is transmitted from the source to the relay and from the relay to the

destination node, respectively.⁶ An illustration of the key parameters in the time allocation considered is provided in Fig. 2.3. Here, the source and the relay nodes have a harvest-use battery, in which the harvested energy is used immediately as soon as it becomes available. When source is transmitting, the relay uses that time to listen because energy is not being available. As soon as energy becomes available the relay harvests while the source is still transmitting. This happens because relay doesn't have any storing equipment.

2.3 Performance Analysis of Energy-Harvesting Relaying System

In this section, we evaluate the end-to-end SNR and the ergodic capacity of the relaying system with fixed batteries and energy harvesting as described in Section II. The end-to-end ergodic capacity C (in b/s/Hz) is the average of the minimum between the rate at the first hop (R_1) and the one at the second hop (R_2), represented by

$$C = \mathbb{E}(\min(R_1, R_2)),$$

where $\mathbb{E}(\cdot)$ indicates the expectation operator. Rates R_1 and R_2 are given by

$$R_1 = \frac{(1 - \tau)}{2} \log_2(1 + \gamma_{\text{TR}}), \quad (2.1)$$

$$R_2 = \frac{(1 - \tau)}{2} \log_2(1 + \gamma_{\text{RS}}), \quad (2.2)$$

where γ_{TR} denotes the received SINR at the relay, and γ_{RS} indicates the received SNR at the sink. The effect of the interference at the receiver is considered as an

⁶The source harvests energy when the relay is transmitting and, hence, TS is not required at the source.

AWGN which is the worst effect of interference.

2.3.1 First Hop (Transmitter to Relay)

During this phase, node T transmits the data signal, consuming power P_1 from its fixed battery B_1 and an additional power Q_T from its harvesting battery. The SINR at the relay node can then be written as

$$\gamma_{\text{TR}} = \frac{(P_1 + Q_T)h}{K_R + \sum_{i=1}^N I_i}, \quad (2.3)$$

where $K_R = P_{L_R} \sigma_R^2 B$, with σ_R^2 indicating the variance of the AWGN, P_1 indicates the instantaneous power of the fixed battery B_1 , and $Q_T = \frac{(1-\tau)Q_t}{1+\tau}$. and P_{L_R} representing the path-loss at the relay, given by $P_{L_R} = K d_R^{-\dot{\alpha}}$. Here K represents the frequency dependent constant, d_R is the distance between the transmitter and the relay node and $\dot{\alpha}$ an environmental/terrain dependent path-loss exponent $\dot{\alpha} > 2$ [LWZ⁺16]. The transmitter-to-relay SINR, γ_{TR} , is further simplified as

$$\gamma_{\text{TR}} = \frac{\gamma_h}{1 + I_R}, \quad (2.4)$$

where $\gamma_h = \frac{(P_1 + Q_T)h}{K_R}$ and $I_R = \frac{\sum_{i=1}^N I_i}{K_R}$. The received data is assumed to be decoded correctly only when the SINR is greater than a predefined threshold γ .

⁷Time for harvesting = $\frac{(1-\tau)T_{\text{sym}}}{2}$ and time for transmitting signal is given by = $\frac{(1-\tau)T_{\text{sym}}}{2} + \tau T_{\text{sym}}$ which makes total harvesting power $\frac{(1-\tau)Q_t\tau}{1+\tau}$

2.3.2 Second Hop (Relay to Sink)

For the second hop, the total power at the relaying node is the sum of the power from its fixed battery B_2 and the harvested power from the interference in RF. Therefore, the power at the relay will be

$$P_R = P_2 + Q_R, \quad (2.5)$$

where P_2 denotes the instantaneous power of the fixed battery⁸, and Q_R indicates the power harvested at the relay node. The total energy that is harvested from the received information signal and from the interference signal for a duration of τT_{sym} at each block, is given by

$$E_H = \eta \left[\sum_{i=1}^N I_i + (P_1 + Q_T) h \right] \tau T_{\text{sym}}, \quad (2.6)$$

with η indicating the energy conversion coefficient which varies from 0 to 1 [XA15]. The processing power at the relay, required by the transmit/receive circuitry is negligible compared to the power used for data transmission [GA15]. Therefore, we assume that the relay consumes energy harvested from the received source and interferences signals, for forwarding information to the destination node. The transmission power at the relay node can be written as

$$Q_R = \frac{E_H}{(1 - \tau)T_{\text{sym}}/2}. \quad (2.7)$$

Replacing the value of E_H from (2.6) into (2.7) and substituting it into (2.5), we get

$$P_R = P_2 + \frac{2\tau\eta}{1 - \tau} \left[\sum_{i=1}^N I_i + (P_1 + Q_T)h \right]. \quad (2.8)$$

⁸ P_2 is the power from the fixed battery B_2 considered at the relay node. Hence P_2 is a fixed power.

The SNR at the sink S is then given by

$$\gamma_{\text{RS}} = \frac{P_{\text{R}}g}{K_{\text{S}}},$$

where $K_{\text{S}} = P_{L_{\text{S}}}\sigma_{\text{S}}^2B$, with σ_{S}^2 indicating the variance of the AWGN at the destination node and $P_{L_{\text{S}}}$ representing the path-loss which is given by $P_{L_{\text{S}}} = Kd_{\text{S}}^{-\alpha}$, where d_{S} is the distance between the relay and the sink node [LWZ⁺16]. Inserting the value of P_{R} from (2.8) into γ_{RS} yields

$$\gamma_{\text{RS}} = \frac{\left[P_2 + \frac{2\tau\eta}{1-\tau} \left(\sum_{i=1}^N I_i + (P_1 + Q_{\text{T}})h \right) \right] g}{K_{\text{S}}},$$

which can be further simplified into

$$\gamma_{\text{RS}} = \gamma_{\text{g}} + w(I_{\text{R}} + \gamma_{\text{h}}), \quad (2.9)$$

where $\gamma_{\text{g}} = \frac{gP_2}{K_{\text{S}}}$ and $w = \frac{2\eta\tau K_{\text{R}}g}{K_{\text{S}}(1-\tau)}$. We note that w is a random variable (RV) with the same distribution as of g but with a different variance.

2.4 Closed-form Derivations

Here, we aim to derive a closed-form expression for the CDF of the SINR/SNR of the links, i.e, transmitter-to-relay SINR and relay-to-sink SNR, and also the end-to-end SNR for the energy harvesting DF relaying system with TS approach. By definition, the CDF of SNR at a certain threshold, γ , shows the probability of the instantaneous SNR to be less than γ . This threshold can represent the criterion for a minimum quality-of-service requirement at each node. The CDF of the SINR at the first-hop is formulated as $F_{\gamma_{\text{TR}}}(\gamma) = \Pr(\gamma_{\text{TR}} \leq \gamma)$, and the CDF of

the SNR at the second-hop is given by $F_{\gamma_{\text{RS}}}(\gamma) = \Pr(\gamma_{\text{RS}} \leq \gamma)$, where $\Pr(\cdot)$ denotes the probability and $F_x(x)$ stands for the CDF of RV X at x .

With the channels following independent Rayleigh fading, the probability distribution function (PDF) γ_{h} , is exponential:

$$f_{\gamma_{\text{h}}}(x) = \frac{1}{\bar{\gamma}_{\text{h}}} \exp\left(-\frac{x}{\bar{\gamma}_{\text{h}}}\right), x \geq 0, \quad (2.10)$$

where $\bar{\gamma}_{\text{h}}$ is the average SNR from the transmitter to the relay and is given by $\bar{\gamma}_{\text{h}} = \frac{(P_{\text{T}} + Q_{\text{T}})\Omega_{\text{h}}}{K_{\text{R}}}$.⁹ Similarly, the PDF of the interference, I_{R} , which is the sum of N statistically i.n.i.d. exponential random interferences, each with a mean of μ_i , can be written as [SW08]

$$f_{I_{\text{R}}}(y) = \sum_{i=1}^{v(\mathbf{A})} \sum_{j=1}^{\tau_i(\mathbf{A})} \lambda_{ij}(\mathbf{A}) \frac{\mu_i^{-j}}{(j-1)!} y^{j-1} \exp\left(-\frac{y}{\mu_i}\right), y > 0, \quad (2.11)$$

where matrix $\mathbf{A} = \text{diag}(\mu_1, \mu_2, \dots, \mu_N)$, with $\mu_1 > \mu_2 > \dots > \mu_{v(\mathbf{A})}$ being the diagonal elements in decreasing order, $v(\mathbf{A})$ denotes the number of distinct diagonal elements of \mathbf{A} , $\tau_i(\mathbf{A})$ is the multiplicity of μ_i , and λ_{ij} is the (i, j) th characteristic coefficient of \mathbf{A} as discussed in [SW08].

2.4.1 CDF of the First-Hop SINR

The CDF of the first-hop received SINR, $\Pr(\gamma_{\text{TR}} \leq \gamma)$, can be expanded by inserting the value of γ_{TR} from (2.4) to get

$$\Pr(\gamma_{\text{TR}} \leq \gamma) = \Pr(\gamma_{\text{h}} \leq (1 + I_{\text{R}})\gamma). \quad (2.12)$$

⁹Also the CDF is defined by $F_{\gamma_{\text{h}}}(x) = \mathbb{E}\left(1 - \exp\left(-\frac{x}{\bar{\gamma}_{\text{h}}}\right)\right)$

Using the PDF of γ_h , given in (2.10), the CDF of the first-hop SINR for each value of interference I_R can be expanded as

$$F_{\gamma_{\text{TR}}}(\gamma) = \mathbb{E}_{I_R} \left(1 - \exp \left(-\gamma \left(\frac{1 + I_R}{\gamma_h} \right) \right) \right), \quad (2.13)$$

where \mathbb{E}_{I_R} is the expectation operator with respect to RV I_R . The expression in (2.13) can be expanded by using the definition of expectation [PP02, p. 30], yielding

$$F_{\gamma_{\text{TR}}}(\gamma) = 1 - \int_0^\infty \exp \left(\frac{-\gamma(1+u)}{\gamma_h} \right) f_{I_R}(u) du. \quad (2.14)$$

We now replace the PDF of interference I_R from (2.11) into (2.14) to get

$$F_{\gamma_{\text{TR}}}(\gamma) = 1 - \int_0^\infty \exp \left(\frac{-\gamma(1+u)}{\gamma_h} \right) \sum_{i=1}^{v(\mathbf{A})} \sum_{j=1}^{\tau_i(\mathbf{A})} \lambda_{ij}(\mathbf{A}) \frac{\mu_i^{-j}}{(j-1)!} u^{j-1} \exp \left(\frac{-u}{\mu_i} \right) du. \quad (2.15)$$

In order to solve (2.15), we re-arrange the equation as

$$\begin{aligned} F_{\gamma_{\text{TR}}}(\gamma) &= 1 - \sum_{i=1}^{v(\mathbf{A})} \sum_{j=1}^{\tau_i(\mathbf{A})} \exp \left(\frac{-\gamma}{\gamma_h} \right) \lambda_{ij}(\mathbf{A}) \frac{\mu_i^{-j}}{(j-1)!} \left(\frac{1}{\mu_i} \left(1 + \frac{\gamma \mu_i}{\gamma_h} \right)^{-1} \right) \\ &\quad \times \int_0^\infty \frac{u^{j-1}}{\mu_i} \left(1 + \frac{\gamma \mu_i}{\gamma_h} \right) \exp \left(\frac{-u}{\mu_i} \left(1 + \frac{\gamma \mu_i}{\gamma_h} \right) \right) du. \end{aligned} \quad (2.16)$$

which can be solved in closed-form as,

$$\begin{aligned} F_{\gamma_{\text{TR}}}(\gamma) &= 1 - \sum_{i=1}^{v(\mathbf{A})} \sum_{j=1}^{\tau_i(\mathbf{A})} \exp \left(\frac{-\gamma}{\gamma_h} \right) \lambda_{ij}(\mathbf{A}) \frac{\mu_i^{-j+1}}{(j-1)!} \left(\left(1 + \frac{\gamma \mu_i}{\gamma_h} \right)^{-1} (j-1)! \right. \\ &\quad \left. \times \mu_i^{j-1} \left(1 + \frac{\gamma \mu_i}{\gamma_h} \right)^{-j+1} \right). \end{aligned} \quad (2.17)$$

Therefore, the CDF of the first-hop received SINR is obtained by simplifying (2.17) to get

$$F_{\gamma_{\text{TR}}}(\gamma) = 1 - \sum_{i=1}^{v(\mathbf{A})} \sum_{j=1}^{\tau_i(\mathbf{A})} \exp\left(\frac{-\gamma}{\bar{\gamma}_{\text{h}}}\right) \lambda_{ij}(\mathbf{A}) \left(1 + \frac{\gamma \mu_i}{\bar{\gamma}_{\text{h}}}\right)^{-j}. \quad (2.18)$$

The closed-form expression for CDF for the first-hop SINR is dependent on the average SNR from transmitter to relay, $\bar{\gamma}_{\text{h}}$, mean of random interference, μ_i and the threshold γ .

2.4.2 CDF of the Second Hop SNR

Here, a closed-form expression for the CDF of the second-hop received SNR, $\Pr(\gamma_{\text{RS}} \leq \gamma)$ is obtained. The analysis is difficult due to the presence of randomness both in the RF interfering signals and in the channels. The transmit power at the relay follows a random exponential distribution according to [GA15]. Since the channel between the relay and the source is also a random parameter, the SNR will have the impact of these two random parameters multiplied.

We start by defining $z = \gamma_{\text{h}} + I_{\text{R}}$ to simplify (2.9). Then, the target CDF becomes

$$F_{\gamma_{\text{RS}}}(\gamma) = \Pr(\gamma_{\text{g}} + wz \leq \gamma) = \mathbb{E}_z \mathbb{E}_{\gamma_{\text{g}}} \left(1 - \exp\left(-\frac{\gamma - \gamma_{\text{g}}}{\bar{w}z}\right)\right), \quad (2.19)$$

where $\bar{w} = \frac{2\tau\eta K_{\text{R}}\Omega_{\text{g}}}{K_{\text{S}}(1-\tau)}$, \mathbb{E}_z and $\mathbb{E}_{\gamma_{\text{g}}}$ are the expectation operators with respect to RVs z and γ_{g} , respectively. We note that the PDF for γ_{g} is an exponential function given by

$$f_{\gamma_{\text{g}}}(\gamma_{\text{g}}) = \frac{1}{\bar{\gamma}_{\text{g}}} \exp\left(-\frac{\gamma_{\text{g}}}{\bar{\gamma}_{\text{g}}}\right), \quad (2.20)$$

where $\bar{\gamma}_{\text{g}} = \frac{P_2\Omega_{\text{g}}}{K_{\text{S}}}$. In order to solve (2.19), we first solve the expectation with

respect to γ_g , to get

$$\mathbb{E}_{\gamma_g} (\Pr(\gamma_g + wz \leq \gamma)) = 1 - \frac{1}{\gamma_g} \exp\left(\frac{-\gamma}{z\bar{w}}\right) \int_0^\gamma \exp\left(-\frac{\gamma_g}{\gamma_g} + \frac{\gamma_g}{\bar{w}z}\right) d\gamma_g. \quad (2.21)$$

Solving the integral in (2.21) and replacing it into (2.19) yields

$$\Pr(\gamma_g + wz \leq \gamma) = \mathbb{E}_z \left(\int_0^\infty \left(1 - \frac{\bar{w}z}{\gamma_g - \bar{w}z} \exp\left(-\frac{\gamma}{\gamma_g}\right) + \frac{\bar{w}z}{\gamma_g - \bar{w}z} \exp\left(\frac{-\gamma}{z\bar{w}}\right) \right) f(z) dz \right). \quad (2.22)$$

Solving the expectation with respect to z in (2.22) is challenging because of the outer expectations \mathbb{E}_z and inner expectation \mathbb{E}_{γ_g} are multiplied, which becomes computationally difficult to solve. Recall that z is defined as $z = \gamma_h + I_R$, which itself is a summation of two random variables with different distributions. Since γ_h and I_R are independent, we get the joint distribution, $f_{\gamma_h, I_R}(x, y) = f_{\gamma_h}(x)f_{I_R}(y)$. The PDF of z is then calculated by inserting the individual PDFs, $f_{\gamma_h}(x)$ and $f_{I_R}(y)$, from (2.10) and (2.11), and integrating according to [GA15, p. 6428, eq. 13], yielding

$$f_z(z) = \frac{1}{\gamma_h} \exp\left(\frac{-z}{\gamma_h}\right) \sum_{i=1}^{v(\mathbf{A})} \sum_{j=1}^{\tau_i(\mathbf{A})} \lambda_{ij}(\mathbf{A}) \left(1 - \frac{\mu_i}{\gamma_h}\right)^{-j} \left(1 - \exp(-a_i z) \sum_{k=0}^{j-1} \frac{a_i^k}{k!} z^k\right), \quad (2.23)$$

where $a_i \triangleq \frac{1}{\mu_i} - \frac{1}{\gamma_h}$.

Then, by inserting the PDF of z from (2.23) into (2.22), we obtain

$$\begin{aligned}
 F_{\gamma_{\text{RS}}}(\gamma) = & 1 - \sum_{i=1}^{v(\mathbf{A})} \sum_{j=1}^{\tau_i(\mathbf{A})} \lambda_{ij}(\mathbf{A}) \left(1 - \frac{\mu_i}{\gamma_{\text{h}}}\right)^{-j} \left(\underbrace{\int_{\gamma}^{\infty} \frac{\bar{w}z}{\gamma_{\text{h}}(\gamma_{\text{g}} - \bar{w}z)} \exp\left(\frac{-\gamma}{z\bar{w}} - \frac{z}{\gamma_{\text{h}}}\right) dz}_{J_1} \right. \\
 & + \underbrace{\frac{1}{\gamma_{\text{h}}} \exp\left(-\frac{\gamma}{\gamma_{\text{g}}}\right) \int_{\gamma}^{\infty} \frac{\bar{w}z}{\gamma_{\text{g}} - \bar{w}z} \exp\left(\frac{-z}{\gamma_{\text{h}}}\right) dz}_{J_2} \\
 & \left. - \underbrace{\sum_{k=0}^{j-1} \frac{a_i^k}{k!} \int_{\gamma}^{\infty} \frac{1}{\gamma_{\text{h}}} \exp\left(-\frac{\gamma}{\bar{w}z} - \frac{z}{\gamma_{\text{h}}}\right) \exp(-a_i z) z^k dz}_{J_3} \right). \quad (2.24)
 \end{aligned}$$

Since there is an additional fraction multiplied with the same entity in the exponential function present in the integral $F_{\gamma_{\text{RS}}}(\gamma)$ in (2.24), therefore obtaining closed-form for is challenging. We start by dividing (2.24) into three integrals, where the first and the second integrals are solved by using the generalized incomplete Gamma functions given in [JZ07]. Details are given below.

2.4.2.1 Closed-Form Expression for J_1

The integral J_1 has a fraction of a same entity multiplied to an exponential function.

We start with the ratio $\frac{\bar{w}z}{\gamma_{\text{g}} - \bar{w}z}$ in (2.24), which can be simplified as

$$\frac{\bar{w}z}{\gamma_{\text{g}} - \bar{w}z} = - \left(\frac{\gamma_{\text{g}} - \gamma_{\text{g}} - \bar{w}z}{\gamma_{\text{g}} - \bar{w}z} \right) = -1 + \left(1 - \frac{\bar{w}z}{\gamma_{\text{g}}} \right)^{-1}, \quad (2.25)$$

The term $\left(1 - \frac{\bar{w}z}{\gamma_{\text{g}}} \right)^{-1}$ can be approximated to $1 + \frac{\bar{w}z}{\gamma_{\text{g}}}$ for $\frac{\bar{w}z}{\gamma_{\text{g}}} \rightarrow 0$. Thus, we have

$$\frac{\bar{w}z}{\gamma_{\text{g}} - \bar{w}z} \simeq \frac{\bar{w}z}{\gamma_{\text{g}}}. \quad (2.26)$$

Now, we recall the formulation for generalized incomplete Gamma function given by [CZ94, p. 372],

$$\Gamma(\hat{\alpha}, x; b) = \int_{\hat{\alpha}}^{\infty} t^{\hat{\alpha}-1} \exp(-t - bt^{-1}) dt, \quad (2.27)$$

which will later be used for obtaining a closed-form expression for J_1 .

Lemma 1. *Using the recurrence relation for the incomplete generalized Gamma function in [CTV96, p. 101], the following equality can be obtained*

$$\Gamma(\hat{\alpha} + 1, x; b) = \hat{\alpha}\Gamma(\hat{\alpha}, x; b) + b\Gamma(\hat{\alpha} - 1, x; b) + x^{\hat{\alpha}} \exp(-x - bx^{-1}), \quad \hat{\alpha} \geq 0. \quad (2.28)$$

Proof. The proof is provided in Appendix A. □

The result of Lemma 1, when $\hat{\alpha} = 1$ referred to A.1, along with the estimation result given in (2.26) will give a solution for the first integral J_1 , according to

$$J_1 = \frac{\bar{\gamma}_g}{\gamma_g \gamma_h} \left(\Gamma \left(0, \frac{\gamma}{\gamma_h}; \frac{\gamma}{\gamma_h \gamma_g w} \right) - \gamma \exp(-\gamma - b\gamma^{-1}) + \Gamma \left(1, \frac{\gamma}{\gamma_h}; \frac{\gamma}{\gamma_h \gamma_g w} \right) \right). \quad (2.29)$$

2.4.2.2 Closed-Form Expression for J_2

To obtain a closed-form expression for J_2 shown in (2.24), we use the approximation result in (2.26), yielding

$$J_2 = \frac{\bar{w}}{\gamma_h \gamma_g} \exp\left(-\frac{\gamma}{\gamma_g}\right) \int_{\gamma}^{\infty} z \exp\left(\frac{-z}{\gamma_h}\right) dz,$$

which allows us to obtain a closed-form expression for J_2 as

$$J_2 = -\frac{\bar{w}}{\gamma_h \gamma_g} \left(1 - \frac{\gamma}{\gamma_h} \right) \exp\left(-\gamma \left(\frac{1}{\gamma_g} + \frac{1}{\gamma_h} \right)\right). \quad (2.30)$$

2.4.2.3 Closed-Form Expression for J_3

To solve this integral, we use (2.27) to get,

$$J_3 = \frac{1}{\gamma_h} \exp(a_i) \sum_{k=0}^{j-1} \frac{1}{k!} (-a_i)^k \sum_{m=0}^k \binom{k}{m} \frac{b_i^{-1}}{(-b_i)^m} \Gamma\left(m+1, b_i \gamma; \frac{b_i \gamma}{w}\right), \quad (2.31)$$

where $b_i = \frac{1}{\gamma_h} + \frac{a_i}{1+\gamma}$ and a_i is defined right after (2.23).

Finally, we obtain the closed-form solution for the CDF of $F_{\gamma_{\text{RS}}}(\gamma)$, by inserting the solution from (2.29), (2.30) and (2.31) into (2.24), yielding

$$\begin{aligned} F_{\gamma_{\text{RS}}}(\gamma) = & 1 - \sum_{i=1}^{v(\mathbf{A})} \sum_{j=1}^{\tau_i(\mathbf{A})} \lambda_{ij}(\mathbf{A}) \left(1 - \frac{\mu_i}{\gamma_h}\right)^{-j} \frac{\bar{w}}{\gamma_g} \left(-\gamma \exp(-\gamma - b\gamma^{-1}) + \Gamma\left(1, \frac{\gamma}{\gamma_h}; \frac{\gamma}{\gamma_h \gamma_g w}\right)\right) \\ & + \Gamma\left(0, \frac{\gamma}{\gamma_h}; \frac{\gamma}{\gamma_h \gamma_g w}\right) - \frac{\bar{w}}{\gamma_g \gamma_h} \left(1 - \frac{\gamma}{\gamma_h}\right) \exp\left(-\gamma \left(\frac{1}{\gamma_h} + \frac{1}{\gamma_g}\right)\right) \\ & - \frac{1}{\gamma_h} \exp(a_i) \sum_{k=0}^{j-1} \frac{1}{k!} (-a_i)^k \sum_{m=0}^k \binom{k}{m} \frac{b_i^{-1}}{(-b_i)^m} \Gamma\left(m+1, b_i \gamma; \frac{b_i \gamma}{w}\right). \end{aligned} \quad (2.32)$$

2.4.3 CDF of the End-to-End SNR

The end-to-end SNR is defined by the probability that the instantaneous output SNR falls below a certain threshold which is already defined as γ . Mathematically, it is written as

$$\Pr(\min(\gamma_{\text{TR}}, \gamma_{\text{RS}}) \leq \gamma) = \Pr((\gamma_g + wz)\mathbb{1} \leq \gamma), \quad (2.33)$$

where $\mathbb{1}$ symbolizes an indicator of RV, with $\mathbb{1} = 1$ for $\gamma_{\text{TR}} > \gamma$ and 0 otherwise. This RV also indicates that the power at the relay is not only the power coming from its fixed battery B_2 , but also the random replenished energy from the interference. Let us introduce the RV $\hat{z} = (\gamma_h + I_R)\mathbb{1}$. Then, the CDF of end-to-end SNR is

calculated by inserting the value of $f_z(\hat{z})$ given below into (2.22), yielding

$$f_z(\hat{z}) = \mathbb{1} \frac{1}{\gamma_h} \exp\left(\frac{-\hat{z}}{\gamma_h}\right) \sum_{i=1}^{v(\mathbf{A})} \sum_{j=1}^{\tau_i(\mathbf{A})} \lambda_{ij}(\mathbf{A}) \left(1 - \frac{\mu_i}{\gamma_h}\right)^{-j} \times \left(1 - \exp\left(-a_i \frac{\hat{z} - \gamma}{1 + \gamma}\right) \sum_{k=0}^{j-1} \frac{a_i^k}{k!} \left(\frac{\hat{z} - \gamma}{1 + \gamma}\right)^k\right). \quad (2.34)$$

Thus, the PDF of the end-to-end SNR, $\gamma_{\text{end-to-end}}$, is obtained as

$$F_{\gamma_{\text{end-to-end}}}(\gamma) = 1 - \sum_{i=1}^{v(\mathbf{A})} \sum_{j=1}^{\tau_i(\mathbf{A})} \lambda_{ij}(\mathbf{A}) \left(1 - \frac{\mu_i}{\gamma_h}\right)^{-j} \left(\underbrace{\int_{\gamma}^{\infty} \frac{1}{\gamma_h} \frac{\bar{w}\hat{z}}{\gamma_g - \bar{w}\hat{z}} \exp\left(\frac{-\gamma}{\hat{z}\bar{w}} - \frac{\hat{z}}{\gamma_h}\right) d\hat{z}}_{K_1} + \underbrace{\frac{1}{\gamma_h} \exp\left(-\frac{\gamma}{\gamma_g}\right) \int_{\gamma}^{\infty} \frac{\bar{w}\hat{z}}{\gamma_g - \bar{w}\hat{z}} \exp\left(\frac{-\hat{z}}{\gamma_h}\right) d\hat{z}}_{K_2} - \underbrace{\sum_{k=0}^{j-1} \frac{a_i^k}{k!} \int_{\gamma}^{\infty} \frac{1}{\gamma_h} \exp\left(-\frac{\gamma}{\bar{w}\hat{z}} - \frac{\hat{z}}{\gamma_h}\right) \exp\left(-a_i \frac{\hat{z} - \gamma}{1 + \gamma}\right) \left(\frac{\hat{z} - \gamma}{1 + \gamma}\right)^k d\hat{z}}_{K_3} \right). \quad (2.35)$$

Obtaining a closed-form solution for (2.35) is done using a similar method as in subsection 2.4.2. It is noted that the solutions to the first and the second integrals are already known from (2.29) and (2.30). In the third integral, we use the Taylor series expansion for $(\hat{z} - \gamma)^k$ [Bea05] and we again use the identity of generalized incomplete Gamma function given in [CZ94, p. 372]. Details are given below.

2.4.3.1 Closed-Form Expression for K_3

The third integral K_3 is solved by using direct substitution of a Taylor series expansion of $(\hat{z} - \gamma)^k$ with respect to \hat{z} [GA15, p. 6430] and the identity of the

generalized incomplete [JZ07, Eq. (3.351.1), Eq.(3.334)]. This gives

$$K_3 = \frac{1}{\gamma_h} \exp\left(\frac{a_i \gamma}{1 + \gamma}\right) \sum_{k=0}^{j-1} \frac{1}{k!} \left(\frac{-a_i \gamma}{1 + \gamma}\right)^k \sum_{m=0}^k \binom{k}{m} \frac{b_i^{-1}}{(-b_i \gamma)^m} \Gamma\left(m + 1, b_i \gamma; \frac{b_i \gamma}{\gamma_g w}\right). \quad (2.36)$$

We now obtain the closed-form solution for the CDF of the end-to-end SNR by inserting the solution from (2.29), (2.30) and (2.36), into (2.24), yielding

$$\begin{aligned} F_{\gamma_{\text{end-to-end}}}(\gamma) = & 1 - \sum_{i=1}^{v(\mathbf{A})} \sum_{j=1}^{\tau_i(\mathbf{A})} \lambda_{ij}(\mathbf{A}) \left(1 - \frac{\mu_i}{\gamma_h}\right)^{-j} \frac{\bar{w}}{\gamma_g} (-\gamma \exp(-\gamma - b\gamma^{-1}) \\ & + \Gamma\left(1, \frac{\gamma}{\gamma_h}; \frac{\gamma}{\gamma_h \gamma_g w}\right) + \Gamma\left(0, \frac{\gamma}{\gamma_h}; \frac{\gamma}{\gamma_h \gamma_g w}\right)) \\ & - \frac{\bar{w}}{\gamma_g \gamma_h} \left(1 - \frac{\gamma}{\gamma_h}\right) \exp\left(-\gamma \left(\frac{1}{\gamma_h} + \frac{1}{\gamma_g}\right)\right) - \frac{1}{\gamma_h} \exp\left(\frac{a_i \gamma}{1 + \gamma}\right) \\ & \times \sum_{k=0}^{j-1} \frac{1}{k!} \left(\frac{-a_i \gamma}{1 + \gamma}\right)^k \sum_{m=0}^k \binom{k}{m} \frac{b_i^{-1}}{(-b_i \gamma)^m} \Gamma\left(m + 1, b_i \gamma; \frac{b_i \gamma}{\gamma_g w}\right). \end{aligned} \quad (2.37)$$

The closed-form expressions derived for end-to-end SNR and the SNR at individual links provide an insight to identify how RF interference and solar energy have improved the average end-to-end rate and the rate of individual hops significantly. The transmission power at the relay P_R is different from conventional systems as it not only depends on the energy from interference but also from the information signal. Therefore the distribution of received SNR at the sink is determined by the distributions of relay-to-sink channel power gain as well as the distribution of the transmitter-to-relay channel power represented by z . Further detail is provided in the numerical results section.

2.4.4 Ergodic Capacity

In this subsection, we analytically derive the ergodic capacity of the relaying system which is calculated by taking the average of the minimum between the rate at the first hop and that at the second hop [CG07], formulated in b/s/Hz as

$$\begin{aligned}
 C &= \mathbb{E} \left(\min \left(\frac{(1-\tau)}{2} \log_2(1 + \gamma_{\text{TR}}), \frac{(1-\tau)}{2} \log_2(1 + \gamma_{\text{RS}}) \right) \right) \\
 &= \mathbb{E} \left(\frac{1-\tau}{2} \log_2(1 + \min(\gamma_{\text{TR}}, \gamma_{\text{RS}})) \right) \\
 &= \frac{1-\tau}{2} \int_0^\infty \log_2(1 + \gamma_{\text{end-to-end}}) f_{\gamma_{\text{end-to-end}}}(\gamma_{\text{end-to-end}}) d\gamma_{\text{end-to-end}}, \quad (2.38)
 \end{aligned}$$

where $f_{\gamma_{\text{end-to-end}}(\cdot)}$ is the PDF of the RV $\gamma_{\text{end-to-end}} = \min(\gamma_{\text{TR}}, \gamma_{\text{RS}})$. We now solve (2.38) by using integration by parts as follows:

$$\begin{aligned}
 C &= \frac{1-\tau}{2} \left(\log_2(1 + \gamma_{\text{end-to-end}}) \left(F_{\gamma_{\text{end-to-end}}}(\gamma_{\text{end-to-end}}) - 1 \right) \right) \Big|_0^\infty \\
 &\quad - \frac{1-\tau}{2 \ln 2} \int_0^\infty \frac{1}{1 + \gamma_{\text{end-to-end}}} \left(F_{\gamma_{\text{end-to-end}}}(\gamma_{\text{end-to-end}}) - 1 \right) d\gamma_{\text{end-to-end}} \\
 &= \frac{1-\tau}{2 \ln 2} \int_0^\infty \frac{1}{1 + \gamma_{\text{end-to-end}}} \left(1 - F_{\gamma_{\text{end-to-end}}}(\gamma_{\text{end-to-end}}) \right) d\gamma_{\text{end-to-end}}.
 \end{aligned}$$

Here, $F_{\gamma_{\text{end-to-end}}}(\gamma_{\text{end-to-end}})$ denotes the CDF of the RV $\gamma_{\text{end-to-end}}$ and is calculated by using (2.37).

2.5 Numerical Results and Discussion

In this section, we numerically evaluate the effect of energy harvesting, power from the fixed batteries and energy conversion coefficient on the ergodic capacity and the end-to-end SNR of the studied relaying system. In all the figures, we assume that the power of the fixed battery at the transmitter node T is equal to the power

of the fixed battery at the relay R , hence, $P = P_1 = P_2$.¹⁰ The variance of the Rayleigh fading with complex channel fading gains, i.e., Ω_h and Ω_g are considered in terms of total power to noise power at each link, in dB, which cater attenuation due to path loss for each channel fading gain, e.g., h and g . The path loss for transmitter to relay hop, P_{LR} is different than the path-loss for relay to sink, P_{RS} , therefore the system model works same even when considered for different distances. The number of interference signals at the relay is set to $N = 5$ with normalized $\mu = 0.3$, and the TS parameter is set to $\tau = 0.4$, unless otherwise stated. Values for Q_t and η are taken from studies shown in [MYG⁺14]. For numerical results, we use mathematical theorems and equations for calculating generalized incomplete gamma function which are then calculated through MATLAB is explained in Appendix A.2. Table 1 is added for showing the boundaries of the results.

Table 2.1: Simulation parameters

Parameters	Default value	Parameters	Default value
N	5	η	0.3 else stated
$\mu_i, i = 1, \dots, 5$	0.3	γ	0.2 dB
τ	0.4 else stated	$\sigma_S^2 B$	1 else stated
Ω_h	1 else stated	P	1 dB else stated
K_R	1 else stated	$\sigma_R^2 B$	1 else stated
K_S	1 else stated	Ω_g	1 else stated

In Fig. 2.4, we start by plotting the CDF of the first-hop SINR $F_{\gamma_{TR}}(\gamma)$, the CDF of the second-hop SNR $F_{\gamma_{RS}}(\gamma)$, and the CDF of the end-to-end SNR $F_{\gamma_{\text{end-to-end}}}$ versus the power consumed from the fixed batteries P , at $\gamma = 0.2$ with $Q_t = 1$ dB. The figure includes both analytical and Monte-Carlo simulation results to verify the correctness of the closed-form derivations. From the graphs, we observe that the CDF of the received SNR at the second hop is greater than the one of the SINR at the first hop, for most of the time. It is noted that the CDF of the end-to-end SNR is similar to the CDF of the second hop SNR $F_{\gamma_{RS}}(\gamma)$. This is

¹⁰Note that the power is normalized and considered in dB

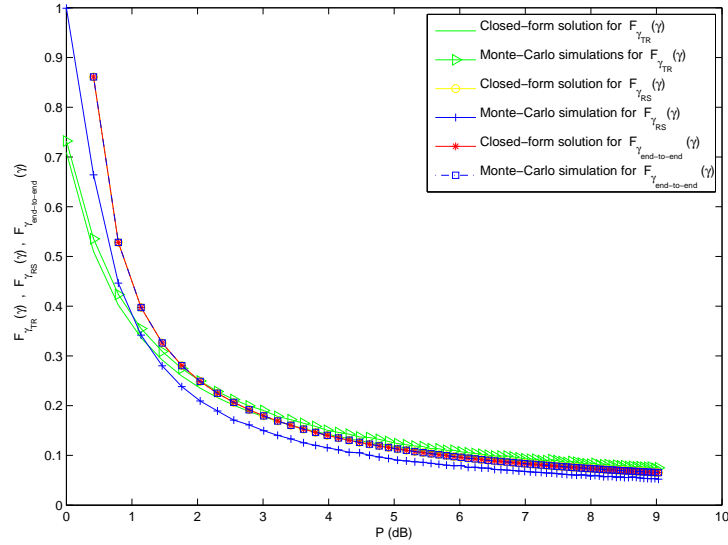


Figure 2.4: The CDF of γ_{TR} (first hop), CDF of γ_{RS} (second hop), and the CDF of the end-to-end SNR $\gamma_{\text{end-to-end}}$ versus the power consumed from the fixed batteries P , when $\gamma = 0.2$, $\eta = 0.3$ and $Q_t = 1\text{dB}$.

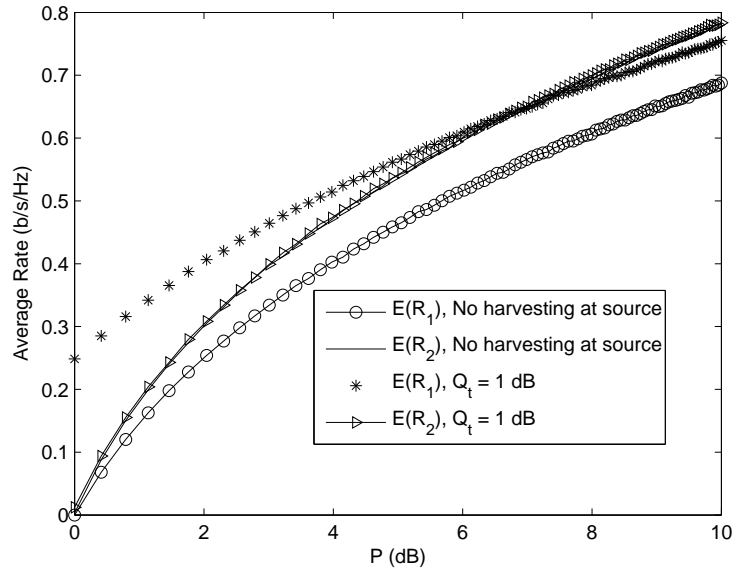


Figure 2.5: Average rates at the first and second hops ($\mathbb{E}(R_1), \mathbb{E}(R_2)$) versus P with $\eta = 0.3$.

due to the fact that, for the settings used in this figure, the first hop SINR is the minimum of the SINR at the first and the the SNR at the second hop for most of the time. Further, the plots confirm that the results obtained from the closed-form expressions match to the ones obtained from the Monte-Carlo simulations, hence

indicating that the obtained closed-form expressions yield accurate measures of the CDF of the individual links' SNRs and the end-to-end SNR.

Fig. 2.5 shows the plots for $\mathbb{E}(R_1)$ (the average rate at the first hop) and $\mathbb{E}(R_2)$ (the average rate at the second hop) versus the power level of the fixed batteries P , at $\eta = 0.3$ and for various values of Q_t . From the plots, we note that when $P = 0\text{dB}$ and no harvesting is available at the source, the average rate of the second hop is slightly higher than the one at the first hop. The relay harvests energy both from source signal and RF interference and, hence, under the above-mentioned conditions, the second hop achieves a slightly higher rate than the first hop. When $Q_t = 1\text{dB}$, and at the same time the energy conversion coefficient at the relay remains small ($\eta = 0.3$), the average rate at the first hop $\mathbb{E}(R_1)$ dominates $\mathbb{E}(R_2)$. This happens because the solar energy at the transmitter is strong compared to the RF energy level at the relay node. We also observe that the difference between the two rates decreases at higher power values P of the fixed batteries, indicating that energy harvesting is less beneficial in devices with higher powers.

Fig. 2.6 includes the plots for the CDF of the SINR at the first-hop γ_{TR} and the CDF of the SNR at the second hop γ_{RS} , versus Q_t , at $\eta = 0.3$, $P = 1\text{dB}$ and $\gamma = 0.2$. From the graph, we notice that not only the CDF of the first hop SINR ($F_{\gamma_{\text{TR}}}(\gamma)$) decreases with the increase in the solar energy, but also the CDF of the second hop SNR ($F_{\gamma_{\text{RS}}}(\gamma)$) shows similar trend.

Fig. 2.7 illustrates the plots for the average rates $\mathbb{E}(R_1)$, $\mathbb{E}(R_2)$ and C versus the time-switching parameter τ with $\eta = 0.3$, $\mu = 0.3$, $P = 1\text{dB}$, and various values of Q_t . It is noted that when $Q_t = 0.5\text{dB}$, $\mathbb{E}(R_2)$ shows bell curve while $\mathbb{E}(R_1)$ is monotonically decreasing; reason being, although with increasing τ , more energy will be available at the relay node through harvesting, but at the same time, less time is available for information transmission. This conflicting effect, make the shape of $\mathbb{E}(R_2)$ with respect to τ being bell-shape. When solar energy increases,

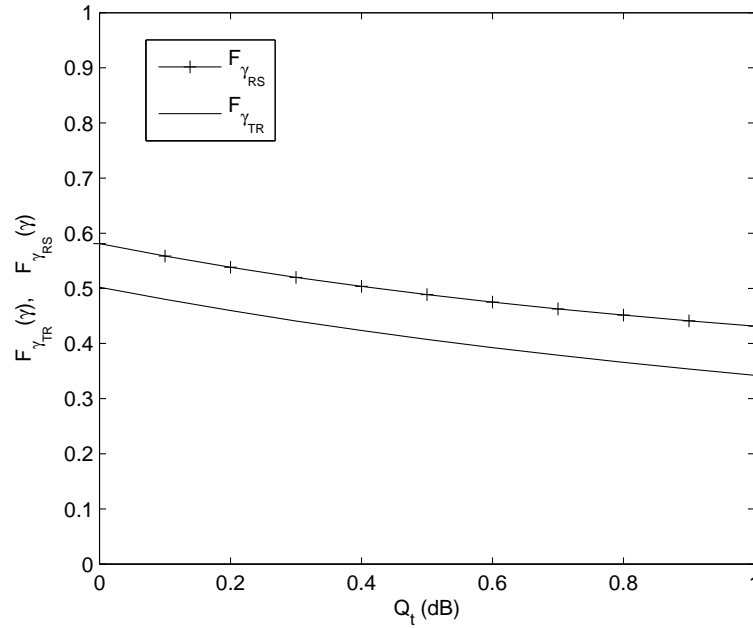


Figure 2.6: $F_{\gamma_{TR}}(\gamma)$ and $F_{\gamma_{RS}}(\gamma)$ versus Q_t at $\gamma = 0.2$ with $\eta = 0.3$ and $P = 1$ dB.

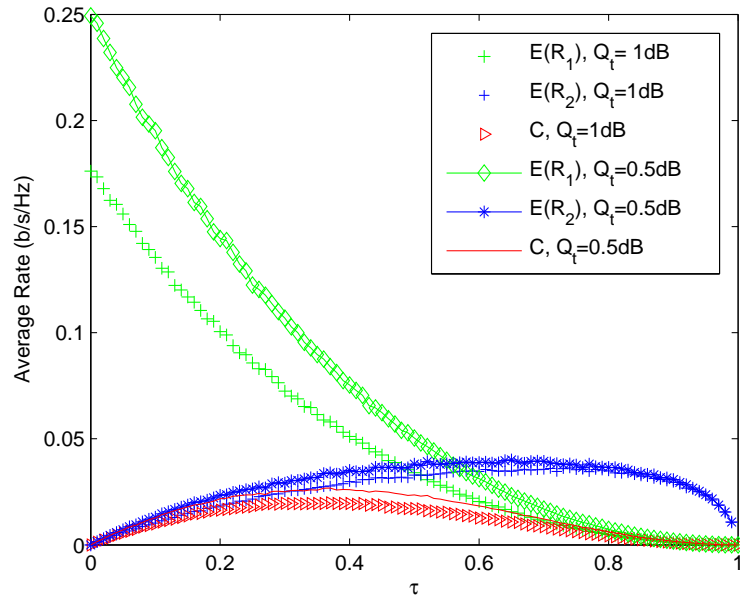


Figure 2.7: Average rates at the first and second hops, $(\mathbb{E}(R_1), \mathbb{E}(R_2))$, versus τ , with $\eta = 0.3$ and various values of Q_t .

e.g., $Q_t = 1$ dB, the two curves coincide each other at smaller values of $\tau = 0.5$. This happens because with higher Q_t , $\mathbb{E}(R_1)$ will be bigger. Hence, the amount of time which will be used for harvesting, instead of information transmission reduces

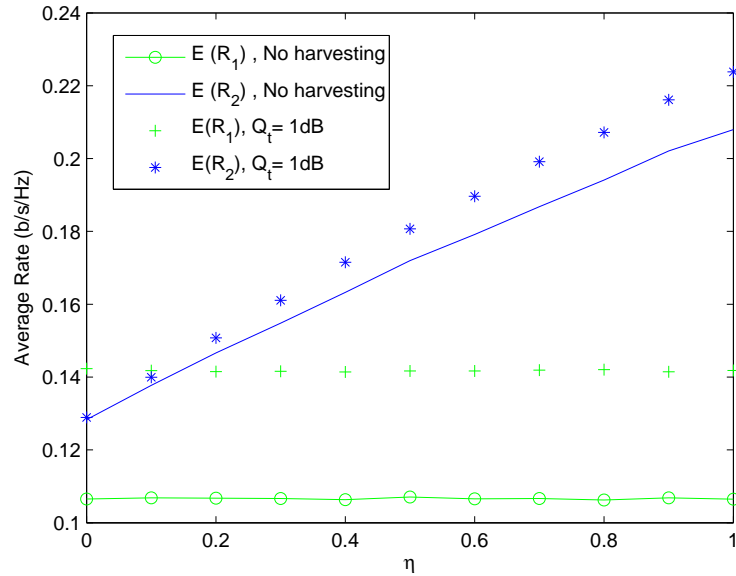


Figure 2.8: Average rates (first-hop and second-hop) versus the energy conversion coefficient η , for $P = 1\text{dB}$ and various values of Q_t .

$\mathbb{E}(R_1)$ quickly and hence, the two curves coincide at a smaller value of τ , when compared to the case with $Q_t = 0.5\text{dB}$. Generally, the trend shows that the higher the solar energy is, less time should be allocated for harvesting in the second hop.

In Fig. 2.8, we present the plots for the average rate at the first-hop and the average rate at the second-hop versus energy conversion coefficient η at $P = 1\text{dB}$ with various values of Q_t . At small values of η , i.e., $\eta < 0.1$, with $Q_t = 1\text{dB}$, the average rate at the first-hop is slightly higher than that at the second-hop, due to the small energy conversion coefficient at the relay harvesting battery. As η increases, i.e., $\eta > 0.1$, the average rate at the second hop dominates the average rate at the first hop.

Fig. 2.9 shows the plots for the average rates versus Q_t with $\eta = 0.3$ and $P = 1\text{dB}$. The figure shows three different rate plots defined by the average rate at the first hop, the average rate at the second hop and the average end-to-end ergodic rate C . We notice that $\mathbb{E}(R_1)$ increases rapidly with Q_t , while the average rate at the second hop increases slowly. When $Q_t = 0\text{dB}$, we observe that the

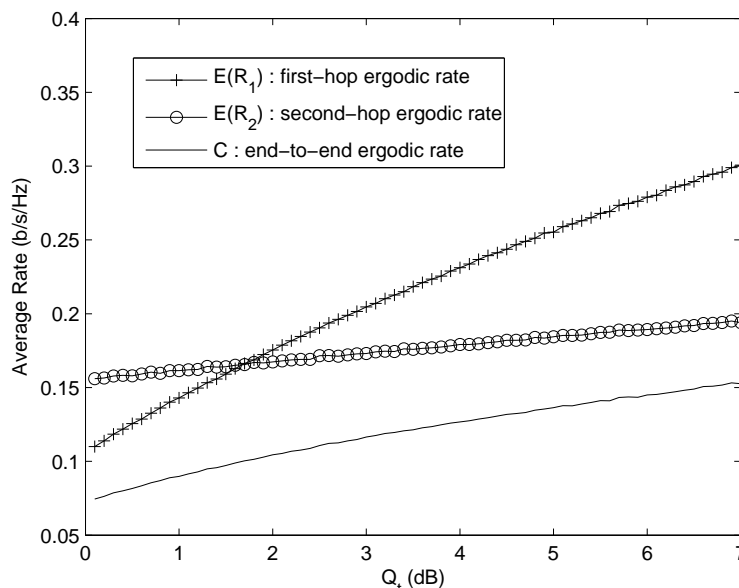


Figure 2.9: Average rates (first hop, second hop and end-to-end) versus Q_t at $\eta = 0.3$ with $P = 1$ dB.

$\mathbb{E}(R_2)$ is higher than $\mathbb{E}(R_1)$ due to the presence of interference energy from RF at the relay node that can be harvested. As Q_t increases, e.g., $Q_t > 1.5$ dB, the average rate at the first hop becomes larger than that at the second hop. This happens due to the fact that in $\mathbb{E}(R_1)$ the transmitter node has a direct access to solar energy, whereas in case of $\mathbb{E}(R_2)$, the harvested power gets affected by the Rayleigh fading channel h . Furthermore, the total end-to-end capacity C increases with Q_t , showing that the higher the solar energy is, the better the end-to-end ergodic rate is. The numerical results validate the mathematical expression for the ergodic capacity in (2.38).

Fig. 2.10 shows the plots for the average SNR/SINR at the second-hop and the first-hop, versus Q_t , at $\eta = 0.3$ and $P = 1$ dB. As observed, both values increase when solar energy increases. Meanwhile, at $Q_t = 0$ dB, the average SNR at the second hop is higher than the average SINR at the first hop. This is due to the fact that while Q_t is small, i.e., $Q_t = 0$ dB, the relay still has access to harvesting power from the external RF interference sources. At $Q_t = 1.5$ dB, the two plots

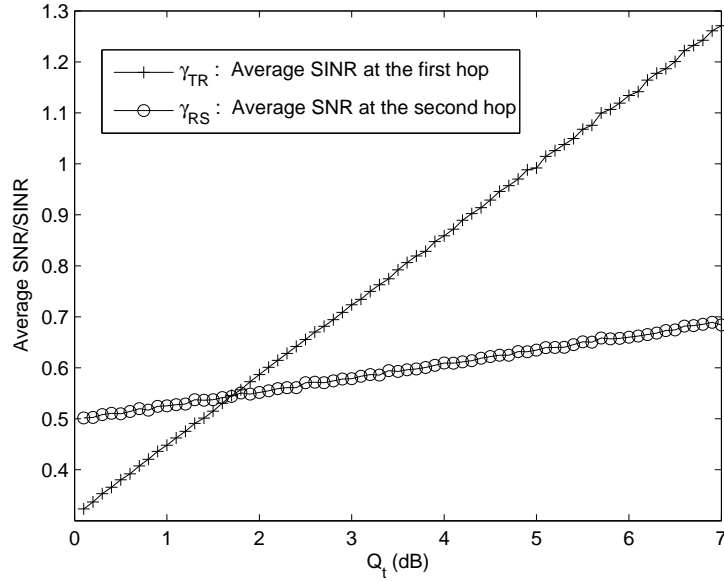


Figure 2.10: Average SNR/SINR versus Q_t at $\eta = 0.3$ with $P = 1$ dB.

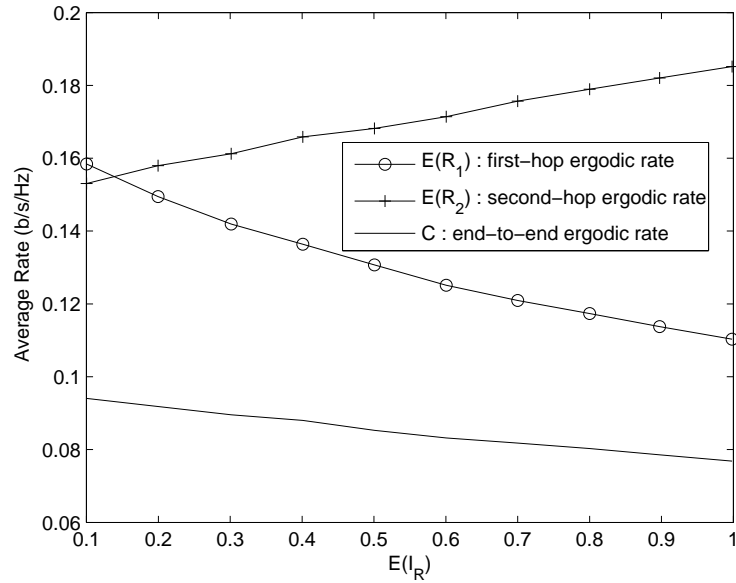


Figure 2.11: Average rates (first hop, second hop and end-to-end) versus average interference at the relay $\mathbb{E}(I_R)$, with $\tau = 0.4$, $Q_t = 1$ dB and varying μ .

coincide each other. Overall, the first-hop SINR increases more rapidly with Q_t compared to the second hop SNR.

Finally, Fig. 2.11 demonstrates the plots for the average rate at the first hop, the average rate at the second hop, and the average end-to-end ergodic rate C ,

versus the average interference power at the relay $\mathbb{E}(I_R)$, with $\eta = 0.3$, $P = 1\text{dB}$ and $Q_t = 1\text{dB}$. When $Q_t = 1\text{dB}$ and the average interference power is small, i.e., $\mathbb{E}(I_R) < 0.2$, the first-hop rate is slightly higher than the one at the second hop. The average interference adversely affects the rate of the first hop, therefore $\mathbb{E}(R_1)$ is always decreasing with $\mathbb{E}(I_R)$; whereas it improves the rate of the second hop through the energy harvesting. Since the source harvests solar energy, the rate of the first hop with small values of interference is better than the rate of the second hop. With an increase in the average interference at the relay, $\mathbb{E}(R_2)$ gives higher values due to the fact that the interference is added as an additional source of energy harvesting as shown in (2.9). Furthermore, the average end-to-end capacity C shows a monotonic decrease with $\mathbb{E}(I_R)$, revealing that the more the average interference is, the less the end-to-end ergodic rate will be.

2.6 Chapter Summary

In this chapter, we investigated the system performance of a dual-hop decode-and-forward relaying system, in which the transmitter and the relay are equipped with fixed, as well as, energy-harvesting batteries. Harvesting at the transmitter is done through solar energy source, whereas interference from the RF is used as the energy harvesting source at the relay. Time switching is used for energy harvesting and information transmission at the relay. We showed that energy harvesting at the transmitter and at the relay node can improve the end-to-end SNR. Novel closed-form expressions were derived for the CDF of the SNR at each hop, and also for the end-to-end SNR. The analytical expression for the end-to-end ergodic capacity was also obtained. Numerical results were provided and show the correctness of the estimation used in obtaining the closed-form expressions in this chapter. The effect of energy conversion efficiency and the fixed-battery

powers on the CDF of the SNR for the individual links were also investigated. The results further demonstrated that with the addition of energy harvesting at the source node and the relay, significant improvement in the system throughput can be achieved. Future work includes consideration of input power constraints at the fixed batteries and catering inter-cell interference and hardware impairments.

2.7 Experts Recommendation

For experts recommendation, this chapter provide details for a system in which transmitter and destination communicate through relay. Energy harvesting batteries are used at transmitter and relay nodes. Impact of energy harvesting is considered and discussed to provide a solution for energy constrained devices. This chapter paves path for vendors and give guidelines to experimenters to use energy harvesting in order to increase end to end rate and improve system performance. As mentioned in the Table 1, the boundaries of this work is also discussed. The closed-form expressions gives simplicity and provides solutions which are easy to be implemented in real life system designs in communications.

Chapter 3

Performance Analysis of Energy

Harvesting Systems Using

Harvest-Use Approach: Energy and

Spectral Efficiency

This chapter focuses on the performance analysis and optimal transmission power allocation techniques for point-to-point communication powered through a fixed-power battery as well as a harvest-use battery. For the considered energy harvesting, a switching scheme is used such that in each time frame, the source node either harvests energy or transmits information to the destination node. Given the switching within a communication time frame, energy harvesting may not necessarily be beneficial in terms of improving the maximum achievable spectral efficiency or energy efficiency of the system. Here, we investigate and provide the conditions under which the harvesting can improve the system performance in two different cases. In the first, the power is optimally adapted to the variations of the channel and in the second case the transmission power is fixed. We also prove that the

energy efficiency oriented optimal power level monotonically decreases with the harvesting. Furthermore, we provide closed-form expressions for the maximum achievable spectral or energy efficiency of the system and also for the condition under which the harvesting is beneficial. These closed-form expressions are then validated by Monte-Carlo simulations. Finally, the impact of important parameters, namely, the time switching parameter, the circuit powers and the harvested energy, on the system performance and on the condition for harvesting beneficialness is investigated through numerical results.

3.1 Introduction

Green wireless communication technologies have attracted significant attention in the last few years as to provide possible solutions to the energy limitation problems in information and communication technologies (ICT) [UBPEG02]. In fact, due to the increase in the number of mobile users and the demand for higher data rates, base stations (BS) are required to increase their transmission power, which in turn, results in higher greenhouse gases, pollution, and also higher costs [HBB11]. Battery technologies, on the other hand, have not progressed with the same pace, which has resulted in deepening the gap between the increasing demand for power and the battery capabilities for the storage [FVDM⁺12]. Wireless communication faces many challenges which includes spectrum challenge, energy saving and energy challenge in developing countries (DCs) [FVDM⁺12], and have incited research in investigating new ways to get energy from re-usable sources [MHL10].

Recently, the world has seen dramatic growth in data rate demand and the wireless portable devices such as mobile phones and laptops which require the energy to deliver such data demands has become an important concern for telecommunication and information communities [KBS16]. Due to this high speed multimedia rich data,

the network capacity of base stations has increased which leads to global CO₂ emission that are threat to global warming [RT14]. Also, the limited battery capacity is another concern which still remains unsolved in wireless network designs [TD15]. In addition to that, the ICT report shows the the increase in CO₂ emissions from 0.53 billion tonnes (Gt) in 2002 to 1.43Gt in 2020 [W⁺08]. Reducing energy costs and carbon emissions has pushed academics and the related industries to explore new paradigm of research Green communication [Wu12]. Green communication has emerged to provide an environment friendly solution to the escalating expansion of wireless networks [KBS16]. Above mentioned issues add to importance of energy saving in wireless communication.

Challenges in developing countries (DCs) are not only the poor access to resources but also taking into account the social and ecological consequences of specific energy source [KLG11]. Along with other issues, spectrum limitation is seeking attention. Due to hundreds of wireless communicating devices in real world all the time. Keeping these technical aspects in mind, energy harvesting provides a solution to all of them.

3.1.1 Motivation and Related Works

Green communications provide ecological friendly approaches that aim at improving the energy efficiency and the spectral efficiency of the communication system [BCR⁺12]. Energy efficiency, which is defined as the data transferred per unit energy consumed, in the unit of b/J/Hz, has recently received a great deal of focus, see e.g. [MHL10] and [SMN15]. The problems of improving energy efficiency and maximizing throughput have been widely investigated in literature. However, it was demonstrated that increasing energy efficiency can result in decreasing data rates in many cases [PD10] and [XZ14]. Recently, energy harvesting has emerged

as a new technology that has a great potential to improve energy efficiency, while maintaining spectral efficiency [ZZH12].

In the past few years, there have been significant research work on EH communications with the main focus on the development of EH protocols and models for improving the rate of the system [RM10]. EH is used to improve the performance of energy efficient wireless sensor networks as discussed in [MSK⁺16]. Optimization of the rate of a multiple-input single-output (MISO) system with EH capability at the transmitter and receiver is provided in [GGG15]. Also, water-filling algorithm for finite battery capacity was proposed for improving the point-to-point communication with energy allocation at finite time slots in [HZ12]. The optimal transmission strategy for discrete as well as continuous energy arrivals for point-to-point systems with known profile of the harvested energy is discussed in [YU12] and [BG14]. Despite the major effect that EH technology can have on the life and the performance of battery-limited communication devices, the majority of the research works in the literature is focused on devices with only harvesting sources at the transmitter and no fixed battery [OTY⁺11]. Actually, it is inevitable that some sort of a limited fixed battery is implemented within the communication system nodes [LMD⁺16]. Hence, a detailed study is required to see how and whether EH can improve the performance of the communication system with fixed, but very limited power battery. Since in TS, transmission time is divided in between data transmission and harvesting energy, the harvesting may not be necessarily beneficial, and a thorough investigation is required on this is yet to be carried out study.

3.1.2 Contributions

In this chapter, we consider a point-to-point communication system equipped with an EH battery source in addition to its fixed battery, operating under Rayleigh flat fading. The HU technique is used with the TS approach.¹ For the system considered here, we investigate and discuss the impact of EH on the system performance. As transmission time is divided through TS, EH may not necessarily be beneficial for the system in terms of increasing energy efficiency (EE) or spectral efficiency (SE). Hence, we investigate the conditions under which EH can improve system performance given by two different cases: 1) when the transmit power is optimally adapted to the variations of the channel, and 2) when the transmission power is fixed. In order to find the EH beneficialness condition² in the latter case, we first obtain the optimal transmission power allocation strategies that maximize EE or SE, with EH used at the transmitter of the system. The maximum achievable energy efficiency is obtained by using fractional programming to get EE-optimal power level \bar{P}_u . We prove that \bar{P}_u monotonically decreases with EH power level. Furthermore, the closed-form expressions for the maximum achievable EE and SE, and also EH beneficialness conditions, are obtained in various scenarios. Validation of the numerical results is carried out by using Monte-Carlo simulations. The effect of different parameters, such as EH power, TS ratio and the circuit powers, are discussed and analyzed.

To summarize, the main contributions of this chapter are enlisted below:

- The advantage of having solar EH at the transmitter along with the fixed, but limited, battery, on the performance of the point-to-point system is investigated. To the best of the author's knowledge, this work is first to

¹As storing energy for future use would also be beneficial, HSU is being considered in an ongoing work project.

²Hereafter, by EH beneficialness condition, we mean the condition at which the performance of the system is improved through EH.

address this. Section 3.2 describes the system model.

- The conditions under which EH can improve the system performance in terms of maximum achievable EE or SE under two different cases, namely, 1) when the transmit power is optimally adapted to the variations of the fading channel and 2) when transmission power is fixed, are derived and discussed. This has been described in Section 3.3, which starts with optimum power allocation, derivation of closed-form expression for EE and SE maximization.
- The optimal TS parameter τ to maximize EE and SE is also calculated for EH beneficialness condition.
- The maximum achievable EE is obtained by using fractional programming to get the optimal power level \bar{P}_u . We prove that \bar{P}_u monotonically decreases with EH power level.
- Closed-form expressions for the maximum achievable SE, the EE and the EH beneficialness condition, are obtained. Monte-Carlo simulations are carried out to validate these closed-form expressions. In Section 3.4, we investigate the performance improvement analysis of the system using EH with optimal and fixed transmission power. Also, closed-form expressions are derived for maximum achievable EE, SE and the EH beneficialness condition are discussed in Section 3.4.
- Finally, the impact of power from the fixed battery, TS parameter, the circuit powers and the solar harvesting energy level on the system performance and on the EH beneficialness condition, is investigated through numerical results. Numerical results are evaluated for the optimal and fixed power allocation to show the effect of EH on improving system EE and SE are given in Section 3.5, followed by the chapter summary in Section 3.6.

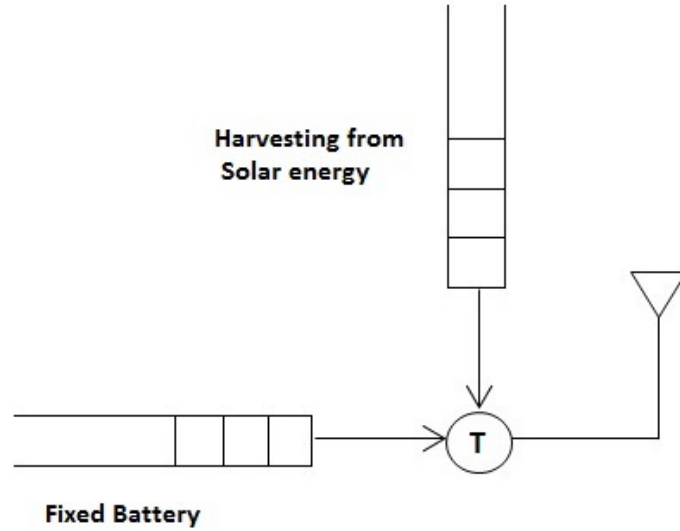


Figure 3.1: System model.

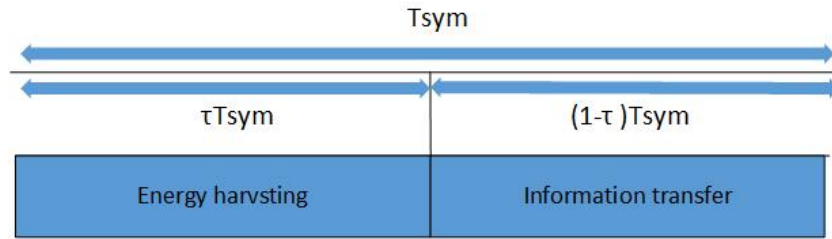


Figure 3.2: Illustration of key parameters in time switching protocol for harvesting energy and information transfer.

3.2 System Model

We consider a system model for a point-to-point communication over a wireless fading channel, in which the transmitter T is equipped with a fixed battery as well as a solar EH battery, as presented in Fig. 3.1. Channels follow the block-fading model, i.e., each of the channel gain is invariant during each fading block, but varies independently from one block to another. The length of each fading block is denoted by T_b . The symbol duration is given by $T_{\text{sym}} = 1/B$, where B is the system bandwidth. We assume that the fading block duration is an integer multiplication of the symbol duration. Furthermore, the noise is considered additive white Gaussian noise (AWGN). The channel state information (CSI) is estimated

at the receiver and is assumed to be fed back to transmitter through an error-free feedback channel.³ The channel power gain, denoted γ , is assumed to be Rayleigh fading, with probability density function (PDF) already given in (2.10).

In this system, transmitter T has a fixed battery, referred to as battery B_1 and operating fixed battery with power P_t , and an additional EH battery which implements the HU approach where, as aforementioned, energy cannot be stored and must be used immediately for information transmission when it becomes available. The proposed model can replenish energy from different sources. Here the harvesting relies on solar energy. Energy collected through harvesting is assumed to be available at the end of the harvesting time [RSV11b]. As no energy buffering is used, the energy causality constraints are not applicable here. Rechargeable batteries that consider energy causality constraints for energy storage through harvesting are discussed in [KHZS07].

The device either harvests energy or transmits data. Therefore, the TS approach is used at the transmitter for harvesting energy and transmitting information, as described in Fig. 3.2. In detail, T_{sym} denotes the time slot during which the communication between the source and the destination takes place. τT_{sym} , for which τ satisfies $0 \leq \tau \leq 1$, is the fraction of time during which the transmitter harvests energy, and the remaining slot time $(1 - \tau)T_{\text{sym}}$ is used for information transmission.

In this case, the spectral efficiency, in units of b/s/Hz, is given by

$$\text{SE} = (1 - \tau)\mathbb{E} \left[\log_2 \left(1 + \left(P_t(t) + \frac{Q\tau}{1 - \tau} \right) \frac{\gamma}{K_{\mathcal{L}}} \right) \right], \quad (3.1)$$

where $P_t(t)$ is the instantaneous transmission power at time t , and Q is the solar

³The CSI is only required at the transmitter when the transmit power is optimally adapted to the variations of the channel. In the cases of fixed transmission power, instantaneous knowledge of the channel is not required at the transmitter.

EH power level.⁴ Therefore, the total transmission power is $P_t(t) + \frac{Q\tau}{1-\tau}$. $\mathbb{E}[\cdot]$ indicates the expectation operator, $K_{\mathcal{L}} = P_L\sigma_n^2B$, with P_L indicating the path loss, and σ_n^2 represents the AWGN variance.

On the other hand, energy efficiency, which is defined as the number of bits per unit power consumed from the fixed battery, is formulated as the ratio of information rate to the sum of total transmission power $P_t(t)$ and total circuit power P_c . Given that the rate and energy consumption are determined by the transmit power, EE can be optimized by adaptively allocating power based on the channel conditions and the system's requirements. Hence, the instantaneous transmit power, $P_t(t)$, is replaced by $P_t(\gamma)$ to show that the transmission power is a function of the channel power gain γ . Hence, $P_{\text{total}}(t) = P_{c2}\tau + (1-\tau)\left(P_c + \frac{1}{\varepsilon}\mathbb{E}[P_t(\gamma)]\right)$, where P_c is the circuit power, ε is the power amplifier efficiency with the range of $0 \leq \varepsilon \leq 1$, and P_{c2} is the circuit power during the harvesting time τT_{sym} . Therefore, the total achievable EE can be expressed as:⁵

$$\eta = \frac{(1-\tau)\mathbb{E}\left[\log_2\left(1 + \left(P_t(t) + \frac{Q\tau}{1-\tau}\right)\frac{\gamma}{K_{\mathcal{L}}}\right)\right]}{P_{c2}\tau + (1-\tau)\left(P_c + \frac{1}{\varepsilon}\mathbb{E}[P_t(\gamma)]\right)}. \quad (3.2)$$

In order to investigate the EH beneficialness condition, we consider two scenarios, specifically when the transmit power is optimally adapted to channel variations and when the transmit power is fixed. Hence, we first need to find the optimal power strategy that gives the maximum achievable EE or SE based on what is considered as the dominant performance metric in the system so that the above mentioned cases can be further discussed in detail.

⁴The total harvesting power is given by $\frac{Q\tau T_{\text{sym}}}{(1-\tau)T_{\text{sym}}}$, where T_{sym} cancels out in (3.1).

⁵Hereafter, we remove the time index whenever the concept is clear from the text.

3.3 Optimum Power Allocation

Recently, there has been many research results on the trade-off between the achievable SE and EE in wireless systems [ZZH12]. We hence consider two different systems in terms of designing EE and SE performance metrics. Our investigation starts with analysing the EH beneficialness condition to see whether it can benefit the system's achievable EE. To do so, we first need to identify the power allocation that maximizes EE when EH is implemented at the transmitter.

3.3.1 Energy-Efficient Power allocation without Input Power Constraint

In this section, we consider the EE-maximization problem when no constraint is imposed on the total power of the fixed battery. The ensuing results will pave the way for the power-constrained EE-maximization problem considered later in this section. We start by formulating the EE-maximization problem, given η as per (3.2),

$$\eta_{\text{opt}} = \max_{P_t(\gamma) \geq 0} \frac{(1 - \tau) \mathbb{E} \left[\log_2 \left(1 + \left(P_t(\gamma) + \frac{Q\tau}{1 - \tau} \right) \frac{\gamma}{K_{\mathcal{L}}} \right) \right]}{P_{c2}\tau + (1 - \tau) \left(P_c + \frac{1}{\varepsilon} \mathbb{E}[P_t(\gamma)] \right)}, \quad (3.3)$$

where $\mathbb{E}_{\gamma}[\cdot]$ is the expectation operator over the channel power gain γ . Note that the maximum achievable EE with additional energy due to harvesting is different from the traditional EE.

The EE-maximization can further be normalized with $K_{\mathcal{L}}$, yielding

$$\eta_{\text{opt}} = \max_{P_r(\gamma) \geq 0} \frac{(1 - \tau) \mathbb{E}_{\gamma} \left[\log_2 \left(1 + \left(P_r(\gamma) + \frac{Q_r \tau}{1 - \tau} \right) \gamma \right) \right]}{K_{\mathcal{L}} \left(\tau P_{\text{cr}2} + (1 - \tau) P_{\text{cr}} + (1 - \tau) \frac{1}{\varepsilon} \mathbb{E}_{\gamma} [P_r(\gamma)] \right)}. \quad (3.4)$$

Here power ratios of signal-to-noise, circuit-to-noise, harvest-to-noise power, and circuit-to-noise during harvesting, are represented by $P_r(\gamma) = P_t(\gamma)/K_{\mathcal{L}}$, $P_{\text{cr}} = P_c/K_{\mathcal{L}}$, $Q_r = Q/K_{\mathcal{L}}$ and $P_{\text{cr}2} = P_{c2}/K_{\mathcal{L}}$, respectively. The problem in (3.4) involves maximization of a ratio of two functions of $P_r(\gamma)$, and is not concave [Sch76, KMLN12]. However, the denominator of (3.4) is affine and the numerator is concave in the transmission power. Hence, the EE-maximization objective function is a strictly quasi-concave function in $P_r(\gamma)$, with a unique global maximum. A general methodology is used for the transformation of quasi-concave optimization into a concave optimization problem through fractional programming [Sch76]. Using variable transformation with inverse power dissipation parameter for $t = \tau P_{\text{cr}2} + (1 - \tau) P_{\text{cr}} + (1 - \tau) \frac{1}{\varepsilon} \mathbb{E}_{\gamma} [P_r(\gamma)]$, the EE-maximization problem is converted to

$$\eta_{\text{opt}} = \max t^{-1} \left((1 - \tau) \mathbb{E}_{\gamma} \left[\log_2 \left(1 + \left(P_r(\gamma) + \frac{Q_r \tau}{1 - \tau} \right) \gamma \right) \right] \right) \quad (3.5)$$

$$\text{subject to: } t^{-1} \left(\tau P_{\text{cr}2} + (1 - \tau) P_{\text{cr}} + (1 - \tau) \frac{1}{\varepsilon} \mathbb{E}_{\gamma} [P_r(\gamma)] \right) = 1 \quad (3.6)$$

$$P_r(\gamma) \geq 0. \quad (3.7)$$

The objective function in (3.5) is concave in $P_r(\gamma)$ and continuously differentiable, and the equality constraint is affine. Therefore, the Karush-Kuhn-Tucker (KKT) conditions are both sufficient and necessary for the optimal solution to exist.

Considering the Lagrangian multiplier λ , the Lagrangian function is formulated as

$$L(P_r(\gamma), t) = t^{-1} \left((1 - \tau) \mathbb{E}_\gamma \left[\log_2 \left(1 + \left(P_r(\gamma) + \frac{Q_r \tau}{1 - \tau} \right) \gamma \right) \right] \right) - \lambda \left(\left(t^{-1} \left(\tau P_{cr2} + (1 - \tau) P_{cr} + (1 - \tau) \frac{1}{\varepsilon} \mathbb{E}_\gamma [P_r(\gamma)] \right) - 1 \right) \right) - \mu P_r(\gamma). \quad (3.8)$$

On the basis of complementary slackness, if the strict inequality $P_r > 0$ holds, then we have $\mu = 0$. hence, the stationary conditions are:

$$\frac{\partial L(P_r(\gamma), t)}{\partial P_r(\gamma)} = \mathbb{E}_\gamma \left[\frac{(1 - \tau)(\gamma)}{1 + \left(P_r(\gamma) + \frac{Q_r \tau}{1 - \tau} \right) \gamma} \right] - \mathbb{E}_\gamma \left[\frac{\lambda(1 - \tau)}{\varepsilon} \right] - \mu = 0, \quad (3.9)$$

$$\frac{\partial L(P_r(\gamma), t)}{\partial t} = (1 - \tau) \mathbb{E}_\gamma \left[\log_2 \left(1 + \left(P_r(\gamma) + \frac{Q_r \tau}{1 - \tau} \right) \gamma \right) \right] - \lambda \left(\tau P_{cr2} + (1 - \tau) P_{cr} + (1 - \tau) \frac{1}{\varepsilon} \mathbb{E}_\gamma [P_r(\gamma)] \right) = 0. \quad (3.10)$$

Now, the EE-maximization power allocation strategy can be derived using (3.9), according to

$$P_r(\gamma) = \left[\frac{\varepsilon}{\lambda} - \frac{1}{\gamma} - \frac{Q_r \tau}{1 - \tau} \right]^+, \quad (3.11)$$

where $[x]^+$ returns the $\max(0, x)$. We note that the power allocation (3.11) is different from traditional water-filling in the sense that (3.11) is a scaled and shifted version of traditional water-filling power allocation. This is due to the presence of the additional term of the harvesting power $\frac{Q_r \tau}{1 - \tau}$, and the TS parameter τ . The expectation in (3.10) can be solved to find a closed-form expression for the optimal power allocation strategy. In order to obtain λ , we insert (3.11) into (3.10)

and solve the expectation operators, yielding

$$\begin{aligned}
 (1 - \tau) \log_2(\beta) e^{-\beta} + (1 - \tau) \text{Ei}(\beta) - \left[(1 - \tau) e^{-\beta} \log_2 \left(\frac{\beta(1 - \tau)}{(1 - \tau) + \beta\tau Q_r} \right) \right] \\
 - \frac{\beta\varepsilon(1 - \tau)P_{\text{cr}2}\tau}{((1 - \tau) + \beta\tau Q_r)} - \frac{(1 - \tau)^2 P_{\text{cr}}\beta\varepsilon}{((1 - \tau) + \beta\tau Q_r)} - \frac{(1 - \tau)^2 e^{-\beta}}{(1 - \tau) + \beta\tau Q_r} \\
 + \frac{\beta(1 - \tau)^2 \text{Ei}(\beta)}{(1 - \tau) + \beta\tau Q_r} = 0. \tag{3.12}
 \end{aligned}$$

where $\beta = \frac{\lambda(1 - \tau)}{\varepsilon(1 - \tau) - \tau Q_r \lambda}$, and $\text{Ei}(\beta)$ indicates the exponential integral defined by $\text{Ei}(\beta) = \int_{\beta}^{\infty} \frac{e^{-t}}{t} dt$ [BV04]. Let us assume β^* is the optimal β that solves (3.12). The average input power at this point can hence be found as $\bar{P}_u = \mathbb{E}_{\gamma}[P_t(\gamma)]|_{\beta=\beta^*}$, wherein $P_t(\gamma) = \frac{P_r(\gamma)}{K_{\mathcal{L}}}$, for which $P_r(\gamma)$ is given in (3.11). Using \bar{P}_u , one can show that the unconstrained EE-maximization problem can be simplified into a SE-maximization problem, subject to an input power constraint with the constraint power level set at \bar{P}_u .

3.3.2 Effect of Q_r on \bar{P}_u

The EE-optimal power allocation strategy (3.11) depends on β^* , which itself depends on the harvesting power Q_r . However, the effect of Q_r on β^* , and in turn, on the optimum power allocation, cannot be analysed clearly from (3.11) and (3.12). Here, we want to analyse the effect of Q_r on the maximum achievable EE, and in turn, on \bar{P}_u . We first start by analysing the effect of Q_r on \bar{P}_u .

Lemma 2. *The optimum input power \bar{P}_u monotonically decreases with the harvesting power Q_r .*

Proof. The proof is provided in Appendix B. □

The result of Lemma 2 implies that the average power associated with the maximum achievable power-unconstrained EE is a decreasing function of Q_r . See

Appendix B.1 for details.

3.3.2.1 Special Case - Neglecting the Circuit Power

We consider the special case, where the circuit power during harvesting is neglected, i.e., $P_{\text{cr2}} = 0$. The purpose of this special case is to find out how other parameters along with EH affect the maximum achievable EE of the system.

We start by investigating the achievable EE using the power allocation strategy in (3.11) when $P_{\text{cr2}} = 0$. In this case, the total power consumed at the transmitter is $(1 - \tau) \left(P_c + \frac{1}{\varepsilon} \mathbb{E}[P_t(t)] \right)$. Thus, the maximum achievable EE when $P_{\text{cr2}} = 0$ is given by

$$\eta = \frac{\mathbb{E} \left[\log_2 \left(1 + \left(P_t + \frac{Q\tau}{1 - \tau} \right) \frac{\gamma}{K_{\mathcal{L}}} \right) \right]}{P_c + \frac{1}{\varepsilon} \mathbb{E}[P_t]}. \quad (3.13)$$

Note that the achievable EE in (3.13) is different from the one derived in (3.2).⁶ The factor $1 - \tau$ is not present in (3.13). In this case, the EE-maximization problem simplifies to

$$\eta_{\text{opt}} = \max_{P_r(\gamma) \geq 0} \frac{\mathbb{E}_{\gamma} \left[\log_2 \left(1 + \left(P_r(\gamma) + \frac{Q_r\tau}{1 - \tau} \right) \gamma \right) \right]}{K_{\mathcal{L}} \left(P_{\text{cr}} + \frac{1}{\varepsilon} \mathbb{E}_{\gamma} [P_r(\gamma)] \right)}. \quad (3.14)$$

The EE-maximization power allocation strategy can now be found by using similar steps as for obtaining (3.11) in subsection 3.3.1.

⁶Here again the total harvesting power has a term τT_{sym} , which cancels out eventually.

The closed-form expression to obtain β is derived as

$$\begin{aligned} & \log_2(\beta) e^{-\beta} + \text{Ei}(\beta) - \left[e^{-\beta} \log_2 \left(\frac{\beta(1-\tau)}{(1-\tau) + \beta\tau Q_r} \right) \right] \\ & - \frac{(1-\tau)P_{\text{cr}}\beta\varepsilon}{(1-\tau) + \beta\tau Q_r} - \frac{(1-\tau)e^{-\beta}}{(1-\tau) + \beta\tau Q_r} + \frac{\beta(1-\tau)\text{Ei}(\beta)}{(1-\tau) + \beta\tau Q_r} = 0. \end{aligned} \quad (3.15)$$

Using the results of the last section, the power-unconstrained EE-maximization problem simplifies into a power-constrained SE-maximization problem, with a limit set at \bar{P}_u . Accordingly, the EE-maximization power allocation strategy with an input power constraint set at P_{max} can be derived when $\mathbb{E}_\gamma[P_r(\gamma)] = \min\left(\frac{\bar{P}_u}{K_{\mathcal{L}}}, \frac{P_{\text{max}}}{K_{\mathcal{L}}}\right)$.

3.3.3 Optimal Power Allocation to Maximize SE

Next, we calculate the optimal power allocation to maximize SE. By following similar steps as in (3.5) to (3.10), the SE-optimal power allocation strategy can be found according to,

$$P_r(\gamma) = \left[\frac{(1-\tau)}{\lambda} - \frac{1}{\gamma} - \frac{Q_r\tau}{1-\tau} \right]^+. \quad (3.16)$$

This power allocation is also a scaled and shifted version of the traditional water-filling power allocation. We can see that (3.16) is different that the EE-power allocation strategy in (3.11). Following the steps in (3.12), the closed-form expression for finding the optimal value for the Lagrangian multiplier is given by,

$$(1-\tau) \log_2(\alpha(1-\tau)) e^{-\alpha} + (1-\tau)\text{Ei}(\alpha) - \left((1-\tau) \log_2 \left(\frac{\alpha(1-\tau)^2}{1-\tau + \alpha\tau Q_r} \right) e^{-\alpha} \right) = 0, \quad (3.17)$$

where $\alpha = \frac{(1-\tau)\lambda}{(1-\tau)^2 - \tau Q_r \lambda}$.

3.4 Performance Improvement Analysis

In this section, we consider the conditions under which EH can improve the system performance, when the input power is optimally allocated so that the system performance is maximized. Specifically, two different cases are considered. 1) Case I: when the power is adapted to the variations of the channel so that either EE or SE of the system is maximized, and 2) Case II: when transmit power is fixed. The EE-optimum power allocation strategy is given in (3.11) and the SE-optimum power allocation strategy is given in (3.16). We further investigate these conditions when the TS factor τ is fixed or variable.

3.4.1 Adaptive Transmit Power Allocation

Here, we assume that the transmit power is adapted to the channel variations, and we investigate the conditions under which implementing EH can benefit the system performance. We analyze two different performance measures, EE and SE.

3.4.1.1 Effect of Harvesting on the System's η_{opt}

We start this by formalizing the maximum achievable EE using the EE-optimal power allocation given in (3.11). This yields

$$\eta_{\text{opt}} = \frac{(1 - \tau) \mathbb{E}_{\gamma} \left[\log_2 \left(\frac{\varepsilon \gamma}{\varepsilon \beta - \frac{\beta Q_r \tau}{1 - \tau}} \right) \right]}{K_{\mathcal{L}} \tau P_{\text{cr}2} + K_{\mathcal{L}} (1 - \tau) P_{\text{cr}} + \frac{K_{\mathcal{L}} (1 - \tau)}{\varepsilon} \mathbb{E}_{\gamma} \left[\frac{1}{\beta} - \frac{1}{\gamma} \right]}, \quad (3.18)$$

where β is defined after (3.12). Further, a closed-form expression for (3.18) can be obtained as follows:

$$\eta_{\text{opt}} = \frac{(1 - \tau) \left(-\log_2(\beta\varepsilon)e^{-\beta} + \frac{\text{Ei}(\beta)}{\beta\varepsilon - \beta\frac{Q_r\tau}{1-\tau}} \right)}{K_{\mathcal{L}} \left(\tau P_{\text{cr}2} + (1 - \tau)P_{\text{cr}} + \frac{(1 - \tau)}{\varepsilon} \left(\frac{e^{-\beta}}{\beta} + \text{Ei}(\beta) \right) \right)} \quad (3.19)$$

To analyze whether EH improves the EE of the system or not, we investigate the effects of τ on the maximum EE. We note that η_{opt} given in (3.19) is a function of the EH parameter τ . Basically, we want to find an answer on how much time should be spent in harvesting. To do so, we first take the derivative of η_{opt} with respect to τ , where η_{opt} is given in (3.19), to get

$$\begin{aligned} \frac{\partial \eta_{\text{opt}}}{\partial \tau} = & \frac{1}{d} \left(\left(K_{\mathcal{L}} P_{\text{cr}2} \tau + K_{\mathcal{L}} P_{\text{cr}} (1 - \tau) + \frac{d_1 (1 - \tau)}{\varepsilon} \right) \left(d_2 + \beta d_2 \left(\frac{2 - Q_r - \tau - \tau^2 + Q_r \tau^2}{(1 - \tau + Q_r \tau)} \right) \right) \right. \\ & \left. - \left((1 - \tau) d_2 + \frac{d_3}{\frac{1}{\beta} + \frac{Q_r \tau}{1 - \tau}} \right) \left(K_{\mathcal{L}} P_{\text{cr}2} - K_{\mathcal{L}} P_{\text{cr}} - \frac{e^{-\beta} K_{\mathcal{L}}}{\beta \varepsilon} - K_{\mathcal{L}} d_3 \right) \right) \end{aligned} \quad (3.20)$$

where $d = K_{\mathcal{L}} \left(\tau P_{\text{cr}2} + (1 - \tau)P_{\text{cr}} + \frac{(1 - \tau)}{\varepsilon} d_1 \right)^2$, $d_1 = \frac{e^{-\beta}}{\beta} + d_3$, $d_2 = \log_2(\beta)e^{-\beta}$ and $d_3 = \text{Ei}(\beta)$. Here d is the denominator of (3.20) and is always positive. We note that (3.20) is a complex equation and even after mathematical manipulation to find the second derivative with respect to τ , (3.20) does not give any information about the trend of η_{opt} with respect to τ . Therefore, this complex case is numerically analyzed and presented through simulations in the numerical result section. For the remaining cases, we provide closed-form solutions for the EH beneficialness condition which are discussed in the following two parts.

3.4.1.2 Effect of Harvesting on η_{opt} when $P_{\text{cr}2} = 0$

Now, we consider the maximum achievable EE presented in (3.14) when $P_{\text{cr}2} = 0$, by using the EE-optimal power allocation given in (3.11), yielding

$$\eta_{\text{opt}} = \frac{\mathbb{E}_{\gamma} \left[\log_2 \left(\frac{\gamma}{\beta} + \frac{\gamma\tau Q_r}{1-\tau} \right) \right]}{K_{\mathcal{L}} P_{\text{cr}} + \frac{K_{\mathcal{L}}}{\varepsilon} \mathbb{E}_{\gamma} \left[\frac{1}{\beta} - \frac{1}{\gamma} \right]}, \quad (3.21)$$

The closed-form expression for (3.21) can be obtained as

$$\eta_{\text{opt}} = \frac{\log_2(\beta)e^{-\beta} + \text{Ei}(\beta) \left(\frac{1}{\beta} + \frac{Q_r\tau}{1-\tau} \right)^{-1}}{K_{\mathcal{L}} P_{\text{cr}} + \frac{K_{\mathcal{L}}}{\varepsilon} \left(\frac{e^{-\beta}}{\beta} + \text{Ei}(\beta) \right)}. \quad (3.22)$$

We aim to investigate the effects of the EH parameter τ on the maximum achievable EE when $P_{\text{cr}2} = 0$. We note that η in (3.22) is a function of τ . Similar to the previous case, we aim to provide an answer to the question on how much time should be spent in harvesting energy. To do so, we first take the derivative of η_{opt} with respect to τ , where η_{opt} is given in (3.21), to get

$$\frac{\partial \eta_{\text{opt}}}{\partial \tau} = \frac{-\text{Ei}(\beta) \left(\frac{1}{\beta} + \frac{Q_r\tau}{1-\tau} \right)^{-2}}{(1-\tau)^2 K_{\mathcal{L}} \left(P_{\text{cr}} + \frac{1}{\varepsilon} \left(\frac{e^{-\beta}}{\beta} + \text{Ei}(\beta) \right) \right)}. \quad (3.23)$$

Equation (3.23) is always negative. Therefore, η_{opt} is maximum when $\tau = 0$. This means that, when $P_{\text{cr}2} = 0$, no harvesting is the best approach to achieve the maximum EE in the system.

3.4.1.3 Effect of Harvesting on SE_{opt}

Now we analyze the effects of EH on the maximum achievable SE of the system, SE_{opt} . We start by formulating SE_{opt} when the optimal power allocation given in (3.16) is used, to get

$$SE_{\text{opt}} = (1 - \tau) \mathbb{E}_\gamma \left[\log_2 \left(\frac{\gamma}{\alpha} + \frac{Q_r \tau \gamma}{1 - \tau} \right) \right]. \quad (3.24)$$

The closed-form expression for (3.24) is found as

$$SE_{\text{opt}} = -\log_2 \left(1 + \frac{Q_r \tau \alpha}{1 - \tau} \right) e^{-\alpha} - \text{Ei}(\alpha). \quad (3.25)$$

In order to investigate the effect of τ on the maximum SE, we first analyse whether (3.25) is concave with respect to τ . We start by finding the first-derivative of SE_{opt} from (3.24) with respect to τ , yielding

$$\frac{\partial SE_{\text{opt}}}{\partial \tau} = \mathbb{E}_\gamma \left[\frac{\frac{Q_r \gamma}{1 - \tau}}{\frac{\gamma}{\alpha} + \frac{Q_r \tau \gamma}{1 - \tau}} \right] - \mathbb{E}_\gamma \left[\log_2 \left(\frac{\gamma}{\alpha} + \frac{Q_r \tau \gamma}{1 - \tau} \right) \right]. \quad (3.26)$$

We further take the second derivative $\frac{\partial^2 SE_{\text{opt}}}{\partial^2 \tau}$, to get

$$\begin{aligned} \frac{\partial^2 SE_{\text{opt}}}{\partial^2 \tau} &= -\frac{\mathbb{E}_\gamma [m_1]}{(1 - \tau)^2} - \left(\mathbb{E}_\gamma [m] + \frac{\mathbb{E}_\gamma [m_1 \tau]}{\mathbb{E}_\gamma [m(1 - \tau)^2]} \right) \left(\frac{\mathbb{E}_\gamma [m_1]}{\mathbb{E}_\gamma [m(1 - \tau)^2 + m_1 \tau(1 - \tau)]} \right) \\ &\quad - \frac{\mathbb{E}_\gamma [m_1]}{(1 - \tau)^2} \mathbb{E}_\gamma \left[\log_2 \left(m + \frac{m_1 \tau}{1 - \tau} \right) \right] \leq 0, \end{aligned} \quad (3.27)$$

where $m = \frac{\gamma}{\alpha}$ and $m_1 = Q_r \gamma$. Given that $\frac{\partial^2 SE_{\text{opt}}}{\partial^2 \tau}$ is always negative, SE_{opt} is concave in τ . With a concave function in τ meaning that the SE_{opt} will have a

maximum at non-zero τ unless $\frac{\partial \text{SE}_{\text{opt}}}{\partial \tau} \Big|_{\tau=0} \leq 0$, we obtain

$$\begin{aligned} \frac{\partial \text{SE}_{\text{opt}}}{\partial \tau} \Big|_{\tau=0} &= \mathbb{E}_{\gamma} [Q_r \gamma] - \mathbb{E}_{\gamma} [\log_2(\gamma)] \\ &= -Q_r e^{-\alpha} (\alpha + 1) + \log_2(\alpha) e^{-\alpha} + \text{Ei}(\alpha), \end{aligned} \quad (3.28)$$

where α is defined after (3.17). In order to find the EH beneficialness condition, we need to investigate the condition under which $\frac{\partial \text{SE}_{\text{opt}}}{\partial \tau} \Big|_{\tau=0} > 0$. The condition can hence be simplified into

$$Q_r > \frac{\log_2(\alpha) e^{-\alpha} + \text{Ei}(\alpha)}{e^{-\alpha} (\alpha + 1)}. \quad (3.29)$$

The result in (3.29) can be validated through numerical results presented in Section 3.5.

3.4.2 Fixed Transmit Power

Here, we analyze the maximum achievable EE and SE when the transmit power is fixed. We also investigate the cases under which adding EH can benefit the system.

3.4.2.1 Effect of Harvesting on the System EE

We start by investigating the achievable EE for a system with fixed transmit power. We derive the expression for the first derivative of EE η_{fix} in (3.2) with respect to

τ , when the transmit power is fixed, according to

$$\begin{aligned} \frac{\partial \eta_{\text{fix}}}{\partial \tau} = & \frac{1}{(\tau P_{\text{cr}2} + (1 - \tau)(P_{\text{cr}} + P_{\text{r}}))^2} \left(\left(\tau P_{\text{cr}2} + (1 - \tau)(P_{\text{cr}} + P_{\text{r}}) \right) \mathbb{E}_{\gamma} \left[\frac{\frac{Q_{\text{r}}\gamma}{1 - \tau}}{1 + \left(P_{\text{r}} + \frac{Q_{\text{r}}\tau}{1 - \tau} \right)} \right] \right. \\ & - \left(\tau P_{\text{cr}2} + (1 - \tau)(P_{\text{cr}} + P_{\text{r}}) \right) \mathbb{E}_{\gamma} \left[\log_2 \left(1 + \left(P_{\text{r}} + \frac{Q_{\text{r}}\tau}{1 - \tau} \right) \gamma \right) \right] \\ & \left. - (P_{\text{cr}2} - P_{\text{cr}} - P_{\text{r}})(1 - \tau) \mathbb{E}_{\gamma} \left[\log_2 \left(1 + \left(P_{\text{r}} + \frac{Q_{\text{r}}\tau}{1 - \tau} \right) \gamma \right) \right] \right). \end{aligned} \quad (3.30)$$

The denominator term $(\tau P_{\text{cr}2} + (1 - \tau)(P_{\text{cr}} + P_{\text{r}}))^2$ is always positive. So, in order to define the sign of $\frac{\partial \eta_{\text{fix}}}{\partial \tau}$, we only consider the numerator of (3.30) and call it t_{fix} .

We take the second derivative of t_{fix} with respect to τ , yielding

$$\frac{\partial^2 t_{\text{fix}}}{\partial^2 \tau} = \frac{\mathbb{E}_{\gamma} \left[-\frac{P_{\text{cr}2} Q_{\text{r}} \gamma}{(1 - \tau)^2} - \frac{Q_{\text{r}} \gamma P_{\text{cr}} (1 + \tau)}{1 - \tau} \right]}{\mathbb{E}_{\gamma} \left[1 + \left(P_{\text{r}} + \frac{Q_{\text{r}}\tau}{1 - \tau} \right) \gamma \right]} \leq 0. \quad (3.31)$$

Since (3.31) is always negative, then η_{fix} is concave in τ . Therefore, EH could be beneficial if $\left. \frac{\partial \eta_{\text{fix}}}{\partial \tau} \right|_{\tau=0} > 0$. Hence, the EH beneficialness condition can be found by

examining the condition of η_{fix} when $\left. \frac{\partial \eta_{\text{fix}}}{\partial \tau} \right|_{\tau=0} > 0$, which is given by

$$Q_{\text{r}} > \frac{P_{\text{cr}2} \left(P_{\text{r}}^{-1} - e^{P_{\text{r}}^{-1}} \text{Ei} (P_{\text{r}}^{-1}) \right)}{P_{\text{cr}} \left(P_{\text{r}}^{-1} - P_{\text{r}}^{-2} e^{P_{\text{r}}^{-1}} \text{Ei} (P_{\text{r}}^{-1}) \right)}. \quad (3.32)$$

Hence, if Q_{r} is bigger than the right-hand-side (RHS) of (3.32), then EH could be beneficial to the system and the optimal value for τ can be found from $\frac{\partial \eta_{\text{fix}}}{\partial \tau} = 0$.

Otherwise, harvesting does not improve the EE of the system and should not be

used.

3.4.2.2 Effect of Harvesting on the System η_{fix} when $P_{\text{cr}2} = 0$

We investigate the effect of τ on the achievable EE with fixed transmit power when $P_{\text{cr}2} = 0$. We derive the expression for the first derivative of η_{fix} presented in (3.14) taken with respect to τ , as

$$\frac{\partial \eta_{\text{fix}}}{\partial \tau} = \mathbb{E}_{\gamma} \left[\frac{\frac{Q_r}{(1-\tau)^2}}{1 + \left(P_r + \frac{Q_r \tau}{1-\tau} \right) \gamma} \right] \geq 0. \quad (3.33)$$

We note that the first-derivative is always positive. The result obtained in (3.33) gives very valuable information, namely, that the EE is always increasing with τ . This means that for a case with fixed power transmission and $P_{\text{cr}2} = 0$, the more time is taken for harvesting energy, the higher the achievable EE will be.

3.4.2.3 Effect of Harvesting on the System SE_{fix}

For analyzing the effect of EH on the system's SE with fixed transmit power, we start by taking the first derivative of the SE in (3.1), which gives

$$\frac{\partial SE_{\text{fix}}}{\partial \tau} = \mathbb{E}_{\gamma} \left[\frac{\frac{Q_r \gamma}{1-\tau}}{1 + \left(P_r + \frac{Q_r \tau}{1-\tau} \right) \gamma} \right] - \mathbb{E}_{\gamma} \left[\log_2 \left(1 + \left(P_r + \frac{Q_r \tau}{1-\tau} \right) \gamma \right) \right]. \quad (3.34)$$

Then taking the second derivative of the equation (3.34) with respect to τ , we get

$$\begin{aligned} \frac{\partial^2 SE_{\text{fix}}}{\partial^2 \tau} &= - \mathbb{E}_{\gamma} \left[\frac{Q_r \gamma \left(1 + \left(P_r + \frac{Q_r \tau}{1-\tau} \right) \gamma \right) + \frac{Q_r \gamma}{1-\tau}}{(1-\tau)^2 \left(1 + \left(P_r + \frac{Q_r \tau}{1-\tau} \right) \gamma \right)^2} \right] - \mathbb{E}_{\gamma} \left[\frac{\frac{Q_r \gamma}{(1-\tau)^2}}{1 + \left(P_r + \frac{Q_r \tau}{1-\tau} \right) \gamma} \right] \\ &\leq 0. \end{aligned} \quad (3.35)$$

The decreasing trend in (3.35) shows that SE_{fix} is concave in τ . For further investigation, we expand the expectations in (3.34) to get a closed-form expression, which leads to

$$SE_{\text{fix}} = \frac{Q_r}{1-\tau} \left(\left(P_r + \frac{Q_r\tau}{1-\tau} \right)^{-1} - \left(P_r + \frac{Q_r\tau}{1-\tau} \right)^{-2} e^{\left(P_r + \frac{Q_r\tau}{1-\tau} \right)^{-1}} \text{Ei} \left(P_r + \frac{Q_r\tau}{1-\tau} \right)^{-1} \right) + e^{\left(P_r + \frac{Q_r\tau}{1-\tau} \right)^{-1}} \text{Ei} \left(P_r + \frac{Q_r\tau}{1-\tau} \right)^{-1} \quad (3.36)$$

In order to find the EH beneficialness condition, we determine $\left. \frac{\partial SE_{\text{fix}}}{\partial \tau} \right|_{\tau=0}$ according to

$$\left. \frac{\partial SE_{\text{fix}}}{\partial \tau} \right|_{\tau=0} = \mathbb{E}_\gamma \left[\frac{Q_r \gamma}{1 + P_r \gamma} \right] - \mathbb{E}_\gamma [\log_2 (1 + P_r \gamma)]. \quad (3.37)$$

Further, solving (3.37) at $\left. \frac{\partial SE_{\text{fix}}}{\partial \tau} \right|_{\tau=0} > 0$, the EH beneficialness condition is found as follows

$$Q_r > \frac{-e^{P_r^{-1}} \text{Ei}(P_r)^{-1}}{P_r^{-1} - P_r^{-2} e^{P_r^{-1}} \text{Ei}(P_r)^{-1}}. \quad (3.38)$$

Hence, if Q_r is bigger than the RHS of (3.38), then EH could be beneficial to the system. Otherwise, EH does not improve the SE of the system and should not be used.

3.5 Numerical Results

In this section, we numerically evaluate the effect of the harvesting power Q_r , the TS parameter τ , the power from fixed battery, the circuit powers P_{cr} and P_{cr_2} on the achievable EE (b/J/Hz) and SE (b/s/Hz) of the system. In all the figures, we assume that the power of the fixed battery at the transmitter device is represented

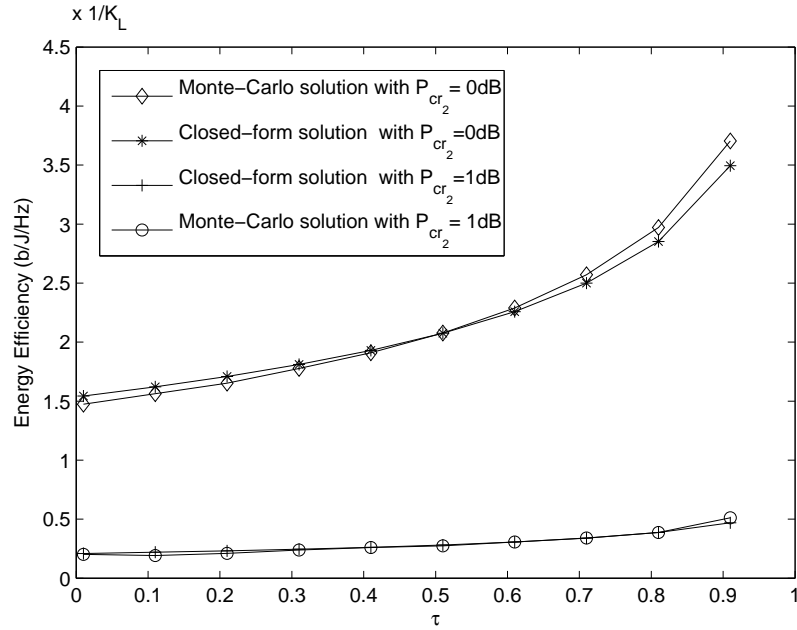


Figure 3.3: EE versus TS parameter τ , when $Q_r = 0.5\text{dB}$, $P_{cr} = 0\text{dB}$ and P_{cr_2} varies.

by P and ε is set to 0.2, unless otherwise stated.

3.5.1 Case I: Adaptive Power Allocation

In this section, we discuss the adaptive power allocation to see how EH can improve the maximum achievable EE and SE of the system.

We start by plotting the EE versus the TS parameter τ at $Q_r = 0.5\text{dB}$, when $P_{cr} = 0\text{dB}$ and considering various values of the circuit power P_{cr_2} . Fig. 3.3 includes both analytical and Monte-Carlo simulation results to verify the correctness of the closed-form derivations. From the graphs, we observe that EE is higher when $P_{cr_2} = 0\text{dB}$ compared to the case when $P_{cr_2} = 1\text{dB}$. Furthermore, the plots confirm the matching between the results obtained from the closed-form expressions and the ones from the simulations, hence indicating the correctness of the analysis. As observed from the plots, EE increases with τ , hence indicating that the more time is spent for harvesting, the higher the EE that can be achieved.

Similarly, Fig. 3.4 includes the plots for SE versus the TS parameter τ with

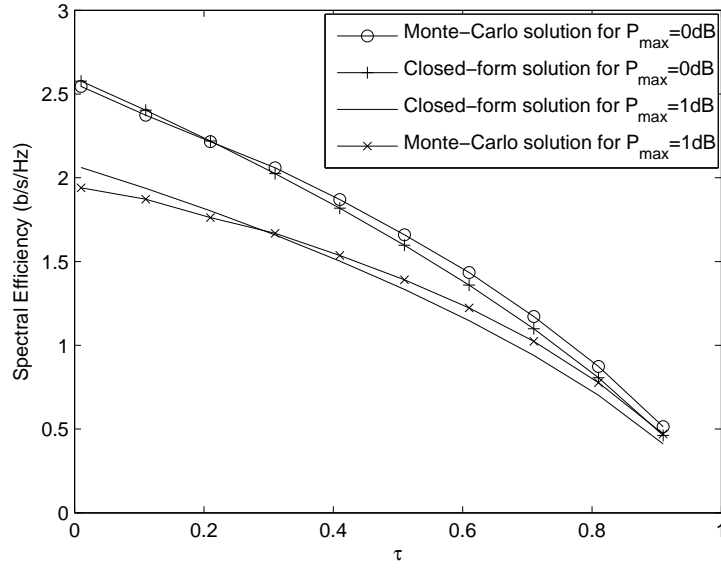


Figure 3.4: SE versus TS parameter τ , with $Q_r = 0.5\text{dB}$ and various values of P_{\max} .

$Q_r = 0.5\text{dB}$ and various values of P_{\max} . The figure includes both analytical and Monte-Carlo simulation results to show the correctness of closed-form expressions for SE. It is noted that the SE decreases with τ at $P_{\max} = 1\text{dB}$ quicker than the one at $P_{\max} = 0\text{dB}$. Also, SE has a decreasing trend with τ which is just opposite to the EE trend in Fig. 3.3.

Numerical results for the EE versus τ are presented in Fig. 3.5 for various values of P_{cr} and P_{cr2} . We notice that EE increases with the TS parameter until it reaches its maximum value around $\tau = 0.5$. After the maximum point, EE decreases. This can also be validated by the mathematical analysis done for η_{opt} in (3.22). Also, the maximum EE is achieved at low values of circuit powers, i.e., $P_{cr} = 0\text{dB}$ and $P_{cr2} = 0\text{dB}$.

Fig. 3.6 illustrates EE versus τ at $P_{cr} = 1\text{dB}$ and $P_{cr2} = 0\text{dB}$ with various values of harvesting power Q_r . It is noted that the higher the harvesting power is, the higher EE can be achieved. Also, EE increases with τ until it reaches a maximum point after which it decreases with τ . When the value for Q_r is bigger, the maximum EE can be achieved at a higher value of τ , hence indicating that

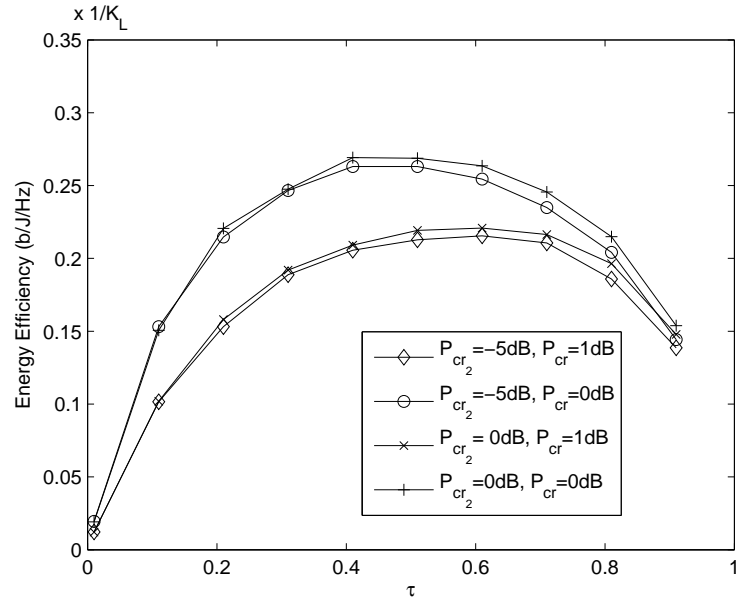


Figure 3.5: EE versus τ with various values of P_{cr} and P_{cr_2} .

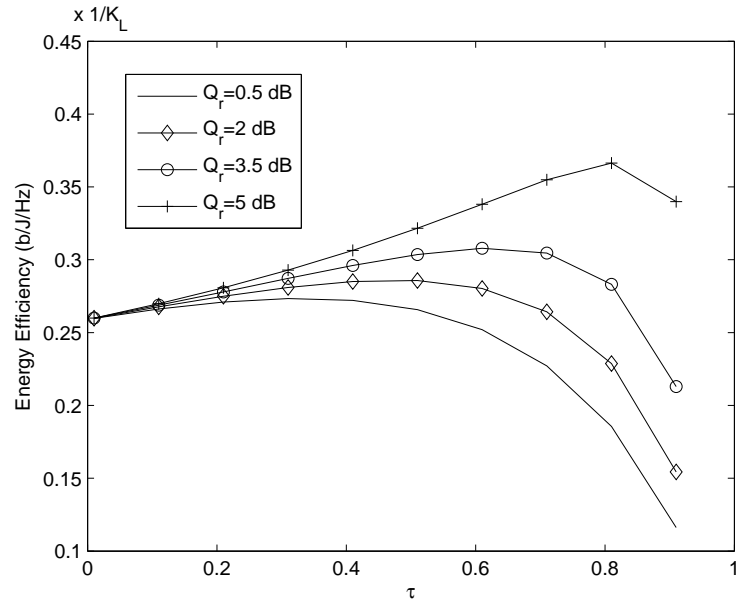


Figure 3.6: EE versus τ with $P_{cr} = 1\text{dB}$ and $P_{cr_2} = 0\text{dB}$ and various values of Q_r .

when EH power is stronger, spending more time for harvesting could be beneficial in terms of maximum achievable EE.⁷

⁷The significance of having two circuit power, i.e., P_{cr} and P_{cr_2} tells that there are two different circuits used in the system. One circuit is for transmission and the other one is for harvesting. They do not operate on same power so you can not basically just add them together. The circuit powers are used in different portions of time.

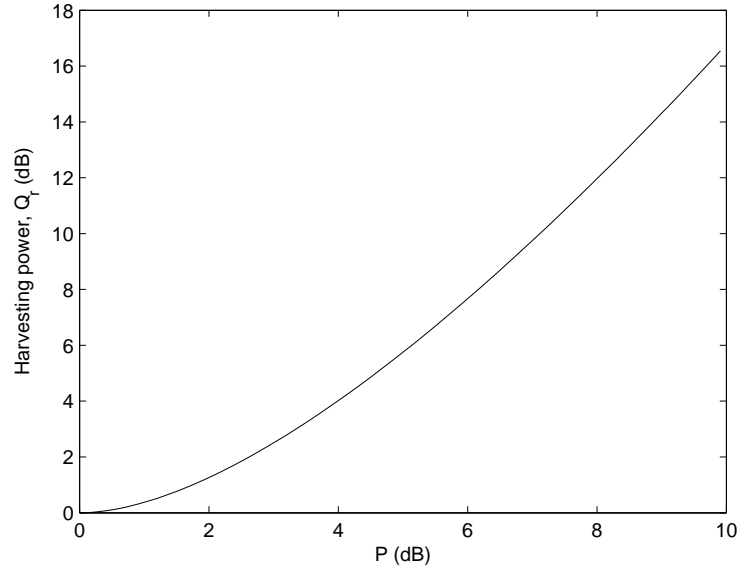


Figure 3.7: Q_r versus power consumed from fixed battery P at $\tau = 0$ with $P_{cr2} = 0\text{dB}$ and $P_{cr} = 0\text{dB}$.

3.5.2 Case II: Fixed Transmit Power

In this section, we present the numerical results for a system with fixed transmit power, to see how EH may improve the maximum achievable EE and SE.

We start by Fig. 3.7, where we present the plot for the harvesting power Q_r versus power P consumed from the fixed battery, with $P_{cr2} = 0\text{dB}$ and $P_{cr} = 0\text{dB}$ for $\left. \frac{\partial EE}{\partial \tau} \right|_{\tau=0} = 0$ referring to (3.32). The figure shows the condition under which EH is beneficial for improving the EE of the system. The upper side of the curve is when EH can benefit the system in terms of improving the maximum achievable EE and the lower side of the curve corresponds to EH in fact decreasing the maximum achievable EE. This happens since the harvested energy is small compared to the power level of the fixed battery. Hence, the time spent for harvesting will be more beneficial if it were spent for signal transmission. The figure also shows that the higher the consumed power from the fixed battery, the higher the harvesting power should be for EH to benefit the system.

Fig. 3.8 illustrates EE versus τ at $P_{cr2} = 0\text{dB}$ and $P_{cr} = 0\text{dB}$ for various values

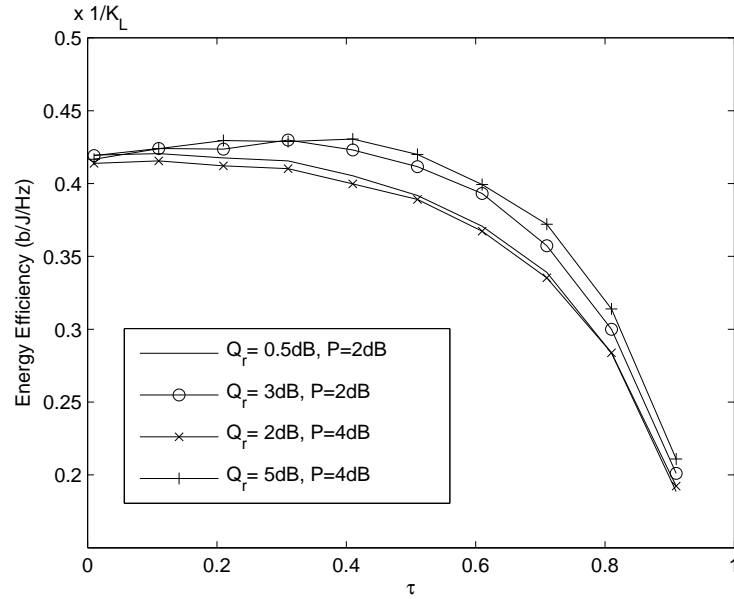


Figure 3.8: EE versus TS parameter τ at $P_{cr2} = 0\text{dB}$ and $P_{cr} = 0\text{dB}$ with various values of harvesting power Q_r and power consumed from fixed battery P.

of harvesting power Q_r and power from the fixed battery P which are taken from Fig. 3.7. We note that at higher values of harvesting power, i.e., $Q_r = 5\text{dB}$, EE increases until it reaches $\tau = 0.45$ after which EE decreases with τ . Similarly, at lower values of power from the fixed battery and the harvesting power, i.e., $Q_r = 0.5\text{dB}$, EE decreases with τ although with a slow slope compared to the case when $Q_r = 5\text{dB}$. This means that the best use of the time is to transmit information rather than to harvest energy.

Results of the SE versus TS parameter τ at $P_{\max} = 1\text{dB}$ with various values of harvesting power Q_r are plotted in Fig. 3.9. The graph demonstrates that SE does monotonically decrease with τ for all values of the harvesting power. The figure shows that maximum SE is achieved at $\tau = 0$, which means that it is rather beneficial to transmit information than to harvest energy. =This result also confirms our derivation for SE case with fixed power transmission given in (3.36) and (3.38).

Fig. 3.10 shows EE versus power P at $\tau = 0.5$ for various values of P_{cr} and

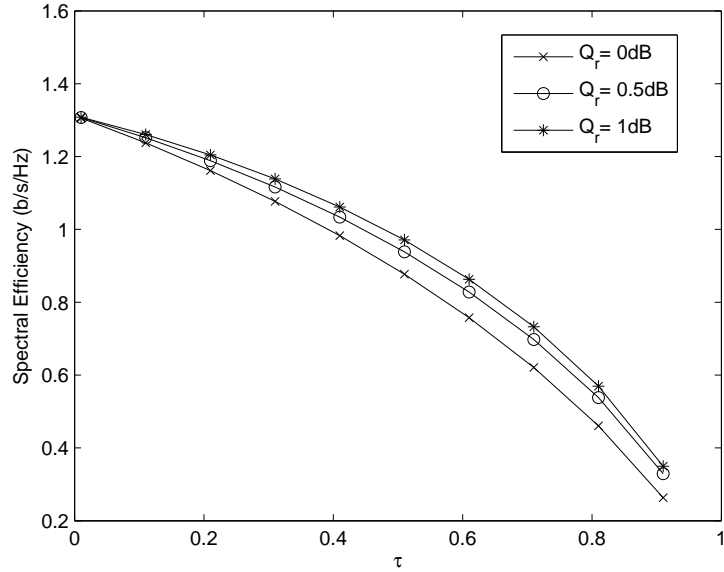


Figure 3.9: SE versus TS parameter τ at $P_{\max} = 1\text{dB}$ with various values of harvesting power Q_r .

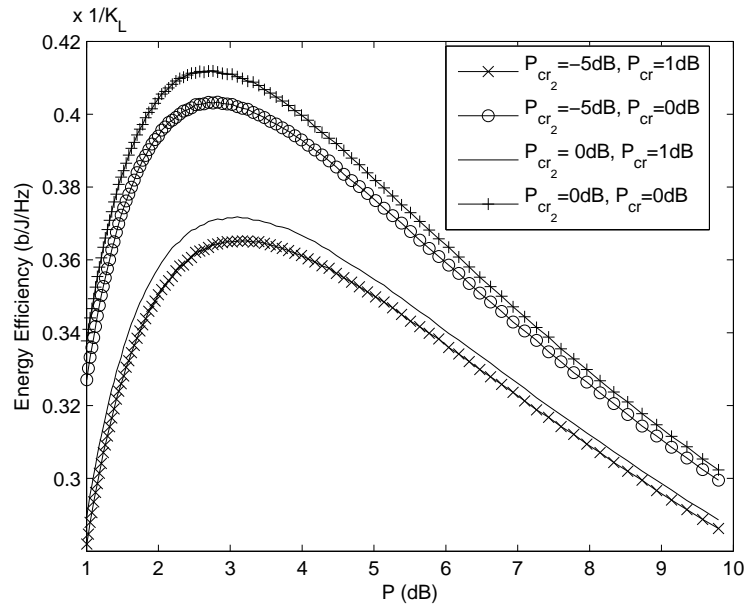


Figure 3.10: EE versus power P at $\tau = 0.5$ for various values of P_{cr} and P_{cr2} .

P_{cr2} . As observed, higher EE can be achieved at smaller values of power. For this case, we assume that $P_{cr2} < P_{cr}$. At low power, i.e., $P = 1\text{dB}$, EE increases until it reaches its optimal value, after that it decreases towards zero. The bell shaped curve shows that addition of harvesting power improves EE and benefits the system

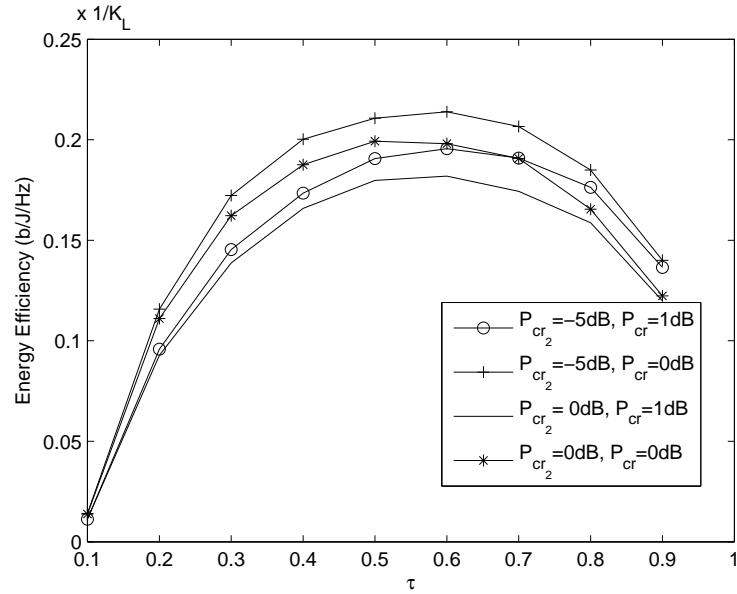


Figure 3.11: EE versus TS parameter τ at $P = 1\text{dB}$ for various values of P_{cr} and P_{cr_2} .

even at low power values. Furthermore, at $P > 2.5\text{dB}$ with circuit powers, i.e., $P_{\text{cr}_2} = 0\text{dB}$ and $P_{\text{cr}} = 0\text{dB}$, the maximum EE is achieved. This result shows that EH can be beneficial for EE-maximization with fixed transmit power.

Fig. 3.11 includes plots of EE versus τ at $P = 1\text{dB}$ for different values of P_{cr} and P_{cr_2} , when the input power is fixed. As shown, EE increases with τ . At $\tau = 0.55$, the maximum EE is achieved when $P_{\text{cr}} = 0\text{dB}$ and $P_{\text{cr}_2} = -5\text{dB}$. Also, EE keeps increasing for most of the values of the TS parameter until it reaches $\tau = 0.69$, after that EE decreases with τ . The mathematical expression for η_{fix} given in (3.31) which compares the simulation result to the theoretical results obtained in (3.31).

Fig. 3.12 evaluates the plots of EE versus power from the fixed battery P for various values of τ , P_{cr} and P_{cr_2} . It is noted that when $P_{\text{cr}} = 0\text{dB}$ and $P_{\text{cr}_2} = 0\text{dB}$, the maximum EE is achieved at $P = 2\text{dB}$. However, at higher value of power, i.e., $P = 6\text{dB}$, EE decreases with P , although with a slow slope.

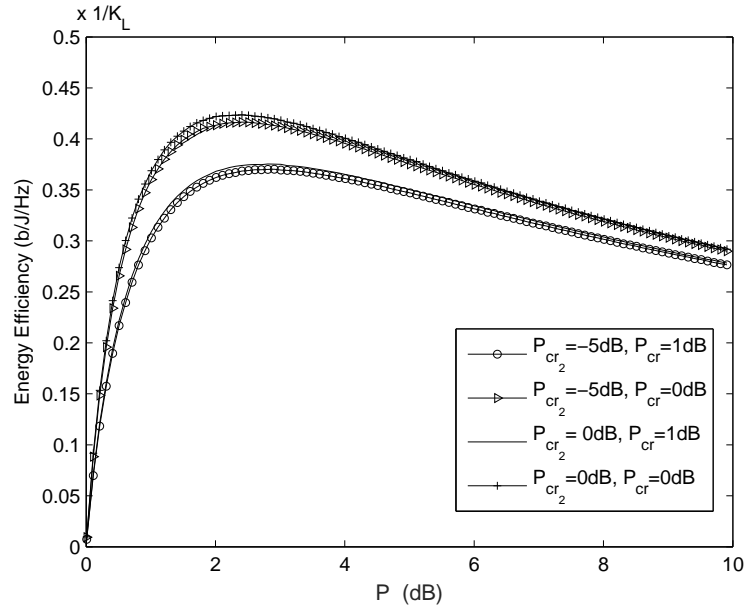


Figure 3.12: EE versus power from the fixed battery P with various values of τ , P_{cr} and P_{cr_2} .

3.6 Chapter Summary

In this chapter, performance analysis and optimal power allocation techniques for point-to-point communication powered equipped with fixed battery as well as EH was considered. A time switching approach where the transmitter switches between harvesting energy and transmitting information was used. We investigated and provided conditions under which EH can improve the system performance in terms of EE or SE. We discussed the case when power is optimally adapted to the variations of channel and another one where transmit power is fixed. Novel closed-form expressions for the maximum achievable EE, SE and EH beneficialness condition were derived. We also proved that the EE-optimum input power decreases with the EH power level. Numerical results validated the correctness of the closed-form expressions. EH has been analysed to improve the system performance in terms of maximum achievable EE and SE. SE however can improve the EH for specific values of the considered parameters, i.e, higher values of Q_r and P_{max} will

somehow improve the SE. This motivates us to look for such cases where SE along with EE can benefit the system under EH constraints. The next chapter will give us more detail about how SE and EE can jointly optimize in presence of EH batteries.

Chapter 4

Weighted Trade-off between Energy Efficiency and Spectral Efficiency for Systems with Energy Harvesting Batteries

This chapter proposes a new power allocation scheme to jointly optimize EE and SE of a point-to-point system, equipped with fixed as well as EH battery. TS is used such that in each frame, the node either harvests energy or transmits information. First, a multi-objective optimization problem (MOP) is formulated which jointly optimizes EE and SE. The priority level of EE and SE can be varied by introducing importance weight. Second, the MOP is further transformed into single-objective optimization problem (SOP) by using importance weight through fractional programming. Using KKT conditions, the optimum power allocation scheme without input power constraint is calculated. Also, the closed-form expressions are derived. The impact of TS parameter, importance weight, circuit powers and solar harvesting energy level on the achievable trade-off performance is

investigated through numerical results.

4.1 Introduction

EE can be achieved either by maximizing bit rate or reducing power per unit [LXX⁺11]. EE and SE are two major metrics in wireless communication systems which are hard to balance [CZXL11], hence research interests have been shifted towards studying EH which promises to provide a reliable approach to improve EE, while maintaining SE [BTA16], [ZZH12].

4.1.1 Motivation and Related Work

In past few years, there have been significant research on EH communications with main focus on developments of EH protocols that improve rate and efficiency of the system [CZXL11]. As, EE and SE do not always coincide and conflicts most of the times, therefore balancing the EE-SE is critical [XLZ⁺11], [DRC⁺13]. EE and SE in downlink orthogonal frequency division multiple access (OFDMA) networks is addressed in [XLZ⁺11]. The QoS requirements in the wireless communication systems mostly require more than one QoS to be maintained [Mie12], [TSAH14]. The solution of such problems which involve more than one QoS requirement is done by using MOP [Mie12]. The EE-maximization problem for OFDMA systems is first converted into a MOP. By using weighted sum method, MOP is then transformed into SOP. Knowing the imperfect channel estimation, the inverse of EE and SE are combined in weighted optimization problem is discussed in [ABAD14]. Joint maximization problem with MOP for EE and effective capacity (EC) is studied in [YMN16]. MOP approach to maximize cognitive radio (CR) system throughput for multi-carrier systems using interference efficiency is described in [MM17]. Optimizing SE-EE tradeoff with green energy utilization for traditional power

grid is studied in [HA13]. Energy-spectral efficiency trade off with simultaneous wireless information and power transfer is presented in [SZS⁺16]. Despite the major effect that EH technology can have on the life and the performance of battery-limited communication devices, the majority of the research works in literature is focused on devices with only harvesting sources at the transmitter with no fixed battery [OTY⁺11]. We note that it is inevitable that some sort of a limited fixed battery is implemented within the communication system nodes [LMD⁺16]. To the author's best knowledge, there has been no work is done in literature which deals with EH MOP system with fixed as well as harvesting batteries. However, a detail study is still required to see how to balance EE and SE with EH battery, is well worth studying.

4.1.2 Contributions

In this chapter, we consider a point-to-point communication system in Rayleigh flat-fading channel that is equipped with an EH battery source in addition to its fixed battery. HU technique is used with TS approach. For the system considered here, we investigate and discuss the impact of energy harvesting on the balancing the EE and SE metric in order to improve system performance. We start by obtaining the optimal transmission power allocation strategy that maximize EE or SE, with EH used at the transmitter of the system. A MOP is formulated which jointly optimize EE and SE. The priority level of EE and SE can be varied by introducing importance weight. The MOP is further converted into SOP by using importance weight through fractional programming. We provide closed-form expressions for the SOP. The impact of TS parameter, importance weight, circuit powers and solar harvesting energy level on the achievable trade-off performance is investigated and analysed.

To summarize, the main contributions of this chapter are enlisted below:

- To the best of author's knowledge, this is the first work which deals with trade-off of EE and SE with solar EH at transmitter along with the fixed battery. Section 4.2 describes the system model.
- MOP is formulated which jointly optimize EE and SE in Rayleigh fading channel. Further, MOP is transformed into SOP using importance weight. Using KKT conditions, the optimum power allocation scheme without input power constraint is derived. Also, closed-form expression are obtained. Section 4.3 starts with EE-SE trade-off as an MOP. Also optimum power allocation, derivation of closed-form expression for EE maximization is provided.
- The impact of TS parameter, importance weight, circuit powers and solar harvesting energy level on the achievable trade-off performance is discussed and analysed. In Section 4.4 numerical results are evaluated with respect to TS parameter, importance weight and solar EH, followed by the chapter summary in Section 4.5.

4.2 System Model

In this chapter, a system model is considered for point-to-point communication over a wireless fading channel with transmitter T equipped with both fixed and solar EH battery as shown in Fig. 3.1. The channel follows block fading model and CSI is estimated at the receiver.

In chapter 3, we have described EE and SE as two individual performance metrics referring to (3.1) and (3.2) respectively. The focus of this chapter is to study the EE-SE trade-off with EH battery source. In order to balance these two conflicting metrics, we first need to find the optimal power allocation in EE-SE

trade-off.

4.3 Optimal Power Allocation in EE-SE Tradeoff

In this section, we consider an EE-maximization problem when no constraint is imposed on the total power of the fixed battery. The results of this section will pave the way for power-constrained EE-maximization problem considered later in this section. We start by formulating the EE-maximization problem, defined by η , according to

$$\eta = \max_{P_t(\gamma) \geq 0} \frac{(1 - \tau) \mathbb{E}_\gamma \left[\log_2 \left(1 + \left(P_t(\gamma) + \frac{Q\tau}{1 - \tau} \right) \frac{\gamma}{K_{\mathcal{L}}} \right) \right]}{P_{c2}\tau + (1 - \tau) \left(P_c + \frac{1}{\varepsilon} \mathbb{E}_\gamma [P_t(\gamma)] \right)}. \quad (4.1)$$

where $\mathbb{E}_\gamma[\cdot]$ is the expectation operator over the channel power gain γ . Note that, the maximum achievable EE with additional harvesting energy is different from the traditional EE.

The EE-maximization problem can further be normalized with $K_{\mathcal{L}}$, yielding

$$\eta = \max_{P_r(\gamma) \geq 0} \frac{(1 - \tau) \mathbb{E}_\gamma \left[\log_2 \left(1 + \left(P_r(\gamma) + \frac{Q_r\tau}{1 - \tau} \right) \gamma \right) \right]}{K_{\mathcal{L}} \left(\tau P_{cr2} + (1 - \tau) P_{cr} + (1 - \tau) \frac{1}{\varepsilon} \mathbb{E}_\gamma [P_r(\gamma)] \right)}. \quad (4.2)$$

Here, the signal-to-noise, circuit-to-noise, harvest-to-noise power and circuit-to-noise during harvesting ratios are represented by $P_r(\gamma) = P_t(\gamma)/K_{\mathcal{L}}$, $P_{cr} = P_c/K_{\mathcal{L}}$, $Q_r = Q/K_{\mathcal{L}}$ and $P_{cr2} = P_{c2}/K_{\mathcal{L}}$.

4.3.1 EE-SE Trade-off as an MOP

In this section EE-SE trade-off is formulated in terms of MOP to provide optimal power allocation under average input constraints. In-order to satisfy different measurements and order of magnitude for EE-SE to able to optimize simultaneously, falls into MOP. The MOP, hence can be written as,

$$\max \text{EE} \quad \text{and} \quad \max \text{SE} \quad (4.3)$$

$$\text{subject to:} \quad \mathbb{E}_\gamma[P_r(\gamma)] \leq \frac{P_{\max}}{K_{\mathcal{L}}}, \quad (4.4)$$

where P_{\max} is the average transmission power limit. Instead of joint maximization of EE and SE, here we minimize the inverse of the objective function in (4.3), to get

$$\min \frac{1}{\text{EE}} \quad \text{and} \quad \min \frac{1}{\text{SE}} \quad (4.5)$$

$$\text{subject to:} \quad \mathbb{E}_\gamma[P_r(\gamma)] \leq \frac{P_{\max}}{K_{\mathcal{L}}}, \quad (4.6)$$

In order to solve MOP in (4.5) and achieve the pareto optimal solutions, generally we convert MOP into SOP, using weighted sum method [MA04]. The objective function in (4.5) can be re-written as,

$$\min \quad \frac{\Delta}{\text{EE}} + \frac{1 - \Delta}{\text{SE}} \quad (4.7)$$

$$\text{subject to:} \quad \mathbb{E}_\gamma[P_r(\gamma)] \leq \frac{P_{\max}}{K_{\mathcal{L}}}, \quad (4.8)$$

The two objective functions in (4.7) are combined by introducing weight, Δ which is defined by $\Delta \in [0, 1]$, which serves as an indicator to set the priority of the two objective functions, EE and SE respectively. The trade-off problem reduces to SE-maximization problem when $\Delta = 0$ and when $\Delta = 1$, the MOP simplifies

into EE-maximization. Here, varying Δ will decide the importance of EE as Δ changes between 0 to 1. Also EE can be written in form of ratio which is already defined (4.2), to get

$$\min \frac{\Delta \left(P_{c_{r2}}\tau + (1 - \tau) \left(P_{c_r} + \frac{1}{\varepsilon} \mathbb{E}_\gamma[P_r(\gamma)] \right) \right) + (1 - \Delta)}{\text{SE}} \quad (4.9)$$

$$\text{subject to: } \mathbb{E}_\gamma[P_r(\gamma)] \leq \frac{P_{\max}}{K_{\mathcal{L}}}, \quad (4.10)$$

(4.9) can be rewritten as maximization function by inverting it and then replacing SE from (3.1) into (4.9), to reduce it as given below

$$\max \frac{(1 - \tau) \mathbb{E}_\gamma \left[\log_2 \left(1 + \left(P_r(\gamma) + \frac{Q_r \tau}{1 - \tau} \right) \gamma \right) \right]}{\Delta \left(P_{c_{r2}}\tau + (1 - \tau) \left(P_{c_r} + \frac{1}{\varepsilon} \mathbb{E}_\gamma[P_r(\gamma)] \right) \right) + (1 - \Delta)} \quad (4.11)$$

$$\text{subject to: } \mathbb{E}_\gamma[P_r(\gamma)] \leq \frac{P_{\max}}{K_{\mathcal{L}}}, \quad (4.12)$$

where $\mathbb{E}_\gamma[.]$ is the expectation operator over the channel power gain γ .

4.3.2 Optimal Power Allocation with No Input Power Constraint

In this subsection, the unconstrained SOP is solved for optimum power allocation scheme of the SOP with input average power constraint. It is noted that the maximization problem in (4.11) involves maximization of a ratio of two functions of $P_r(\gamma)$, and is not concave [Sch76], [SMN15]. However, the numerator is concave in transmission power and denominator of (4.11) is affine. The EE maximization function is strictly quasi-concave function in $P_r(\gamma)$ with a unique global maximum. In-order to transform quasi-concave function into

concave optimization problem we use fractional programming [BV04]. By using the variable transformation with inverse power dissipation parameter for $\phi = \Delta \left(P_{c_{r2}}\tau + (1 - \tau) \left(P_{c_r} + \frac{1}{\varepsilon} \mathbb{E}_\gamma [P_r(\gamma)] \right) \right) + (1 - \Delta)$, the maximization problem in (4.11) is converted into

$$\max \quad \phi^{-1} \left((1 - \tau) \mathbb{E} \left[\log_2 \left(1 + \left(P_r(\gamma) + \frac{Q_r \tau}{1 - \tau} \right) \gamma \right) \right] \right) \quad (4.13)$$

$$\text{subject to: } \phi^{-1} \left(\Delta \left(P_{c_{r2}}\tau + (1 - \tau) \left(P_{c_r} + \frac{1}{\varepsilon} \mathbb{E}_\gamma [P_r(\gamma)] \right) \right) + (1 - \Delta) \right) = 1 \quad (4.14)$$

$$P_r(\gamma) \geq 0 \quad (4.15)$$

The objective function in (4.13) is continuously differentiable, concave in $P_r(\gamma)$, and equality constraint is affine. Therefore, the KKT conditions are both sufficient and necessary for optimal solution [BV04]. If $\hat{\lambda}$ is the Lagrangian multiplier, then the Lagrangian is given by

$$\begin{aligned} L(P_r(\gamma), \phi) &= \phi^{-1} \left((1 - \tau) \mathbb{E}_\gamma \left[\log_2 \left(1 + \left(P_r(\gamma) + \frac{Q_r \tau}{1 - \tau} \right) \gamma \right) \right] \right) \\ &\quad - \hat{\lambda} \left(\left(\phi^{-1} \left(\Delta \left(\tau P_{c_{r2}} + (1 - \tau) P_{c_r} + (1 - \tau) \frac{1}{\varepsilon} \mathbb{E}_\gamma [P_r(\gamma)] \right) + (1 - \Delta) \right) - 1 \right) \right) \\ &\quad - \hat{\mu} P_r(\gamma). \end{aligned} \quad (4.16)$$

From (4.16), due to the complementary slackness we have $\hat{\mu} = 0$ when it holds the strict inequality $P_r(\gamma) > 0$. For optimal power allocation, the stationary conditions

are hence written as,

$$\frac{\partial L(P_r(\gamma), \phi)}{\partial P_r(\gamma)} = \mathbb{E}_\gamma \left[\frac{(1-\tau)(\gamma)}{1 + \left(P_r(\gamma) + \frac{Q_r \tau}{1-\tau} \right) \gamma} \right] - \mathbb{E}_\gamma \left[\frac{\hat{\lambda}(1-\tau)\Delta}{\varepsilon} \right] - \hat{\mu} = 0, \quad (4.17)$$

and

$$\begin{aligned} \frac{\partial L(P_r(\gamma), \phi)}{\partial \phi} &= (1-\tau) \mathbb{E}_\gamma \left[\log_2 \left(1 + \left(P_r(\gamma) + \frac{Q_r \tau}{1-\tau} \right) \gamma \right) \right] \\ &\quad - \hat{\lambda} \left(\Delta \left(\tau P_{cr2} + (1-\tau) P_{cr} + (1-\tau) \frac{1}{\varepsilon} \mathbb{E}_\gamma [P_r(\gamma)] \right) + (1-\Delta) \right) = 0. \end{aligned} \quad (4.18)$$

From (4.17), the optimum power allocation scheme can be derived as,

$$P_r(\gamma) = \left[\frac{\varepsilon}{\hat{\lambda}\Delta} - \frac{1}{\gamma} - \frac{Q_r \tau}{1-\tau} \right]^+, \quad (4.19)$$

where $[x]^+ = \max(0, x)$. We note that the power allocation (4.19) is different from traditional water-filling approach in a sense that (4.19) is a scaled and shifted version of traditional water-filling power allocation. This is due to the presence of an additional harvested power, $\frac{Q_r \tau}{1-\tau}$, and TS parameter, τ . The expectation in (4.18) can be solved to carry out a closed-form expression for the optimal power strategy. We insert (4.19) into (4.18) to obtain value of $\hat{\lambda}$, which yields to

$$\begin{aligned} (1-\tau) \log_2 \left(\hat{\beta} \varepsilon \right) e^{-\hat{\beta}} + (1-\tau) \text{Ei}(\hat{\beta}) - \left[(1-\tau) e^{-\hat{\beta}} \log_2 \left(\frac{\hat{\beta}(1-\tau)}{(1-\tau) + \hat{\beta}\tau Q_r} \right) \right] \\ - \frac{\hat{\beta}(1-\tau)(1-\Delta)}{\Delta((1-\tau) + \hat{\beta}\tau Q_r)} - \frac{\hat{\beta}(1-\tau) P_{cr2} \tau}{(1-\tau) + \hat{\beta}\tau Q_r} - \frac{(1-\tau)^2 P_{cr} \hat{\beta}}{(1-\tau) + \hat{\beta}\tau Q_r} \\ - \frac{(1-\tau)^2 e^{-\hat{\beta}}}{\varepsilon \left((1-\tau) + \hat{\beta}\tau Q_r \right)} + \frac{\hat{\beta}(1-\tau)^2 \text{Ei}(\hat{\beta})}{\varepsilon \left((1-\tau) + \hat{\beta}\tau Q_r \right)} = 0. \end{aligned} \quad (4.20)$$

where $\hat{\beta} = \frac{\Delta\hat{\lambda}(1-\tau)}{\varepsilon(1-\tau) - \tau\Delta Q_r\hat{\lambda}}$, and $\text{Ei}(\hat{\beta}) = \int_{\hat{\beta}}^{\infty} \frac{e^{-t}}{t} dt$ indicates the exponential integral [BV04]. Let us assume $\hat{\beta}^*$ is the optimal $\hat{\beta}$ that solves (4.20). The average input power at this point \bar{P}_u can, hence, be found as $\bar{P}_u = \mathbb{E}_{\gamma}[P_t(\gamma)] \Big|_{\hat{\beta}=\hat{\beta}^*}$, wherein $P_t(\gamma) = \frac{P_r(\gamma)}{K_{\mathcal{L}}}$, for which $P_r(\gamma)$ is given in (4.19). Using \bar{P}_u , one can show that the unconstrained EE-maximization problem can be simplified into a SE-maximization problem, subject to an input power constraint with the constraint power level set at \bar{P}_u .

4.3.3 Special case: without Circuit Power $P_{c,2}$

In this subsection, we consider a special case, where the circuit power during harvesting is neglected, i.e., $P_{c,2} = 0$. The purpose of the special case is to find out how EH effects the priority of EE and SE according to the circumstances.

We start by investigating the power allocation scheme in (4.19) when $P_{c,2} = 0$. In this case, the total power consumed at the transmitter is given by $(1-\tau) \left(P_c + \frac{1}{\varepsilon} \mathbb{E}[P_t(t)] \right)$. The maximum achievable EE without $P_{c,2}$ is given by,

$$\eta = \frac{\mathbb{E} \left[\log_2 \left(1 + \left(P_t + \frac{Q\tau}{1-\tau} \right) \frac{\gamma}{K_{\mathcal{L}}} \right) \right]}{P_c + \frac{1}{\varepsilon} \mathbb{E}[P_t]}. \quad (4.21)$$

The achievable EE in (4.21) is different from the one calculated in (4.2). The EE-maximization problem is hence defined by,

$$\eta_{\text{opt}} = \max_{P_r(\gamma) \geq 0} \frac{\mathbb{E}_{\gamma} \left[\log_2 \left(1 + \left(P_r(\gamma) + \frac{Q\tau}{1-\tau} \right) \gamma \right) \right]}{K_{\mathcal{L}} \left(P_{c,r} + \frac{1}{\varepsilon} \mathbb{E}_{\gamma} [P_r(\gamma)] \right)}. \quad (4.22)$$

Using the similar steps in 4.3, the objective function can be solved by converting MOP into SOP by using weighted sum method. The joint maximization function from (4.22) is hence written as

$$\max \frac{(1-\tau)\mathbb{E}\left[\log_2\left(1+\left(P_r(\gamma)+\frac{Q_r\tau}{1-\tau}\right)\gamma\right)\right]}{\Delta(1-\tau)\left(P_{cr}+\frac{1}{\varepsilon}\mathbb{E}_\gamma[P_r(\gamma)]\right)+(1-\Delta)} \quad (4.23)$$

Using the results of the last section and following the similar steps from (4.13) to (4.19), the closed-form expression for finding optimal value for Lagrangian multiplier is given by,

$$\begin{aligned} (1-\tau)\log_2(\hat{\beta}\varepsilon)e^{-\hat{\beta}}+(1-\tau)\text{Ei}(\hat{\beta})-\left[(1-\tau)e^{-\hat{\beta}}\log_2\left(\frac{\hat{\beta}(1-\tau)}{(1-\tau)+\hat{\beta}\tau Q_r}\right)\right] \\ -\frac{\hat{\beta}(1-\tau)^2P_{cr}}{(1-\tau)+\hat{\beta}\tau Q_r}-\frac{(1-\tau)^2e^{-\hat{\beta}}}{\varepsilon\left((1-\tau)+\hat{\beta}\tau Q_r\right)} \\ +\frac{\hat{\beta}(1-\tau)^2\text{Ei}(\hat{\beta})}{\varepsilon\left((1-\tau)+\hat{\beta}\tau Q_r\right)}+\frac{(1-\tau)\hat{\beta}(1-\Delta)}{\Delta\left((1-\tau)+\hat{\beta}\tau Q_r\right)}=0. \end{aligned} \quad (4.24)$$

where $\hat{\beta}$ is given after (4.20).

Using the results from last section, the EE-SE trade-off problem under an average input power constraint given in (4.7) and (4.8) is considered, with a limit set at \bar{P}_u . Hence the problem in (4.11) and (4.12) simplified when $\mathbb{E}_\gamma[P_r(\gamma)] = \min\left(\frac{\bar{P}_u}{K_{\mathcal{L}}}, \frac{P_{\max}}{K_{\mathcal{L}}}\right)$.

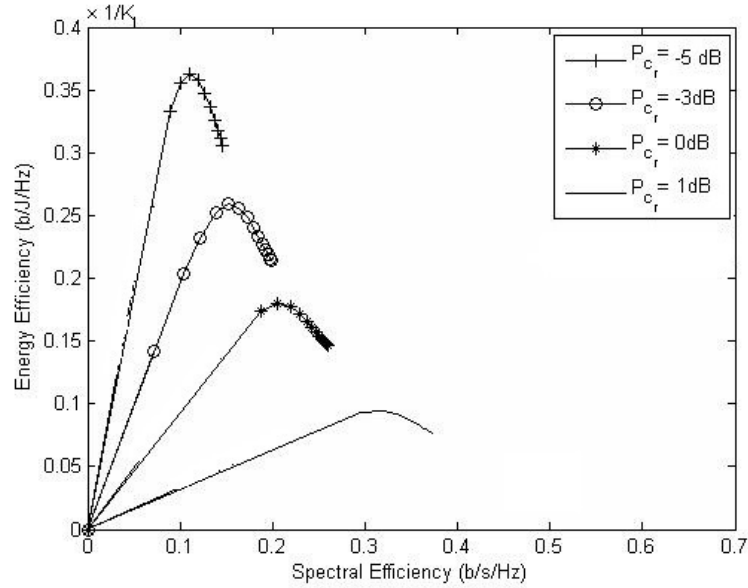


Figure 4.1: EE versus SE for various values of circuit power P_{cr} with $\tau = 0.8$, $Q_r = 0\text{dB}$ and $P_{cr2} = 0\text{dB}$.

4.4 Numerical results

In this section we numerically investigate the impact of TS parameter τ , harvesting power Q_r , circuit powers P_{cr} and P_{cr2} , importance weight Δ on achievable EE (b/J/Hz) and SE(b/s/Hz) of the system. In all figures, ε is set to 0.3, unless otherwise stated. For further investigation, we categorize numerical results into two sections 1) Optimum power allocation and 2) Optimum power allocation without circuit power P_{cr2} .

4.4.1 Optimum Power Allocation

In this section, we present the numerical results for a system with optimum power allocation, to see how the effect of EH and importance weight parameter Δ improves the trade-off of EE and SE.

Firstly, Fig. 4.1 includes the plots for EE versus SE with $\tau = 0.8$, harvesting power $Q_r = 0\text{dB}$, $P_{cr2} = 0\text{dB}$ and various values of P_{cr} . The results illustrate a

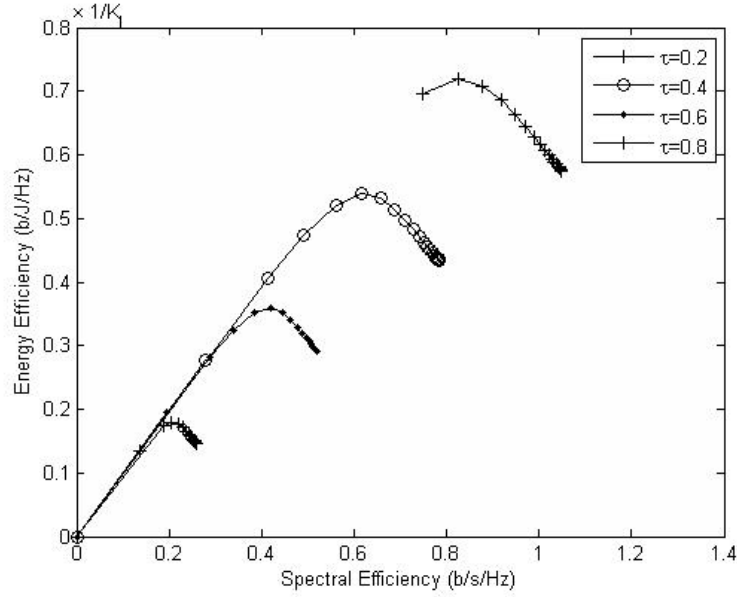


Figure 4.2: EE versus SE with $Q_r = 0\text{dB}$, $P_{cr} = 0\text{dB}$ and $P_{cr2} = 0\text{dB}$ for various values of TS parameter τ .

higher EE against smaller SE at lower circuit powers. The optimal input power for each value for P_{cr} has been shifted to the left, i.e., the EE curve shrinks towards the zero y-axis. In this way, a higher EE is achieved at a lower average operational power.

Fig. 4.2 shows the plots for EE versus SE with $P_{cr} = 0\text{dB}$, harvesting power $Q_r = 0\text{dB}$, $P_{cr2} = 0\text{dB}$ and various values of τ . In this particular setting of Q_r , P_{cr} and P_{cr2} , the figure shows that as τ is increases, both EE and SE increases. So, the choice of τ depends on the chosen Q_r , P_{cr} and P_{cr2} . The EE bell shaped curve expands as τ increases resulting in achieving higher EE, as well as higher SE. Therefore, it is prominent for a system which is required to be both energy and spectral efficient.

In Fig. 4.3, we plot EE versus harvesting power Q_r with $P_{cr} = 0\text{dB}$, $P_{cr2} = 0\text{dB}$, $\tau = 0.5$ and various values of importance weight Δ . The figure shows that EE increases with Q_r . This figure is obtained from theoretical result presented in (4.20). Also, at higher values of Δ , higher EE can be achieved. This indicates that

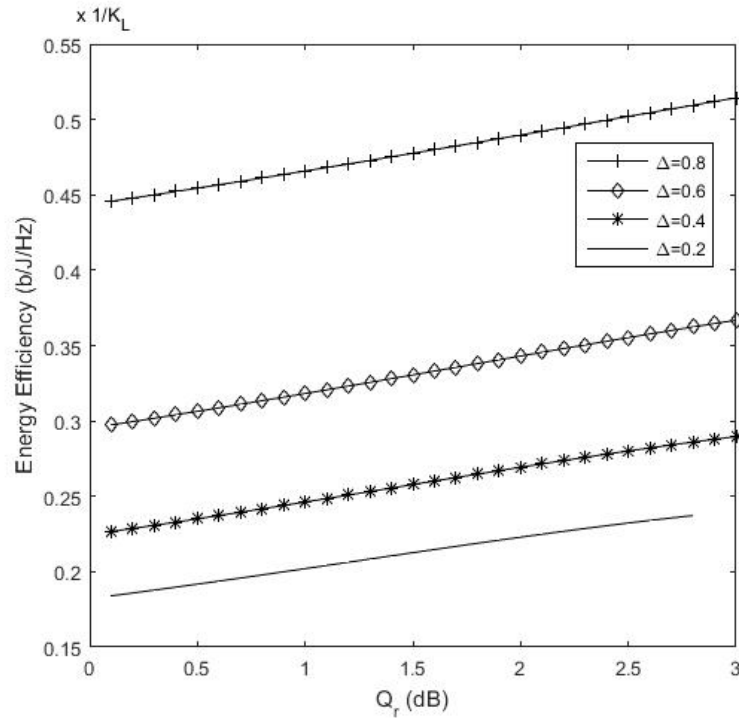


Figure 4.3: EE vs Q_r with $\tau = 0.5$ with $P_{cr} = 0\text{dB}$ and $P_{cr2} = 0\text{dB}$, for various values of Δ .

EE metric is dominant that is why it is increasing continuously. In addition to that, higher EE can be achieved at high Q_r , which shows that when EH power is stronger, we should spend more time in harvesting in order to achieve maximum achievable EE.

Similarly, Fig. 4.4 shows the plots of SE versus Q_r with $P_{cr} = 0\text{dB}$, $P_{cr2} = 0\text{dB}$, $\tau = 0.5$ and various values of importance weight Δ . It is seen from the figure that SE is monotonically decreasing with Q_r for most of the values of importance weight. The figure also reveals that for $\tau = 0.5$, maximum SE is achieved when $\Delta \in [0.6, 0.8]$, which means that its rather beneficial to transmit information than to harvest energy. Also, when Δ is big, SE is decreasing quickly which means that SE-maximization is dominant which confirms the significance of importance weight in trade-off given in (4.7).

Fig. 4.5 represents EE and SE curve versus importance weight Δ with $Q_r = 1\text{dB}$,

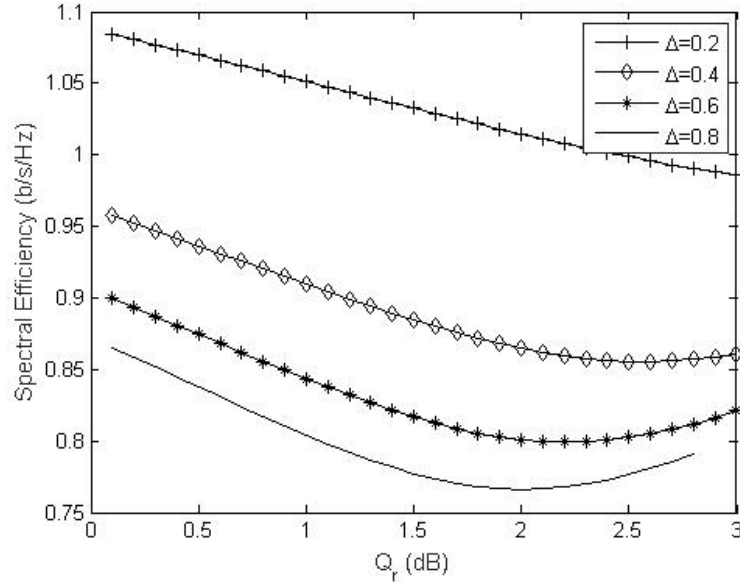


Figure 4.4: SE vs Q_r with $\tau = 0.5$ with $P_{cr} = 0\text{dB}$ and $P_{cr2} = 0\text{dB}$, for various values of Δ .

$\tau = 0.5$ with $P_{cr} = 0\text{dB}$ and $P_{cr2} = 0\text{dB}$. From the figure, it is noted that at smaller values of Δ , both SE and EE are decreasing until it reaches $\Delta = 0.3$ and after that EE increases which shows the importance of EE and diminishes the priority of SE, which supports our design intention. Also, the result presented here depicts the comparison of both theoretical (referring to (4.20)) and simulation result.

Fig. 4.6 includes the plot for EE vs TS parameter τ with $\Delta = 0.7$, $Q_r = 1\text{dB}$ for various values of P_{cr} and P_{cr2} . It is noted that when $P_{cr} = 0\text{dB}$ and $P_{cr2} = 0\text{dB}$, the maximum EE is achieved at $\tau = 0.7$. After reaching its peak value, EE decreases with TS parameter. Also, when $P_{cr} > P_{cr2}$, EE is always increasing due to the fact that allocation strategy for EE-maximization has consumed the whole input power which results in continuously increasing EE. Hence, EE metric is dominant.

4.4.2 Optimum Power Allocation without Circuit Power P_{cr2}

In this subsection, we discuss the optimum power allocation case without circuit power P_{cr2} , to see how Δ , EH and TS parameter can effect the trade-off of EE and

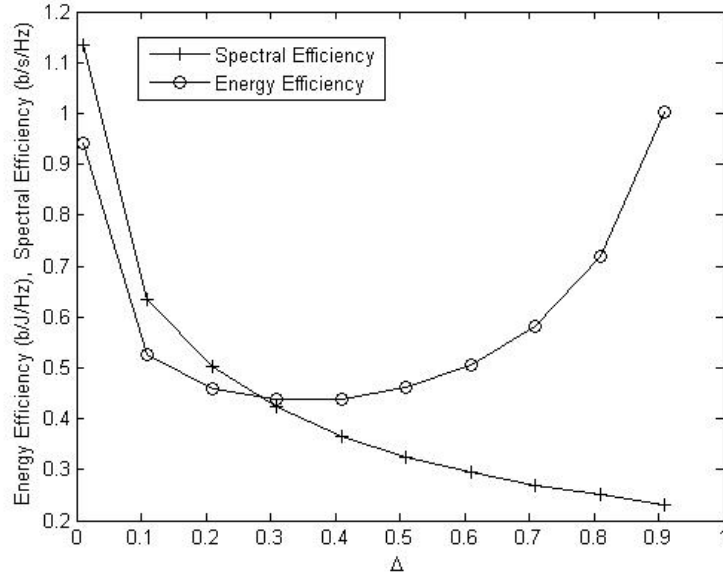


Figure 4.5: EE and SE vs importance weight Δ with $Q_r = 1\text{dB}$, $\tau = 0.5$ with $P_{c_r} = 0\text{dB}$ and $P_{c_{r2}} = 0\text{dB}$.

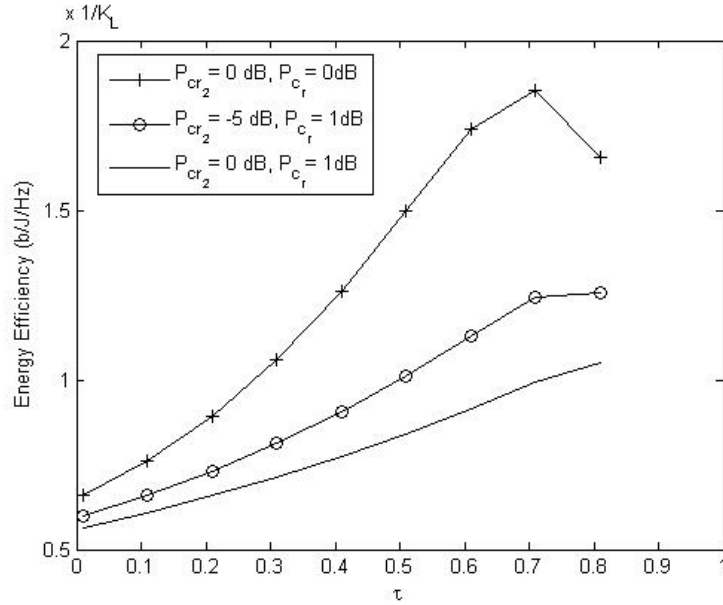


Figure 4.6: EE vs τ with $\Delta = 0.7$, $Q_r = 1\text{dB}$ for various values of P_{c_r} and $P_{c_{r2}}$.

SE.

We plot the results of EE and SE versus τ with $Q_r = 1\text{dB}$ and $P_{c_r} = 0\text{dB}$ for various values of Δ in Fig. 4.7 and Fig. 4.8. From Fig. 4.7, we notice that at $\tau = 0$ and smaller values of importance weight, i.e, $\Delta = 0.1$, maximum EE is achieved.

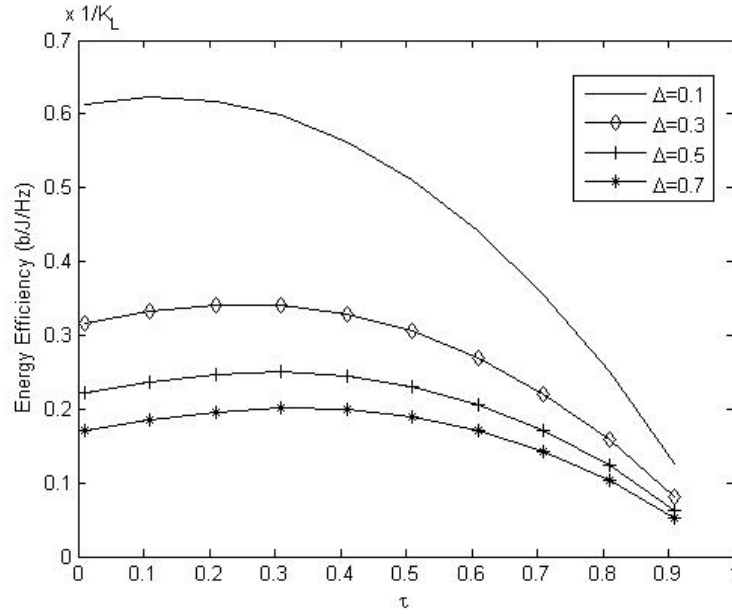


Figure 4.7: EE vs τ for various values of Δ with $Q_r = 1\text{dB}$ and $P_{cr} = 0\text{dB}$.

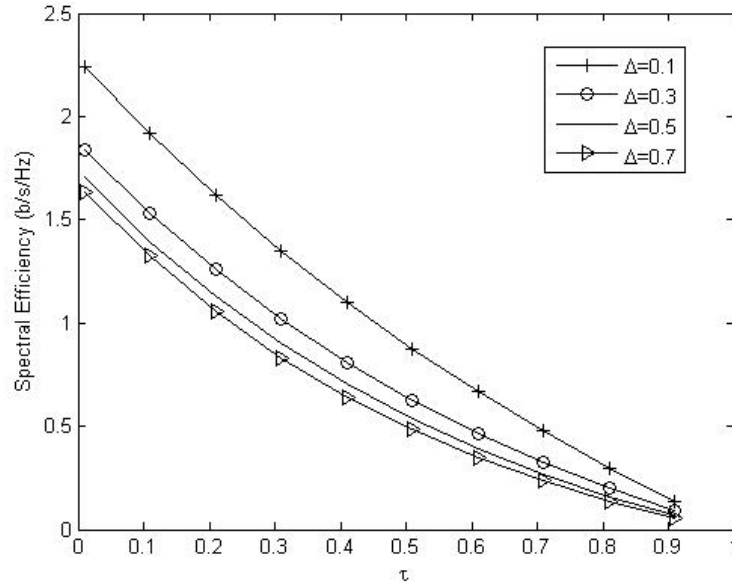


Figure 4.8: SE vs τ for various values of Δ with $Q_r = 1\text{dB}$ and $P_{cr} = 0\text{dB}$.

As τ increases and importance weight Δ is higher, more priority is given to EE therefore, the curve slowly goes to zero. Similarly, from Fig. 4.8, we can see that SE is always decreasing with τ . The higher Δ , i.e, $\Delta = 0.7$, decreases quicker than the one at $\Delta = 0.1$.

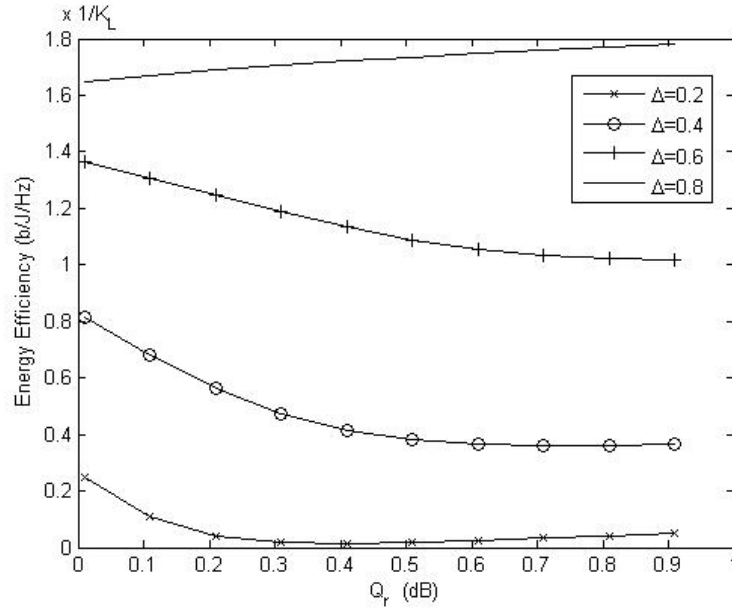


Figure 4.9: EE vs Q_r with $\tau = 0.5$ with $P_{cr} = 0\text{dB}$ and $P_{cr2} = 0\text{dB}$, for various values of Δ .

Fig. 4.9 presents the plots of EE vs Q_r with $\tau = 0.5$ with $P_{cr} = 0\text{dB}$ and $P_{cr2} = 0\text{dB}$, for various values of Δ . Here, it can be observed from figure that at lower values of importance weight parameter, i.e., $\Delta \in [0.2, 0.4, 0.6]$, EE is decreasing with Q_r . Due to this priority of EE will be decreased. As Q_r and Δ increases to a higher value, e.g., $\Delta = 0.8$, EE increases with harvested power. Varying Δ gives us a freedom to choose the priority for the given EE, which confirms the theoretical expression presented in (4.24).

4.5 Chapter Summary

In this chapter optimal power allocation scheme to jointly optimize EE and SE for a point-to-point system, equipped with fixed as well as EH battery is considered. A TS approach in which the transmitter switches between harvesting energy and transmitting information. We formulate MOP which jointly optimize EE and SE. Importance weight is introduced which is varied to set the priority level of

EE and SE. By using fractional programming and KKT conditions, the optimum power allocation scheme without input power constraint is calculated. Also, the closed-form expressions are derived. Numerical results validate the impact of TS parameter, importance weight, circuit powers and solar harvesting energy level on the achievable trade-off performance.

Chapter 5

Conclusion and Future work

5.1 Conclusion

This thesis was dedicated to design and performance analysis of energy harvesting systems. Several conclusion results have arisen from the study carried out to see how energy harvesting improves energy and spectral efficiency of the wireless communication networks.

In chapter 2, we investigated the performance analysis of a dual-hop decode-and-forward relaying system in which transmitter and the relay nodes both are equipped with fixed as well as harvested batteries. Compared to the pre-existed literature such as [GA15] and [NZDK15], the proposed system model shows a significant improvement in system throughput when energy harvesting is used at transmitter and the relay node. Also, the novel closed-form expressions derived for the CDF of the SNR at each hop and the end-to-end SNR is presented which improves overall QoS and system parameters remarkably. The closed-form reduces computational complexity for the receiver architecture for practical systems. Hence, the system parameters provide an insight for significant improvement in end-to-end SNR when both transmitter and relay nodes are equipped with harvesting sources.

Chapter 3 demonstrates the optimal transmission power allocation techniques and performance analysis for a point-to-point communication system which has a fixed as well as harvesting battery separated by time-switching. We investigated and obtained the conditions under which EH can improve system performance in terms of EE and SE of the proposed system model. First, we studied two cases for power such as power is optimally adapted to the variations in the channel and when transmission power is fixed. Second, novel closed-form expressions are derived for maximum achievable EE, SE and EH beneficialness condition. We proved that EE-optimum input power decreases with EH power level. Also, the system parameters demonstrates the conditions under which EH improves overall system performance.

In chapter 4, a power allocation scheme that jointly optimize EE and SE for point-to-point system equipped with both fixed and EH battery is proposed. Firstly, a MOP is formulated which jointly optimize EE and SE. a priority level of EE and SE is decided by introducing importance weight. We then use KKT conditions and fractional programming to convert this MOP into SOP. Again, closed-form expressions are calculated to see the impact of system parameters on achievable trade-off performance. The proposed model provide freedom to choose any value for importance weight to satisfy QoS requirements and flexibility for choosing EE or SE.

5.2 Future Work

From this thesis, we recommend and present following future directions.

- Optimal power allocation for multiple network topologies in 5G.
- Energy harvesting for Internet-of-things (IOT).

- EH based Non-orthogonal multiple access relaying systems.

5.2.1 Optimal power allocation for multiple network topologies in 5G

EH for point-to-point network is considered in Chapter 2 and 3. This contribution however pave ways to consider the optimal power allocation techniques in multiple network topologies. It was assumed that the energy arrivals were constant for the settings used for the proposed model. However, random energy arrivals in EH for multiple network is gaining alot more attention in 5G network. Recently [OU12] use save-and-transmit and best-effort-transmit schemes for unlimited sized battery as presented in [UYE⁺15]. This can be extended in our system model to meet the 5G requirements to prolong battery time. Although it was challenging to derive closed-form expressions for current network topology, however this work presented in this thesis will pave way to extend our system model for multiple network topologies in future networks.

5.2.2 Energy harvesting for Internet-of-things (IOT)

Internet of things (IOT) has predicted to change our lives by providing smart connectivity to the existing architecture, that will not only save time but will also helps in economic growth of information and communication sector [KMS⁺15]. In this regard, big companies such as EnOcean and Cymbet has started looking for solutions where EH can be used to charge sensors which are eventually used for IOT [MS14]. Since the performance analysis proposed for two different harvesting sources in Chapter 1 was limited to solar and RF harvesting, we can extend that to see how it can benefit IOT while keeping the EH architecture at the receiver end.

Also, the work proposed in chapter 2 is fundamental which can be further

extended to see how EH can improve system performance in terms of EE and SE for IOT.

5.2.3 EH based Non-orthogonal multiple access relaying systems

With an immense growth in mobile communication and wireless networks, it is too early to tell the features of 5G networks, but still there are a lot of promising candidates out of which Non-orthogonal multiple access (NOMA) stands out as it will improve the spectral efficiency (SE) of the system which is one of the major challenges faced by vendors and the telecom sector [LDEP16].

In this trend using NOMA with EH relaying system cannot only significantly improve SE but also the user selection schemes based on user distances and harvesting energy together can remarkably improve the system throughput [DPDK16] and ergodic capacity which is a QoS requirement metric for every user. We can extend the system model based on NOMA to see how EH along with user distance can improve the efficiency of the system.

Finally, the future direction is not restricted to only the above mentioned cases but also extendable to multi-disciplinary research areas.

Appendix A

Appendix of Chapter 2

A.1 Proof for Lemma 1

Here, we aim to prove the equation in Lemma 1, given in (2.28). We start by referring to the below recurrence equation

$$\frac{d}{dx} x^{\hat{\alpha}} \exp(-x - bx^{-1}) = \hat{\alpha} x^{\hat{\alpha}-1} \exp(-x - bx^{-1}) + bx^{\hat{\alpha}-2} \exp(-x - bx^{-1}) - x^{\hat{\alpha}} \exp(-x - bx^{-1}),$$

For $\hat{\alpha} = 1$, the expression simplifies to

$$\frac{d(x \exp(-x - bx^{-1}))}{dx} = (1 + bx^{-1} - x) \exp(-x - bx^{-1}). \quad (\text{A.1})$$

Re-arranging (A.1) and taking integration on both sides gives,

$$\begin{aligned} \int_{\gamma}^{\infty} x \exp(-x - bx^{-1}) dx &= \int_{\gamma}^{\infty} bx^{-1} \exp(-x - bx^{-1}) + x \exp(-x - bx^{-1}) \Big|_{\gamma}^{\infty} \\ &+ \int_{\gamma}^{\infty} \exp(-x - bx^{-1}) dx. \end{aligned} \quad (\text{A.2})$$

Different parts of (A.2) can be re-written into generalized incomplete Gamma function [CZ94] as

$$\int_{\gamma}^{\infty} x \exp(-x - bx^{-1}) = \Gamma(2, x; b), \quad (\text{A.3})$$

$$\int_{\gamma}^{\infty} bx^{-1} \exp(-x - bx^{-1}) = \Gamma(0, x; b), \quad (\text{A.4})$$

$$\int_{\gamma}^{\infty} \exp(-x - bx^{-1}) = \Gamma(1, x; b). \quad (\text{A.5})$$

Hence, replacing (A.3)-(A.5) into (A.2) yields,

$$\Gamma(2, x; b) = \Gamma(0, x; b) + x \exp(-x - bx^{-1}) \Big|_{\gamma}^{\infty} + \Gamma(1, x; b). \quad (\text{A.6})$$

Replacing the values for x and b in (A.6), the final expression for generalized incomplete Gamma function can be found as [CZ94]

$$\Gamma\left(2, \frac{\gamma}{\gamma_h}; \frac{\gamma}{\gamma_h \gamma_g w}\right) = \Gamma\left(0, \frac{\gamma}{\gamma_h}; \frac{\gamma}{\gamma_h \gamma_g w}\right) - \gamma \exp(-\gamma - b\gamma^{-1}) + \Gamma\left(1, \frac{\gamma}{\gamma_h}; \frac{\gamma}{\gamma_h \gamma_g w}\right). \quad (\text{A.7})$$

A.2 Calculating Generalized Incomplete Gamma Function

This appendix provide the details for calculating generalized incomplete gamma function for numerical results. As it is known from the literature that the generalized incomplete Gamma function can neither be calculated directly from MATLAB nor MATHEMATICA. In order to do so, we divide the generalized incomplete gamma function in small functions in order to get results in MATLAB. Details are given below.

The generalized incomplete gamma function is given by [CZ94, eq. 27]. We start by using the series expansion of $\exp(\frac{-b}{t})$ taken from [CZ94, eq.2.1], to get

$$\Gamma(\hat{\alpha}, x; b) = \sum_{n=0}^{\infty} \frac{(-b)^n}{n!} \Gamma(\hat{\alpha} - n, x). \quad (\text{A.8})$$

Here, $\Gamma(\hat{\alpha} - n, x)$ varies for different values of $\hat{\alpha}$, is given by

$$\Gamma(\hat{\alpha} - n, x) = x^{\hat{\alpha}-n-1} \exp^{-x}. \quad (\text{A.9})$$

However the value of $\hat{\alpha}$ in our work consider certain values, i.,e., 0, 1, 2. When $\hat{\alpha} = 0$, we have

$$\Gamma(0 - n, x) = x^{-1-n} \exp^{-x}. \quad (\text{A.10})$$

Further, we use identity from [CTV96, Theorem 12, eq. 69] when $\hat{\alpha} = 1$, is given by

$$\Gamma(1 - n, x) = x^{1-n} E_{i_n}(x). \quad (\text{A.11})$$

Similarly we substitute $\hat{\alpha} = 2$ in (A.9), to get

$$\Gamma(2 - n, x) = x^{1-n} \exp^{-x}. \quad (\text{A.12})$$

The expressions calculated in (A.10), (A.11) and (A.12) are substituted back in (A.8) in-order to get their exact values for generalized incomplete gamma function. Hence, the numerical results for generalized incomplete gamma function are calculated through these equations.

Appendix B

Appendix of Chapter 3

B.1 Proof for Lemma 2

We want to prove that \bar{P}_u decreases with increase in harvested power Q_r as presented in Lemma 2. We note that SE, is a concave function of transmission power $\mathbb{E}_\gamma[P_r(\gamma)]$, which is non-decreasing linear function of $P_r(\gamma)$. Hence, EE is a quasi-concave function of $\mathbb{E}_\gamma[P_r(\gamma)]$, and its maximum η can be achieved when $\eta' = 0$, with η' indicating the first derivative of η with respect to $\mathbb{E}_\gamma[P_r(\gamma)]$. This means that EE monotonically increases with $\mathbb{E}_\gamma[P_r(\gamma)]$ until it reaches its maximum and then it becomes a monotonically decreasing function of $\mathbb{E}_\gamma[P_r(\gamma)]$.

Now let us consider a system with fixed circuit powers: P_{cr} , P_{cr2} and EH power of Q_{r1} . We take the first derivative of η of the system with respect to $\mathbb{E}[P_r(\gamma)]$, yielding,

$$\eta' \Big|_{\substack{\mathbb{E}_\gamma[P_r(\gamma)] = \bar{P}_{u1}^* \\ Q_r = Q_{r1}}} = \frac{SE' \left(\bar{P}_{u1}^* + P_{cr} + P_{cr2} - Q_{r1} \right) - SE}{\left(\bar{P}_{u1}^* - Q_{r1} + P_{cr} + P_{cr2} \right)^2} = 0. \quad (\text{B.1})$$

where SE is rate of the system and SE' indicates the first derivative of SE with respect to $\mathbb{E}_\gamma[P_r(\gamma)]$. In more detail, (B.1) implies that for a system with Q_r , η is

maximized when $\mathbb{E}_\gamma[P_r(\gamma)] = \bar{P}_{u_1}^*$, and as a result, $\eta' = 0$ at $\mathbb{E}_\gamma[P_r(\gamma)] = \bar{P}_{u_1}^*$.

Now assume a system with higher energy harvesting power, i.e., $Q_{r_2} = Q_{r_1} + \Delta Q_r$, when $\Delta Q_r \geq 0$. In this system, the input power at which EE is maximized is achieved by $\bar{P}_{u_2}^*$. Now update (B.1) with Q_{r_2} gives

$$\eta' \Big|_{\substack{\mathbb{E}_\gamma[P_r(\gamma)] = \bar{P}_{u_1}^* \\ Q_{r_2} = Q_{r_1} + \Delta Q_r}} = \frac{\text{SE}'\left(\bar{P}_{u_1}^* - (Q_{r_1} + \Delta Q_r) + P_{cr} + P_{cr2}\right) - \text{SE}}{\left(\bar{P}_{u_1}^* - (Q_{r_1} + \Delta Q_r) + P_{cr} + P_{cr2}\right)^2}.$$

Using (B.1), we can further simplify (B.2), according to

$$\eta' \Big|_{\substack{\mathbb{E}_\gamma[P_r(\gamma)] = \bar{P}_{u_1}^* \\ Q_{r_2} = Q_{r_1} + \Delta Q_r}} = \frac{-\text{SE}'(\Delta Q_r)}{\left(\bar{P}_{u_1}^* - (\Delta Q_{r_1} + \Delta Q_r) + P_{cr} + P_{cr2}\right)^2} \leq 0. \quad (\text{B.2})$$

which shows $\eta' \Big|_{Q_r = Q_{r_2}}$ is decreasing at $\mathbb{E}_\gamma[P_r(\gamma)] = \bar{P}_{u_1}^*$, henceforth, η has already reached its maximum, which implies that $\bar{P}_{u_2}^* \leq \bar{P}_{u_1}^*$.

Bibliography

- [ABAD14] Osama Amin, Ebrahim Bedeer, Mohamed H Ahmed, and Octavia A Dobre. Energy efficiency and spectral efficiency trade-off for ofdm systems with imperfect channel estimation. In *Proc. IEEE Int. Conf. Commun. (ICC)*, pages 3553–3558, Australia, Jun. 2014. [Cited on page 79]
- [ABC⁺14] Jeffrey G Andrews, Stefano Buzzi, Wan Choi, Stephen V Hanly, Angel Lozano, Anthony CK Soong, and Jianzhong Charlie Zhang. What will 5g be? *IEEE Journal on selected areas in communications*, 32(6):1065–1082, Jun. 2014. [Cited on page 2]
- [AMBC⁺12] Marco Ajmone Marsan, Stefano Buzzi, Luca Chiaraviglio, Michela Meo, Carmen Guerrero, Filip Idzikowski, Yabin Ye, and Jorge López Vizcaíno. TREND: toward real energy-efficient network design. in *Proc. Int. Sustain. ICT Sustainability (SustainIT)*, Italy, Oct. 2012. [Cited on page 2]
- [BCR⁺12] Aruna Prem Bianzino, Claude Chaudet, Dario Rossi, Jean-Louis Rougier, et al. A survey of green networking research. *IEEE Commun. Sur. & Tut.*, 14(1):3–20, New York, Mar. 2012. [Cited on pages 5 and 48]
- [Bea05] Geoffrey P Beaumont. *Probability and random variables*. Elsevier, 2005. [Cited on page 34]
- [BG14] Alexandre Bodin and Deniz Guenduez. Energy harvesting communication system with a finite set of transmission rates. In *Proc. European Wireless Conf.*, pages 1–6, Spain, May, 2014. [Cited on page 49]
- [BTA16] Fatma Benkhelifa, Kamel Tourki, and Mohamed-Slim Alouini. Simultaneous wireless information and power transfer for spectrum sharing in cognitive radio communication systems. In *Proc. Int. Conf. Commun., (ICC)*, pages 676–681, Malaysia, May. 2016. [Cited on page 79]

BIBLIOGRAPHY

- [BV04] Stephen Boyd and Lieven Vandenbergh. Convex optimization. 2004. *Cambridge Univ. Pr.*, 2004. [Cited on pages 58, 85, and 87]
- [CG07] Sayantan Choudhury and Jerry D Gibson. Ergodic capacity, outage capacity, and information transmission over Rayleigh fading channels. In *Proc. Inf. Theory Appl. Workshop (ITA)*, California, Jan. 2007. [Cited on page 36]
- [Che16] Yunfei Chen. Energy-harvesting af relaying in the presence of interference and nakagami- m fading. *IEEE Trans. Wireless Commun.*, 15(2):1008–1017, Feb. 2016. [Cited on page 16]
- [CLJ⁺15] He Chen, Yonghui Li, Yunxiang Jiang, Yuanye Ma, and Branka Vucetic. Distributed power splitting for SWIPT in relay interference channels using game theory. *IEEE Trans. Wireless Commun.*, 14(1):410–420, Jan. 2015. [Cited on page 4]
- [CQZ14] Hsiao-Hwa Chen, Yi Qian, and Sheng Zhou. Energy conservation and harvesting for green communications. *China Commun.*, 11(3):i–ii, China, Mar. 2014. [Cited on page 3]
- [CSAA16] Yunfei Chen, Kalen T Sabnis, and Raed A Abd-Alhameed. New formula for conversion efficiency of RF EH and its wireless applications. *IEEE Trans. Vehicular Tech.*, 65(11):9410–9414, Nov. 2016. [Cited on pages 4 and 6]
- [CTV96] M Aslam Chaudhry, NM Temme, and EJM Velting. Asymptotics and closed form of a generalized incomplete Gamma function. *J. Comput. Applied Math.*, 67(2):371–379, Mar. 1996. [Cited on pages 32 and 103]
- [CYZ⁺11] Tao Chen, Yang Yang, Honggang Zhang, Haesik Kim, and Kari Horneman. Network energy saving technologies for green wireless access networks. *IEEE Wireless Commun.*, 18(5):30–38, Oct. 2011. [Cited on page 3]
- [CZ94] M Aslam Chaudhry and Syed M Zubair. Generalized incomplete Gamma functions with applications. *J. Comput. Applied Math.*, 55(1):99–123, Oct. 1994. [Cited on pages 32, 34, 102, and 103]
- [CZXL11] Yan Chen, Shunqing Zhang, Shugong Xu, and Geoffrey Ye Li. Fundamental trade-offs on green wireless networks. *IEEE Commun. Mag.*, 49(6), Jun. 2011. [Cited on pages 2 and 79]
- [DCA16] Kemal Davaslioglu, Cemil Can Coskun, and Ender Ayanoglu. New algorithms for maximizing cellular wireless network energy efficiency. *arXiv preprint arXiv:1610.04950*, 2016. [Cited on page 1]

BIBLIOGRAPHY

- [DdCA16] Nhu Tri Do, Daniel Benevides da Costa, and Beongku An. Performance analysis of multirelay RF energy harvesting cooperative networks with hardware impairments. *IET Commun.*, 10(18):2551–2558, Dec. 2016. [Cited on pages 6 and 16]
- [DG16] Kemal Davaslioglu and Richard D Gitlin. 5g green networking: Enabling technologies, potentials, and challenges. In *Proc. IEEE Int. Conf. Wireless and Microwave Tech. (WAMICON)*, pages 1–6, Florida, Apr. 2016. [Cited on page 1]
- [DGK⁺13] Panagiotis Demestichas, Andreas Georgakopoulos, Dimitrios Karvounas, Kostas Tsagkaris, Vera Stavroulaki, Jianmin Lu, Chunshan Xiong, and Jing Yao. 5g on the horizon: key challenges for the radio-access network. *Proc. IEEE Vehicular Tech. Mag.*, 8(3):47–53, Sept. 2013. [Cited on page 2]
- [DPDK16] Panagiotis D Diamantoulakis, Koralia N Pappi, Zhiguo Ding, and George K Karagiannidis. Optimal design of non-orthogonal multiple access with wireless power transfer. In *Proc. IEEE Int. Conf. Commun. (ICC)*, pages 1–6, Malaysia, May, 2016. [Cited on page 100]
- [DPEP14] Zhiguo Ding, Samir M Perlaza, Inaki Esnaola, and H Vincent Poor. Power allocation strategies in energy harvesting wireless cooperative networks. *IEEE Trans. Wireless Commun.*, 13(2):846–860, Feb. 2014. [Cited on page 15]
- [DRC⁺13] Lei Deng, Yun Rui, Peng Cheng, Jun Zhang, QT Zhang, and Mingqi Li. A unified energy efficiency and spectral efficiency tradeoff metric in wireless networks. *IEEE Commun. Lett.*, 17(1):55–58, Jan. 2013. [Cited on page 79]
- [ENS⁺17] Waleed Ejaz, Muhammad Naeem, Adnan Shahid, Alagan Anpalagan, and Minh Jo. Efficient energy management for the internet of things in smart cities. *IEEE Communications Magazine*, 55(1):84–91, 2017. [Cited on page 3]
- [FVDM⁺12] Xenofon Fafoutis, Dusan Vuckovic, Alessio Di Mauro, Nicola Dragoni, and Jan Madsen. Energy-harvesting wireless sensor networks. In *Proc. European Conf. Wireless Sensor Net. (EWSN)*, pages 84–85, Italy, Feb. 2012. [Cited on pages 2 and 47]
- [GA14] Yanju Gu and Sonia Aissa. Interference aided energy harvesting in decode-and-forward relaying systems. In *Proc. IEEE Int. Conf. Commun. (ICC)*, pages 5378–5382, Australia, Jun. 2014. [Cited on pages 6, 15, 16, and 22]

BIBLIOGRAPHY

- [GA15] Yanju Gu and Sonia Aissa. RF-based energy harvesting in decode-and-forward relaying systems: Ergodic and outage capacities. *IEEE Trans. Wireless Commun.*, 14(11):6425–6434, Nov. 2015. [Cited on pages 15, 16, 25, 29, 30, 34, and 97]
- [GBF⁺09] Markus Gruber, Oliver Blume, Dieter Ferling, Dietrich Zeller, Muhammad Ali Imran, and Emilio Calvanese Strinati. EARTH-energy aware radio and network technologies. In *Proc. IEEE Int. Symp. Person. Indoor Mob. Radio Commun. (PIMRC)*, pages 1–5, Japan, Sept. 2009. [Cited on page 2]
- [GGG15] Rajeev Gangula, David Gesbert, and Deniz Gündüz. Optimization of energy harvesting miso communication system with feedback. *IEEE J. Sel. Areas Commun.*, 33(3):396–406, Mar. 2015. [Cited on page 49]
- [GS10] Pulkit Grover and Anant Sahai. Shannon meets Tesla: Wireless information and power transfer. In *Proc. IEEE Int. Symp. Inf. Theory (ISIT)*, pages 2363–2367, Jun. 2010. [Cited on page 15]
- [GSMZ14] Deniz Gunduz, Kostas Stamatiou, Nicolo Michelusi, and Michele Zorzi. Designing intelligent energy harvesting communication systems. *IEEE Commun. Mag.*, 52(1):210–216, Jan. 2014. [Cited on page 5]
- [GW02] Andrea J Goldsmith and Stephen B Wicker. Design challenges for energy-constrained ad hoc wireless networks. *IEEE J. Wireless Commun.*, 9(4):8–27, Aug. 2002. [Cited on page 14]
- [HA13] Tao Han and Nirwan Ansari. On optimizing green energy utilization for cellular networks with hybrid energy supplies. *IEEE Trans. Wireless Commun.*, 12(8):3872–3882, Aug. 2013. [Cited on page 80]
- [HBB11] Ziaul Hasan, Hamidreza Boostanimehr, and Vijay K Bhargava. Green cellular networks: A survey, some research issues and challenges. *IEEE Commun. Surveys Tut.*, 13(4):524–540, Nov. 2011. [Cited on pages 14 and 47]
- [HD88] Peter Harrop and Raghu Das. *Energy harvesting and storage for electronic devices 2009-2019*. IDTechEx, 1988. [Cited on page 4]
- [HGM16] Weiliang Han, Jianhua Ge, and Jinjin Men. Performance analysis for NOMA energy harvesting relaying networks with transmit antenna selection and maximal-ratio combining over Nakagami-m fading. *IET Commun.*, 10(18):2687–2693, Dec. 2016. [Cited on page 16]
- [HH15] Ekram Hossain and Monowar Hasan. 5g cellular: key enabling technologies and research challenges. *Proc. IEEE Instrumentation & Measurement Mag.*, 18(3):11–21, Jun. 2015. [Cited on page 3]

BIBLIOGRAPHY

- [HMLN13] Amir Helmy, Leila Musavian, and Tho Le-Ngoc. Energy-efficient power adaptation over a frequency-selective fading channel with delay and power constraints. *IEEE Trans. Wireless Commun.*, 12(9):4529–4541, Sept. 2013. [Cited on page 5]
- [HZ12] Chin Keong Ho and Rui Zhang. Optimal energy allocation for wireless communications with energy harvesting constraints. *IEEE Trans. on Signal Process.*, 60(9):4808–4818, Sept. 2012. [Cited on pages 15 and 49]
- [IEBA16] Elmehdi Illi, Faissal El Bouanani, and Fouad Ayoub. Performance analysis of dual-hop underwater communication system subject to k - μ shadowed fading channel. In *in Proc. IEEE Int. Conf. Advanced Commun. Sys. Inf. Secur. (ACOSIS)*, pages 1–6, Morocco, Oct. 2016. [Cited on page 16]
- [Ind15] Cisco Visual Networking Index. Cisco visual networking index: global mobile data traffic forecast update, 2014–2019. *Tech. Rep.*, 2015. [Cited on page 1]
- [JZ07] Alan Jeffrey and Daniel Zwillinger. *Table of integrals, series, and products*. Academic Press, Apr. 2007. [Cited on pages 31 and 35]
- [KBS16] MI Khalil, S M Berber, and K W Sowerby. Energy efficiency and spectrum efficiency trade-off over optimal relay location in bidirectional relay networks. In *Proc. IEEE Conf. Anten. and Propa. Wireless Commun. (APWC)*, pages 298–302, Australia, Sept. 2016. [Cited on pages 47 and 48]
- [KHZS07] Aman Kansal, Jason Hsu, Sadaf Zahedi, and Mani B Srivastava. Power management in energy harvesting sensor networks. *ACM Trans. Embedded Comput. Sys.(TECS)*, 6(4):32, Sept. 2007. [Cited on pages 21 and 53]
- [KLG11] Onno J Kuik, Mairon Bastos Lima, and Joyeeta Gupta. Energy security in a developing world. *Wiley Interdisciplinary Reviews: Climate Change*, 2(4):627–634, 2011. [Cited on page 48]
- [KMLN12] Suman Khakurel, Leila Musavian, and Tho Le-Ngoc. Energy-efficient resource and power allocation for uplink multi-user OFDM systems. In *Proc. IEEE Int. Symp. Personal Indoor and Mobile Radio Commun. (PIMRC)*, pages 357–361, Sydney, Sept. 2012. [Cited on page 56]
- [KMS⁺15] Pouya Kamalinejad, Chinmaya Mahapatra, Zhengguo Sheng, Shahriar Mirabbasi, Victor CM Leung, and Yong Liang Guan. Wireless energy harvesting for the internet of things. *IEEE Communications Magazine*, 53(6):102–108, 2015. [Cited on pages 4 and 99]

BIBLIOGRAPHY

- [Kri14] Ioannis Krikidis. Simultaneous information and energy transfer in large-scale networks with/without relaying. *IEEE Trans. Commun.*, 62(3):900–912, Mar. 2014. [Cited on page 4]
- [KZO13] Ioannis Krikidis, Gan Zheng, and Björn Ottersten. Harvest-use cooperative networks with half/full-duplex relaying. In *Proc. IEEE Wireless Commun. and Net. Conf. (WCNC)*, pages 4256–4260, China, April, 2013. [Cited on page 5]
- [LDEP16] Yuanwei Liu, Zhiguo Ding, Maged ElKashlan, and H Vincent Poor. Cooperative non-orthogonal multiple access with simultaneous wireless information and power transfer. *IEEE J. Sel. Areas Commun.*, 34(4):938–953, Apr. 2016. [Cited on pages 16 and 100]
- [LDPR02] Kanishka Lahiri, Sujit Dey, Debashis Panigrahi, and Anand Raghunathan. Battery-driven system design: A new frontier in low power design. In *Proc. ASP-DAC*, page 261, India, Jan. 2002. [Cited on page 2]
- [LFN⁺15] Xiao Lu, Ian Flint, Dusit Niyato, Nicolas Privault, and Ping Wang. Performance analysis of simultaneous wireless information and power transfer with ambient RF energy harvesting. In *in Proc. IEEE Int. Wireless Commun. Network. Conf.(WCNC)*, pages 1303–1308, Doha, Apr. 2015. [Cited on page 16]
- [LKWG11] Christoph Lange, Dirk Kosiankowski, Rainer Weidmann, and Andreas Gladisch. Energy consumption of telecommunication networks and related improvement options. *IEEE IJSTQE Trans.*, 17(2):285–295, Mar. 2011. [Cited on page 2]
- [LMD⁺16] Yuanwei Liu, S Ali Mousavifar, Yansha Deng, Cyril Leung, and Maged ElKashlan. Wireless energy harvesting in a cognitive relay network. *IEEE Trans. Wireless Commun.*, 15(4):2498–2508, Apr. 2016. [Cited on pages 15, 17, 49, and 80]
- [LS15] Yin Li and Ronghua Shi. An intelligent solar energy-harvesting system for wireless sensor networks. *EURASIP J. Wireless Commun. and Network.*, 2015(1):179, Jun. 2015. [Cited on page 4]
- [LWN⁺15] Xiao Lu, Ping Wang, Dusit Niyato, Dong In Kim, and Zhu Han. Wireless networks with rf energy harvesting: A contemporary survey. *IEEE Commun. Sur. & Tut.*, 17(2):757–789, May. 2015. [Cited on pages 19 and 21]
- [LWZ⁺16] Yuanwei Liu, Lifeng Wang, Syed Ali Raza Zaidi, Maged ElKashlan, and Trung Q Duong. Secure d2d communication in large-scale cognitive cellular networks: A wireless power transfer model. *IEEE Trans. Commun.*, 64(1):329–342, Jan. 2016. [Cited on pages 24 and 26]

BIBLIOGRAPHY

- [LXX⁺11] Geoffrey Ye Li, Zhikun Xu, Cong Xiong, Chenyang Yang, Shunqing Zhang, Yan Chen, and Shugong Xu. Energy-efficient wireless communications: tutorial, survey, and open issues. *IEEE Wireless Commun.*, 18(6), Dec. 2011. [Cited on page 79]
- [LZC13] Liang Liu, Rui Zhang, and Kee-Chaing Chua. Wireless information and power transfer: a dynamic power splitting approach. *IEEE Trans. Commun.*, 61(9):3990–4001, Sept. 2013. [Cited on pages 3, 15, and 16]
- [LZL13] Shixin Luo, Rui Zhang, and Teng Joon Lim. Optimal save-then-transmit protocol for energy harvesting wireless transmitters. *IEEE Trans. Wireless Commun.*, 12(3):1196–1207, Mar. 2013. [Cited on pages 15 and 21]
- [MA04] R Timothy Marler and Jasbir S Arora. Survey of multi-objective optimization methods for engineering. *Struct. multidiscip. optim.*, 26(6):369–395, Apr. 2004. [Cited on page 83]
- [Mel10] Nigel P Melville. Information systems innovation for environmental sustainability. *MIS quarterly*, 34(1):1–21, Mar. 2010. [Cited on page 2]
- [MHL10] Guowang Miao, Nageen Himayat, and Geoffrey Ye Li. Energy-efficient link adaptation in frequency-selective channels. *IEEE Trans. Commun.*, 58(2):545–554, Feb. 2010. [Cited on pages 5, 47, and 48]
- [Mie12] Kaisa Miettinen. *Nonlinear multiobjective optimization*, volume 12. Springer, Dec. 2012. [Cited on page 79]
- [MM10] Bhargav Medepally and Neelesh B Mehta. Voluntary energy harvesting relays and selection in cooperative wireless networks. *IEEE Trans. Wireless Commun.*, 9(11):3543–3553, Nov. 2010. [Cited on page 5]
- [MM17] Mohammad Robot Mili and Leila Musavian. Interference efficiency: A new metric to analyze the performance of cognitive radio networks. *IEEE Trans. Wireless Commun.*, Jan. 2017. [Cited on page 79]
- [MS14] Subhas Chandra Mukhopadhyay and NK Suryadevara. Internet of things: Challenges and opportunities. In *Internet of Things*, pages 1–17. Springer Int. Publishing, 2014. [Cited on page 99]
- [MSK⁺16] Chinmaya Mahapatra, Zhengguo Sheng, Pouya Kamalinejad, Victor CM Leung, and Shahriar Mirabbasi. Optimal power control in green wireless sensor networks with wireless energy harvesting, wake-up radio and transmission control. *IEEE Access*, Dec. 2016. [Cited on page 49]

BIBLIOGRAPHY

- [MYG⁺14] Simon Mathew, Aswani Yella, Peng Gao, Robin Humphry-Baker, Basile FE Curchod, Negar Ashari-Astani, Ivano Tavernelli, Ursula Rothlisberger, Md Khaja Nazeeruddin, and Michael Grätzel. Dye-sensitized solar cells with 13% efficiency achieved through the molecular engineering of porphyrin sensitizers. *Nature chemistry*, 6(3):242–247, Mar. 2014. [Cited on page 37]
- [NJC⁺17] Dang Khoa Nguyen, Dushantha Nalin Jayakody, Symeon Chatzinotas, John Thompson, and Jun Li. Wireless energy harvesting assisted two-way cognitive relay networks: Protocol design and performance analysis. *IEEE Access*, Jan. 2017. [Cited on page 4]
- [NK⁺16] Sang Quang Nguyen, Hyung Yun Kong, et al. Performance analysis of energy-harvesting relay selection systems with multiple antennas in presence of transmit hardware impairments. In *Proc. Int. Conf. on Advanced Technologies for Commun. (ATC)*, pages 126–130, Vietnam, Oct. 2016. [Cited on page 16]
- [NMLC12] Prusayon Nintanavongsa, Ufuk Muncuk, David Richard Lewis, and Kaushik Roy Chowdhury. Design optimization and implementation for rf energy harvesting circuits. *IEEE J. Emerging sel. topics circuits and sys.*, 2(1):24–33, Mar. 2012. [Cited on page 21]
- [NZDK15] Ali A Nasir, Xiangyun Zhou, Salman Durrani, and Rodney A Kennedy. Wireless-powered relays in cooperative communications: Time-switching relaying protocols and throughput analysis. *IEEE Trans. Commun.*, 63(5):1607–1622, May, 2015. [Cited on pages 6, 15, and 97]
- [OCF⁺13] Magnus Olsson, Cicek Cavdar, Pål Frenger, Sibel Tombaz, Dario Sabella, and R Jantti. 5green: Towards green 5g mobile networks. In *Proc. IEEE Int. Conf. Wirel. and Mobile Computing, Net. and Commun. (WiMob)*, pages 212–216, Oct. 2013. [Cited on page 5]
- [OTY⁺11] Omur Ozel, Kaya Tutuncuoglu, Jing Yang, Sennur Ulukus, and Aylin Yener. Transmission with energy harvesting nodes in fading wireless channels: Optimal policies. *IEEE J. Sel. Areas Commun.*, 29(8):1732–1743, Sept. 2011. [Cited on pages 5, 49, and 80]
- [OU12] Omur Ozel and Sennur Ulukus. Achieving awgn capacity under stochastic energy harvesting. *IEEE Trans. Information Theory*, 58(10):6471–6483, Oct. 2012. [Cited on page 99]
- [PD10] Raghavendra S Prabhu and Babak Daneshrad. An energy-efficient water-filling algorithm for ofdm systems. In *in Proc. IEEE Int. Conf. Commun. (ICC)*, pages 1–5, South Africa, May. 2010. [Cited on pages 5 and 48]

BIBLIOGRAPHY

- [PKH13] Sungsoo Park, Hyungjong Kim, and Daesik Hong. Cognitive radio networks with energy harvesting. *IEEE Trans. Wireless commun.*, 12(3):1386–1397, Mar. 2013. [Cited on page 5]
- [PP02] Athanasios Papoulis and S Unnikrishna Pillai. *Probability, random variables, and stochastic processes*. Tata McGraw-Hill Education, 2002. [Cited on page 28]
- [PS05] Joseph A Paradiso and Thad Starner. Energy scavenging for mobile and wireless electronics. *IEEE Pervasive Computing*, 4(1):18–27, Mar. 2005. [Cited on page 4]
- [PSZS13] Aaron N Parks, Alanson P Sample, Yi Zhao, and Joshua R Smith. A wireless sensing platform utilizing ambient RF energy. In *Proc. IEEE Topical Conf. on Biomedical Wireless Technologies, Networks, and Sensing Systems (BioWireless)*, pages 154–156, Jan. 2013. [Cited on page 4]
- [RJS⁺17] Akashkumar Rajaram, Dushantha Nalin K Jayakody, Kathiravan Srinivasan, Bin Chen, and Vishal Sharma. Opportunistic-harvesting: Rf wireless power transfer scheme for multiple access relays system. *IEEE Access*, 2017. [Cited on page 3]
- [RM10] Srinivas Reddy and Chandra R Murthy. Profile-based load scheduling in wireless energy harvesting sensors for data rate maximization. In *Proc. IEEE Int. Conf. Commun (ICC)*, pages 1–5, Cape Town, May, 2010. [Cited on page 49]
- [RSV11a] Ramachandran Rajesh, Vinod Sharma, and Pramod Viswanath. Information capacity of energy harvesting sensor nodes. In *Proc. IEEE Int. Symp. Inf. Theory Proc. (ISIT)*, pages 2363–2367, Russia, Jul. 2011. [Cited on pages 4 and 5]
- [RSV11b] Ramachandran Rajesh, Vinod Sharma, and Pramod Viswanath. Capacity of fading Gaussian channel with an energy harvesting sensor node. In *Proc. IEEE Global Commun. Conf. (GLOBECOM)*, pages 1–6, USA, Dec. 2011. [Cited on pages 21 and 53]
- [RSV14] Ramachandran Rajesh, Vinod Sharma, and Pramod Viswanath. Capacity of Gaussian channels with energy harvesting and processing cost. *IEEE Trans. on Inf. Theory*, 60(5):2563–2575, May, 2014. [Cited on page 21]
- [RT14] Irma Uriarte Ramírez and Norma A Barboza Tello. A survey of challenges in green wireless communications research. In *Proc. Int. Conf. Mechatron. Electron. and Automot. Engin. (ICMEAE)*, pages 197–200, Mexico, Nov. 2014. [Cited on page 48]

BIBLIOGRAPHY

- [Sch76] S Schaible. Minimization of ratios. *J. of Optimization Theory and Applic.*, 19(2):347–352, Jun. 1976. [Cited on pages 56 and 84]
- [SK] Sujesha Sudevalayam and Purushottam Kulkarni. Energy harvesting sensor nodes: Survey and implications. *IEEE Commun. Sur. & Tut.*, volume=13, number=3, pages=443–461, year=Sept. 2011. [Cited on page 5]
- [SMN15] Arooj Mubashara Siddiqui, Leila Musavian, and Qiang Ni. Energy efficiency optimization with energy harvesting using harvest-use approach. In *Proc. IEEE Int. Conf. Commun. Workshop (ICCW)*., pages 1982–1987, London, Jun. 2015. [Cited on pages 5, 15, 48, and 84]
- [SP01] Nathan S Shenck and Joseph A Paradiso. Energy scavenging with shoe-mounted piezoelectrics. *IEEE Micro*, 21(3):30–42, May. 2001. [Cited on page 5]
- [SW08] Hyundong Shin and Moe Z Win. MIMO diversity in the presence of double scattering. *IEEE Trans. Inf. Theory*, 54(7):2976–2996, Jul. 2008. [Cited on page 27]
- [SZS⁺16] Jisheng Sun, Wensheng Zhang, Jian Sun, Cheng-Xiang Wang, and Yun-Fei Chen. Energy-spectral efficiency in simultaneous wireless information and power transfer. In *Proc. IEEE Conf. Commun. China (ICCC)*, pages 1–6, CHENGDU, CHINA, July, 2016. [Cited on page 80]
- [TD15] J Thirumaran and S Dhinakaran. Green communications and networking systems—a challenge to current communications and protocols. 2015. [Cited on page 48]
- [THOK15] Hina Tabassum, Ekram Hossain, Adedayo Ogundipe, and Dong In Kim. Wireless-powered cellular networks: Key challenges and solution techniques. *IEEE Commun. Mag.*, 53(6):63–71, Jun. 2015. [Cited on page 15]
- [TSAH14] Jie Tang, Daniel KC So, Emad Alsusa, and Khairi Ashour Hamdi. Resource efficiency: A new paradigm on energy efficiency and spectral efficiency tradeoff. *IEEE Trans. Wireless Commun.*, 13(8):4656–4669, Aug. 2014. [Cited on page 79]
- [TTS⁺16] Yuki Tsunoda, Chikara Tsuchiya, Yuji Segawa, Hajime Sawaya, Minoru Hasegawa, Shohei Ishigaki, and Koichiro Ishibashi. A small-size energy-harvesting electric power sensor for implementing existing electrical appliances into hems. *IEEE Sensors Journal*, 16(2):457–463, 2016. [Cited on page 4]

BIBLIOGRAPHY

- [TY12] Kaya Tutuncuoglu and Aylin Yener. Optimum transmission policies for battery limited energy harvesting nodes. *IEEE Trans. Wireless Commun.*, 11(3):1180–1189, Mar. 2012. [Cited on page 15]
- [UBPEG02] Elif Uysal-Biyikoglu, Balaji Prabhakar, and Abbas El Gamal. Energy-efficient packet transmission over a wireless link. *IEEE ACM Trans. Net.*, 10(4):487–499, Aug. 2002. [Cited on page 47]
- [UYE⁺15] Sennur Ulukus, Aylin Yener, Elza Erkip, Osvaldo Simeone, Michele Zorzi, Pulkit Grover, and Kaibin Huang. Energy harvesting wireless communications: A review of recent advances. *IEEE J. Sel. Areas Commun.*, 33(3):360–381, Mar. 2015. [Cited on page 99]
- [Var08] Lav R Varshney. Transporting information and energy simultaneously. In *Proc. IEEE Int. Symp. Inf. Theory, (ISIT)*, pages 1612–1616, Toronto, Jul. 2008. [Cited on pages 3 and 6]
- [VTY14] Burak Varan, Kaya Tutuncuoglu, and Aylin Yener. Energy harvesting communications with continuous energy arrivals. In *Proc. IEEE, Inf. Theory and Applications Workshop (ITA)*, pages 1–10, San Diego, Feb. 2014. [Cited on pages 17 and 21]
- [W⁺08] Molly Webb et al. Smart 2020: Enabling the low carbon economy in the information age. *The Climate Group. London*, 1(1):1–1, London, Jun. 2008. [Cited on page 48]
- [WAW14] Zhe Wang, Vaneet Aggarwal, and Xiaodong Wang. Optimal energy-bandwidth allocation for energy harvesting interference networks. In *Proc. IEEE Int. Symp. Inf. Theory (ISIT)*, pages 1166–1170, Hawaii, Jun. 2014. [Cited on page 15]
- [Wu12] Jinsong Wu. Green wireless communications: from concept to reality [industry perspectives]. *IEEE Wireless Commun.*, 19(4), Aug. 2012. [Cited on page 48]
- [WYJW14] Xiaonan Wen, Weiqing Yang, Qingshen Jing, and Zhong Lin Wang. Harvesting broadband kinetic impact energy from mechanical triggering/vibration and water waves. *ACS nano*, 8(7):7405–7412, 2014. [Cited on page 3]
- [XA15] Minghua Xia and Sonia Aissa. On the efficiency of far-field wireless power transfer. *IEEE Trans. Sig. Proces.*, 63(11):2835–2847, Jun. 2015. [Cited on page 25]
- [XCFD13] Yan Xia, Hongbin Chen, Lisheng Fan, and Fenliang Dai. Optimal power control for source and relay in energy harvesting relay networks. In *Proc. Int. Conf. Commun. Net. (CHINACOM)*, pages 942–947, China, Aug. 2013. [Cited on page 3]

BIBLIOGRAPHY

- [XLZ⁺11] Cong Xiong, Geoffrey Ye Li, Shunqing Zhang, Yan Chen, and Shugong Xu. Energy-and spectral-efficiency tradeoff in downlink ofdma networks. *IEEE trans. wireless commun.*, 10(11):3874–3886, Nov. 2011. [Cited on page 79]
- [XT12] Zhengzheng Xiang and Meixia Tao. Robust beamforming for wireless information and power transmission. *IEEE Wireless Commun. Lett.*, 1(4):372–375, Aug. 2012. [Cited on page 15]
- [XZ14] Jie Xu and Rui Zhang. Throughput optimal policies for energy harvesting wireless transmitters with non-ideal circuit power. *IEEE J. Sel. Areas Commun.*, 32(2):322–332, Feb. 2014. [Cited on pages 5, 14, and 48]
- [YMN16] Wenjuan Yu, Leila Musavian, and Qiang Ni. Tradeoff analysis and joint optimization of link-layer energy efficiency and effective capacity toward green communications. *IEEE Trans. Wireless Commun.*, 15(5):3339–3353, May. 2016. [Cited on page 79]
- [YU10] Jing Yang and Sennur Ulukus. Transmission completion time minimization in an energy harvesting system. In *Proc. Annual Conf. Inf. Sciences and Sys. (CISS)*, pages 1–6, Princeton, Mar. 2010. [Cited on page 3]
- [YU12] Jing Yang and Sennur Ulukus. Optimal packet scheduling in an energy harvesting communication system. *IEEE Trans. Commun.*, 60(1):220–230, Jan. 2012. [Cited on page 49]
- [YZLZ17] Jiazheng Yuan, Dongyan Zhao, Keping Long, and Yongrong Zheng. Improved immunization strategy to reduce energy consumption on nodes traffic. *Optics Communications*, 389:314–317, Apr. 2017. [Cited on page 2]
- [ZCR⁺17] Deyu Zhang, Zhigang Chen, Ju Ren, Ning Zhang, Mohamad Khattar Awad, Haibo Zhou, and Xuemin Sherman Shen. Energy-harvesting-aided spectrum sensing and data transmission in heterogeneous cognitive radio sensor network. *IEEE Trans. Vehicular Tech.*, 66(1):831–843, Jan. 2017. [Cited on page 5]
- [ZZH12] Xun Zhou, Rui Zhang, and Chin Keong Ho. Wireless information and power transfer: architecture design and rate-energy tradeoff. In *Proc. IEEE Global Commun. Conf. (GLOBECOM)*, pages 3982–3987, California, Nov. 2012. [Cited on pages 5, 49, 55, and 79]
- [ZZZ14] Jing Zhao, Ming Zhao, and Wuyang Zhou. Energy efficiency optimization in energy harvesting cooperative relay systems. In *Proc. Int. Conf. Wireless Commun. and Signal Proc. (WCSP)*, pages 1–6, China, Oct. 2014. [Cited on page 5]